Determination of Trace Levels of Pb (II) in Tap Water by Anodic Stripping Voltammetry with Boron-doped Diamond (BDD) Electrode

Chalermpol Innuph

A Thesis Submitted in Partial Fulfillment of the Requirements for the Degree of Master of Science in Analytical Chemistry

Prince of Songkla University

2008

Thesis Title Determination of Trace Levels of Pb (II) in Tap Water by Anodic Stripping Voltammetry with Boron-doped Diamond (BDD) Electrode

Author Mr. Chalermpol Innuphat

Major Program Analytical Chemistry

Major Advisor

……..…

(Assist. Prof. Dr. Pipat Chooto)

Co-advisor

…….

(Dr. Puchong Wararatananurak)

Examining Committee:

…..…..……..……Chairperson

(Dr. Charuwan Suitcharit)

……..…..……Committee

(Assist. Prof. Dr. Pipat Chooto)

……..……..……Committee

(Dr. Puchong Wararatananurak)

……..…..……Committee

(Dr. Supunnee Duangthong)

The Graduate School, Prince of Songkla University, has approved this thesis as partial fulfillment of the requirements for the Master of Science Degree in Analytical Chemistry

...……..……..

(Assoc. Prof. Dr. Krerkchai Thongnoo)

Dean of Graduate School

ชื่อวิทยานิพนธ์ การหาปริมาณตะกั่ว (II) ปริมาณน้อยในน้ำประปาด้วยวิธีแอโนดิกสทริปปิงโวลแทมเมตรีโดยใช้ขั้วโบรอนโดพไดมอน (BDD)

ผู้เขียน นายเฉลิมพล อินนุพัฒน์

สาขาวิชา เคมีวิเคราะห์

ปีการศึกษา 2550

บทคัดย่อ

การศึกษาวิธีการเตรียมตัวอย่างที่สะดวกและรวดเร็วในการวิเคราะห์หาตะกั่วปริมาณน้อยในน้ำประปาด้วยวิธีแอโนดิกสทริปปิงโวลแทมเมตรีโดยใช้ขั้วโบรอนโดพไดมอน (BDD) โดยการนำตัวอย่างน้ำมาเติมด้วยกรดไนตริกเข้มข้นภายในขวดโพลีเอทิลลีน (polyethylene) ปรับสภาพความเป็นกรด-ด่าง จากนั้นทำการหาสภาวะที่เหมาะสมในการหาปริมาณตะกั่ว เช่น สภาพความเป็นกรด-เบส ชนิดและความเข้มข้นของอิเล็กโตรไลต์ จากการศึกษาพบว่าการตรวจวัดตะกั่วทำได้อย่างมีประสิทธิภาพในช่วงความเป็นกรด-เบส 1.26 อิเล็กโตรไลต์ที่เหมาะสม คือ 0.2 โมลาร์ โพแทสเซียมไนเตรต (KNO_3) ร่วมกับ 0.05 โมลาร์ กรดไนตริก (HNO_3) ซึ่งทำให้ตะกั่วในตัวอย่างน้ำอยู่ในรูปของไอออน จากนั้นนำไปวิเคราะห์เพื่อหาปริมาณโดยใช้เทคนิค สแควร์เวฟ แอโนดิก สทริปปิงโวลแทมเมตรี (SWASV) ซึ่งเทคนิคนี้ประกอบด้วยการทำให้ไอออนของตะกั่วเกิดปฏิกิริยารีดักชันเกาะติดกับขั้วไฟฟ้าที่ทำหน้าที่เป็นแคโทดโดยใช้ศักย์รีดักชัน -1.30 โวลต์ และตามด้วยการให้ตะกั่วหลุดออกจากขั้วไฟฟ้าด้วยการสแกนศักย์ไฟฟ้าทางด้านลบ พีค ออกซิเดชั่นของตะกั่วปรากฏที่ศักย์ -0.460 โวลต์ ศึกษาและปรับสภาวะที่เหมาะสมของการทดลองในส่วนของเครื่องมือวิเคราะห์ (instrumental parameters) ได้แก่ ศักย์ไฟฟ้าที่ก่อให้เกิดการพอกพูนด้วยไฟฟ้า (deposition potential), เวลาที่ใช้ในการก่อให้เกิดการพอกพูนด้วยไฟฟ้า (deposition time), อัตราการสแกน (scan rate), แอมปลิจูด (amplitude) และเวลาในการปรับสมดุล (equilibration time) พบว่าขั้วโบรอนโดพไดมอนให้ความเป็นเส้นตรงของกราฟตะกั่วอยู่ในช่วง 2.0 $\mu g\ L^{-1}$ ถึง 30.0 $\mu g\ L^{-1}$ ด้วยค่าสหสัมพันธ์ของเส้นตรง (r^2) เท่ากับ 0.9994 เมื่อใช้เวลาการพอกพูนด้วยไฟฟ้านาน 10 นาที และที่สภาวะเหมาะสมขีดจำกัดต่ำสุดของการตรวจวัดของตะกั่วเท่ากับ 0.3 $\mu g\ L^{-1}$ การศึกษาความถูกต้องและแม่นยำของวิธีการทำได้โดยการวิเคราะห์วัสดุอ้างอิงมาตรฐานน้ำธรรมชาติ (Standard Reference Material; SRM1640) พบค่าร้อยละของการได้กลับคืนของตะกั่วคือ 98.85 % และให้ค่าความแม่นยำโดยมีค่าเบี่ยงเบนมาตรฐานสัมพัทธ์ (%RSD) อยู่ในช่วงน้อยกว่า 7% นอกจากนี้ได้ทำการศึกษาการรบกวนของไอออนอื่น ๆ ต่อการตรวจวัดตะกั่ว พบว่า Mg^{2+}, Ca^{2+}, Ni^{2+}, Fe^{2+}, Zn^{2+}, Cd^{2+}, Mn^{2+}, Co^{2+}, Al^{3+} และ Cu^{2+} มีผลรบกวนน้อยมากและจากการเปรียบเทียบผลการวิเคราะห์หาปริมาณตะกั่วในตัวอย่างน้ำประปาโดยใช้เทคนิคอินดักทีพลีคัพเพิลพลาสมา ออฟติ

คอลอีมิสชันสเปกโทรเมทรี (ICP-OES) ได้ผลการวิเคราะห์ที่คล้ายคลึงกัน ดังนั้นวิธีการที่ได้ศึกษาขึ้นสามารถนำไปใช้ในการวิเคราะห์หาปริมาณตะกั่วในตัวอย่างน้ำได้อย่างมีประสิทธิภาพ จากการศึกษาพบระดับการปนเปื้อนของตะกั่วในน้ำประปาจำนวน 11 ตัวอย่าง ที่เก็บจากก๊อกน้ำของบ้านเรือนประชาชนที่ตั้งอยู่ในเขตเทศบาลนครหาดใหญ่อยู่ในช่วง 0.0-0.8 $\mu g\ L^{-1}$ ปริมาณการปนเปื้อนของตะกั่วในตัวอย่างน้ำที่ตรวจพบไม่เกิน 10.0 $\mu g\ L^{-1}$ ซึ่งยังคงอยู่ในระดับที่ปลอดภัยสำหรับผู้บริโภคตามมาตรฐานขององค์การอนามัยโลก (WHO)

Thesis Title	Determination of Trace Levels of Pb (II) in Tap Water by Anodic Stripping Voltammetry with Boron-doped Diamond (BDD) Electrode
Author	Mr. Chalermpol Innuphat
Major Program	Analytical Chemistry
Academic Year	2007

ABSTRACT

A simple and rapid method for determination of trace lead in the tap water in Hatyai city by anodic stripping voltammetry with boron-doped diamond (BDD) electrode has been studied. The water samples were added with concentrated nitric acid in closed vessel (polyethylene). The parameters in the preconcentration steps were studied including with the electrolyte influences, pH, concentration and volume. Effective preconcentration of trace lead was achieved in the pH of 1.26. The appropriate electrolyte was found to be 0.2 M potassium nitrate (KNO_3) in 0.05 M nitric acid (HNO_3) to made all lead ionic and BDD was then applied to determine lead ion by square wave anodic stripping voltammetry technique (SWASV). The Pb^{2+} was preconcentrated on the cathode electrode surface at -1.30 V vs Ag/AgCl (3 M KCl). The stripping peak was obtained by scanning potential in the negative direction at -0.460 V. The optimized instrumental parameters include deposition potential, deposition time, scan rate, modulation amplitude and equilibration time. A linear calibration graph was obtained within the Pb^{2+} concentration range of 2.0 µg L^{-1} to 30.0 µg L^{-1} (r^2 = 0.9994) with 10 min accumulation time. The detection limit was found to be 0.3 µg L^{-1}. The accuracy was verified by analyzing the standard reference material; SRM1640 (Trace Elements in Natural Water). The recovery was found to be 98.85% with relative standard deviation (%RSD) less than 7%. Several interferences including Mg^{2+}, Ca^{2+}, Ni^{2+}, Fe^{2+}, Zn^{2+}, Cd^{2+}, Mn^{2+}, Co^{2+}, Al^{3+} and Cu^{2+} were studied and it was found that the method was not significantly affected by these coexisting ions and can be applied satisfactorily to lead determination in water samples. The results from determination of Pb^{2+} using the studied method (ASV) and ICP-OES were compared and found to be in a good agreement. The concentration of lead in various water samples from eleven regions at Hatyai city was found to be in the range of 0.0-0.8 µg L^{-1}, lower than the drinking water contamination standard limited level (<10.0 µg L^{-1}) issued by the World Health Organization (WHO).

ACKNOWLEDGEMENTS

The completion of this thesis would be quite impossible without the help of certain people whom I would like to thank.

I deeply express my sincere thanks to my advisor Assist. Prof. Dr. Pipat Chooto and Dr. Puchong Wararattananurak for their valuable advice and suggestions throughout the course of this work,

I also would like to thank:

The examination committee members of this thesis for their valuable time,

Hatyai Waterwork Offices for map of the tap water pipe in Hatyai city,

Staff of the Department of Chemistry for their help in some technical aspects of this thesis,

Chemistry Glassblowing room for supporting Deionized water and Central Equipment unit of Faculty of Science for determination of lead in tap water sample with Inductively Couple Plasma Optical Emission Spectrometer,

The Graduate School for financial support and Department of Chemistry, Prince of Songkla University for chemicals and equipment,

My parents and my sister for their loves and attention all through my life,

And lastly, my friends in Analytical Chemistry and Heavy metal analysis group who are always of great help.

Chalermpol Innuphat

CONTENTS

CONTENTS (CONTINUED)

CONTENTS (CONTINUED)

CONTENTS (CONTINUED)

CONTENTS (CONTINUED)

LIST OF TABLES

LIST OF TABLES (CONTINUED)

LIST OF TABLES (CONTINUED)

LIST OF FIGURES

LIST OF FIGURES (CONTINUED)

LIST OF FIGURES (CONTINUED)

LIST OF ABBREVIATIONS AND SYMBOLS

AAS	=	Atomic absorption spectroscopy
AdSV	=	Adsorptive stripping voltammetry
ADI	=	Acceptable Daily Intake
AE	=	Auxiliary electrode
ALAD	=	Aminolevulinic acid dehydratase
ASV	=	Anodic stripping voltammetry
AR	=	A standard grade of analytical reagents
BDD	=	Boron-doped diamond
BDL	=	Below the detection limit
CRM	=	Certified Reference Material
CSV	=	Cathodic stripping voltammetry
CV	=	Cyclic voltammetry
DME	=	Dropping mercury electrode
DMF	=	*N,N*-Dimethylformamide
DMSO	=	Dimethylsulfoxide
DPASV	=	Differential pulse Anodic stripping voltammetry
DPP	=	Differential pulse polarography
DPV	=	Differential pulse voltammetry
EPA	=	Environmental Protection Agency

LIST OF ABBREVIATIONS AND SYMBOLS (CONTINUED)

FI	=	Flow injection
HMDE	=	Hanging mercury drop electrode
Hz	=	Hertz
ICP-MS	=	Inductively couple plasma mass spectrometry
LOAEL	=	Lowest observed adverse effect level
Ipa	=	Oxidation peak current
Ipc	=	Reduction peak current
IQ	=	Intelligence quotient
Ir-UMEA	=	Iridium ultramicroelectrode arrays
IUPAC	=	International Union of Pure and Applied Chemistry
LOD	=	Limit of detection
LOQ	=	Limit of quantification
LSV	=	Linear sweep voltammetry
MAC	=	Maximum acceptable concentration
$mg\ L^{-1}$	=	Milligram per liter
min	=	Minute (time)
mM	=	Millimole per liter (Millimolar)
mV	=	Millivolts
$mV\ s^{-1}$	=	Millivolts per second

LIST OF ABBREVIATIONS AND SYMBOLS (CONTINUED)

ND	=	Non detectable
NHE	=	Normal hydrogen electrode
NIST	=	National Institute of Standards and Technology
nM	=	Nanomole per liter (Nanomolar)
NOAEL	=	No observed adverse effect level
PQL	=	Practical quantitation limit
PTWI	=	Provisional tolerable weekly intake
RE	=	Reference electrode
rpm	=	Revolutions per minute
RSD	=	Relative standard deviation
s	=	Second (time)
SASV	=	Subtractive anodic stripping voltammetry
S/B		Signal to background ratio
SD	=	Standard deviation
S/N	=	Signal to noise ratio
SPCE	=	Screen-printed carbon electrodes
SRM	=	Standard Reference Materials
SWV	=	Square wave voltammetry
SWASV	=	Square wave anodic stripping voltammetry

LIST OF ABBREVIATIONS AND SYMBOLS (CONTINUED)

THF	=	Tetrahydrofuran
TMFE	=	Thin-mercury film electrodes
$\mu g\ dL^{-1}$	=	Microgram per deciliter
$\mu g\ g^{-1}$	=	Milligram per gram
$\mu g\ kg^{-1}$	=	Microgram per kilogram
$\mu g\ L^{-1}$	=	Microgram per liter
USGS	=	United States Geological Survey
UV	=	Ultraviolet
v/v	=	Volume by volume
WE	=	Working electrode
WHO	=	World Health Organization
ZPP	=	Zinc protoporphyrin
σ	=	The population standard deviation

CHAPTER 1

INTRODUCTION

1.1 Introduction

Lead is a toxic heavy metal that appears in the environment mainly due to industrial processes. The pollution of lead is one of the most serious environmental problems because of their stability in contaminated sites and complexity of the mechanism for biological toxicity.

Hatyai city is the important traveling and business center in the Southern of Thailand. Profits cause rapid development with the result of high population density in certain areas, increasing busy street traffic and more air pollution from dust and Pb^{2+} exposure in the atmosphere from the combustion (Rojanapraiwong, 1999). The populousness in limited area is the cause of the land management for occupational activities. The survey shows that activities from a lot of the factory buildings in Hatyai including printing houses, lathe and welding shops, car repair shops, car spraypaint shops and electronic repair shops. Where increase dust and Pb^{2+} exposure, causing widespread environmental contamination (Wangwongwatana, 2003). Subsequently, these matters fall and accumulate in the ground. The half-life of Pb^{2+} in the ground is about 90-100 years and it was the least soluble but the solubility can increase in the clay acid condition (Aikamphon, 1979). Drinking water can become contaminated by Pb^{2+}, either at the source due to deposition from environmental sources or in the water distribution system. For example, the study of student blood in the primary school Pattani province aged 6-15 years old, revealed that the students of Municipality 3 School had elevated blood Pb^{2+} levels over 25 μg dL^{-1}. Currently, the World Health Organization (WHO) limit of concern for Human Pb^{2+} intoxication is 10 μg dL^{-1}. Because these children live near the boat plant it where lead oxide (Pb_3O_4) is used to plug a crack of boat wall for protect some percolate water (Geater *et al.,* 1996). Effects of Pb^{2+} on the children nervous system have demonstrated to reduce the IQ scale with the increased concentration in blood. In addition, consistent alterations were observed on attention, visual-motor reasoning skills, social behavior, mathematics and reading abilities (Guilarte, 2005).

Monitoring heavy metal ion levels in water supplies is essential for human health and safety. There are numerous health problems associated with exposure to high levels of metal

ions (e.g., Cd^{2+}, Pb^{2+}, Hg^{2+}, $As^{3+/5+}$) because of their tendency to accumulate in the body, toxicity and low rate of clearance. For instance, the biological half-life of cadmium is 10-30 years while that for lead in bone is more than 20 years (Goyer, 1995). The Environmental Protection Agency (EPA) estimates that nearly 20% of human exposure to lead occurs through contaminated drinking water (EPA, 2005). It is, therefore, critical for humans to experience minimal exposure to these contaminants and this can be ensured through effective water quality monitoring.

Utaphao watercourse in Hatyai, Southern Thailand, is the main suffer way of the wastewater from the established factories which are near watercourse branch. Moreover, it suffers from trash and wastewater from Hatyai city. The water is most deteriorated compared with other branches of Songkhla lake. Considering the water used in Hatyai of 82,143 cubic meter day^{-1}, it is possible to become wastewater of 65,714 cubic meter day^{-1} into Utaphao watercourse (Pochareng and Kamnurtpriwul, 2004). Therefore, the water from Utaphao watercourse to produce tap water might be contaminate with heavy metals such as mercury, lead and cadmium at greater levels and can increase the risk to public health in the future.

Lead is one of the metal worth paying attention due to its undespread used and its effects on human. Once absorbed, lead can be accumulated in the body and greatly threaten the health of human. Furthermore, lead is frequently used as a material for water supply pipes, with the possibiling that the tap water having been in contact with a lead pipe for a long time (e.g., overnight) can contain relatively high amounts of lead. That it is important to monitor lead in drinking water is therefore increasingly recognized (Spataru *et al.,* 2006). Detection of trace level lead in the environment is a highly important yet challenging analytical problem. To determine the environmental toxic trace levels of lead, highly sensitive and selective methods need to be developed. Sensitive methods for the determination of trace amount of lead have received much attention, and many techniques have been employed for the determination. The current EPA-recommended methods for metal ion analysis in water supplies are atomic absorption spectroscopy (AAS), inductively couple plasma mass spectrometry (ICP-MS) and anodic stripping voltammetry (ASV). These methods are highly sensitive; however, they require relatively large volumes of sample for analysis, complicated operation, high cost of maintenance, expensive apparatus and requiring well-controlled experimental conditions. ASV is increasingly employed because its a wide linear dynamic range, low detection limit ($\mu g\ L^{-1}$) and multielement

analysis capability. An additional advantage of ASV over AAS or ICP-MS is the simplicity of the instrumentation, high sensitivity, easy operation, relatively inexpensive**,** small in size and low electrical power requirement (Swain and McGaw, 2006). This electrochemical method is one of the most favorable techniques for the determination of heavy metal ions, mostly carried out at mercury electrodes (Fischer and Berg, 1999; Korolczuk, 2000; Saito *et al.,* 2001 and Cordon *et al.,* 2002). With the increasing awareness of conserving the living environment, mercury-free electrodes for the determination of heavy metal ions became more attractive and more and more work was performed at mercury-free modified electrodes. BDD electrodes has been shown to have a high sensitivity, good selectivity and reproducibility for the determination of Pb^{2+} in tap water samples (Spataru *et al.,* 2006).

Table 1-1 Comparison of the important BDD and Hg electrode properties for anodic stripping voltammetry

Boron-doped diamond (BDD)	**Hg**
Wide cathodic and anodic potential limits	Wide cathodic potential limit
Lower background current	Higher background current
Good sensitivity	Good sensitivity
Chemically inert	Interaction with Cl^-
Reusable surface-no pretreatment required	Easily refreshed surface
Non-toxic	Toxic
Non-volatile	Volatile

Source: (Swain and McGaw, 2006).

It has electrochemical properties very similar to those of Hg, as listed in Table 1-1, but yields better detection figures of merit under the condition of several metal ions contaminants. The lower background current and wider anodic potential limit are its main advantages of BDD over Hg (Swain *et al.,* 2004; Manivannan *et al.,* 2004; Babyak and Smart, 2004 and Wantz *et al.,* 2005). ASV with this electrode has been used to sensitively and accurately quantify contaminant

metal ions in several real samples, such as lake, river and tap waters, as well as digestions of river sediment, waste treatment sludge and soil (Compton *et al.*, 2000; Swain *et al.,* 2004 and Babyak and Smart, 2004). Conductive diamond represents an electrode material that has attracted great interest in electroanalysis, due to its outstanding electrochemical features: wide potential window in aqueous solutions, low background current, long-term stability of the response and low sensitivity to dissolved oxygen (Fujishima *et al.,* 1999). These unique properties of the polycrystalline diamond, together with its extreme robustness, strongly recommend this material to be very well suited for stripping voltammetry analysis of heavy metals, and the results reported thus far are more than promising (Saterlay *et al.,* 2000 and Prado *et al.,* 2002). It is worth noting that practical applications for tap water analysis often require lead determination within the nanomolar concentration range.

This work was aimed at evaluating the potential analytical applications of boron-doped diamond (BDD) electrodes for the determination of Pb^{2+} within the nanomolar concentration range using ASV. In order to assess the practical utility of the method for tap water analysis, preliminary investigation concerning the effect of copper as possible interferent is also reported.

1.1.1 Physical and chemical properties of lead

Heavy metals are the elements that have the specific gravity more than 5 g cm^{-3} such as cadmium (Cd), chromium (Cr), copper (Cu), lead (Pb), mercury (Hg), and zinc (Zn). The high levels of heavy metal accumulated in human are toxic. Generally, only trace amount of heavy metals is found in the environment (Suwannarath, 1995).

Lead is the heavy metal which classified in group IV A of the periodic table. It is a soft, white gray metal. It is easy to beat, press or straighten and soluble in nitric acid (Hill, 1995). A summary of the physical properties of lead is given in Table 1-2.

Table 1-2 Physical and chemical properties of lead

Physical properties	Lead properties
Element symbol	Pb
Atomic mass	207.2
Atomic number	82
Oxidation state	0, 2, 4
Atomic radius	180 pm
Melting point (s.t.p.)	327.46^{o}C
Boiling point (s.t.p.)	1749 ^{o}C
Density (20 ^{o}C)	11.34 g cm^{-3}
Heat of fusion	4.77 kJ·mol^{-1}
Heat of vaporization	179.5 kJ·mol^{-1}
Heat capacity (25 °C)	26.650 J·mol^{-1}·K^{-1}
Electron configuration	[Xe] 4f^{14} 5d^{10} 6s^{2} 6P^{2}
Young's modulus	16 GPa

Source: http://en.wikipedia.org/wiki/Lead (3/02/2007).

1.1.2 Sources and potential exposure of Lead

Lead is the most common of the heavy elements and is widely distributed throughout the environment. It is used in the production of lead acid storage batteries, tetraethyl lead (a gasoline additive), pigments, chemicals and solder. From a drinking water perspective, the almost universal use of lead compounds in plumbing fittings and solder in water distribution systems has an important role. Older distribution systems and plumbing may also be made from lead pipes. Lead is present in tap water as a result of dissolution from natural sources or from household plumbing systems containing lead in pipes, solder or service connections to homes. The relative contribution of drinking water to average daily intake is estimated to be

approximately 10 percent for children and 11 percent for adults. Soils and household dust are significant sources of lead exposure for small children (Health Canada, 1996). Lead can also come from the natural variation such as the explosion of volcanoes and the erosion of soil and rock. In addition, human activities bring about the contamination of lead in the environment such as those in coating, batteries, painting, cosmetic, plastic and printing industries.

Lead can be introduced to human body by exposing into respiratory system and gastrointestinal tract. The consumption of lead contaminated food brings to the lead accumulation in human body. The exposed lead will dissolve in the stomach by hydrochloric acid and some lead chloride can dissolve with water. The dissolved lead can adsorb in Duodenum (5-10 percent) and some lead can be released to large intestine. The exposed lead can distribute and accumulate in the body. The organic lead can not change its form by oxidation, reduction and hydrolysis but it can change the form under the metabolism and binding with glucuronic acid or sulfate. The alkyl leads will oxidize in the liver. The lead adsorbed from intestine can distribute to the liver. Normally the exposed lead can accumulate in liver, kidneys, bone, teeth, brain, lung and spleen. Lead can be released with bile, urine and sweat (ATSDR, 1993).

1.1.3 Toxicity and Health Effect of Lead

Lead is a cumulative general poison with foetuses, infants, young children and pregnant women being most susceptible to adverse health effects. Lead can severely affect the central nervous system. Acute intoxication leads to restlessness, irritability, poor attention span, headaches and loss of memory. Signs of chronic lead toxicity include fatigue, sleeplessness, irritability, headaches, gastrointestinal symptoms and renal disease. Lead also interferes with the activity of several of the major enzymes involved in the biosynthesis of Haemoglobin. Several epidemiological studies have examined the effects of lead exposure on the intellectual abilities and behaviour of young children. Interpretation of these epidemiological data is difficult, and results were inconsistent. However, research on young primates supports the view that lead causes significant behavioral impairment. Lead has been classified as being possibly carcinogenic to humans. The acceptable daily intake (ADI) for compounds classified in this way is derived on the basis of division of the no-observed-adverse-effect level (NOAEL) or lowest-observed-adverse-effect level (LOAEL) in humans or in animals, taking into account the equivocal

evidence of carcinogenicity. For lead, there is also evidence from human studies that adverse effects other than cancer may occur at very low levels, and that a guideline derived for these effects would be protective for the risk of carcinogenic effects. The World Health Organization established a provisional tolerable weekly intake (PTWI) for lead for children of 25 μg kg^{-1}, equivalent to an ADI of approximately 3.5 μg kg^{-1} per day. This provisional tolerable weekly intake (PTWI) was established on the premise that lead is a cumulative poison and that there should be no increase in the body burden of lead from any source, thus avoiding the possibility of adverse biochemical and neurobehavioral effects in infants and young children. It was based on metabolic studies in infants showing that a mean daily lead intake of 3 to 4 μg kg^{-1} was a NOAEL and was not associated with an increase in blood lead levels or in the body burden of lead, whereas a daily intake of 5 μg kg^{-1} or more resulted in lead retention. An unusually small uncertainty factor (less than 2) reflected the conservatism of the end-point, the quality of the metabolic data and use of one of the most susceptible groups in the population. The Maximum Acceptable Concentration (MAC) for lead in drinking water is derived from the ADI, taking into account the average body weight of a two-year-old child, the proportion of total daily intake allocated to drinking water (intake of lead from sources other than water has decreased substantially over the last few years because of the phase-down of the use of lead-soldered cans in the food industry and the phase-out of lead additives in gasoline) and the average daily water consumption for a two-year-old child. The MAC calculated in this manner is approximately 0.008 mg L^{-1}. The practical quantitation limit (PQL) for routine analysis of lead in drinking water is 1 to 10 μg L^{-1}, depending on the presence of other compounds in the water supply. Because the MAC should be measurable and achievable at reasonable cost, the MAC selected for lead in drinking water is 0.010 mg L^{-1}, based on this limit. Because the MAC for lead is based on chronic effects, it is intended to apply to average concentrations in water consumed for extended periods; short-term consumption of water containing lead at concentrations above the MAC does not necessarily pose undue risk to health. In order to minimize exposure to lead introduced into drinking water from plumbing systems, it is also recommended that only the cold water supply be used, after an appropriate period of flushing to rid the system of standing water, for analytical sampling, drinking, beverage preparation and cooking (Health Canada, 1996).

The toxicity of lead after exposure at high level can affect human body in many ways. Many symptoms occurred such as appetite, nausea, vomit, thirsty, the sweet taste in the mouth, headache, stomachache, diarrhea, tiredness and unconsciousness. Long-term exposure of lead decreases performance function of the nervous system. It may also cause weakness in fingers, wrists or ankles. Lead exposure also causes small increase in blood pressure, anemia and severely damage the brain and kidney. EPA has also determined that lead is human carcinogenic (ATSDR, 2005). The lead level in blood and corresponding human health effect are presented in Table 1-3.

Table 1-3 Lead level in blood and corresponding human health effect

Lead level in blood ($\mu g\ dL^{-1}$)	**Health effect**
25	- Inhibition of ALAD enzyme
40	- Zinc protoporphyrin (ZPP) level high; nervous and renal system dysfunction.
50	- Hemoglobin produces system dysfunction.
60	- Severe stomach-ache (colic pain)
70	- Anemia
80	- Duramater inflammation in children.
100	- Duramater inflammation in adult.

Source: (Daecharat, 2002)**.**

The World Health Organization have been established the maximum allowable of the heavy metal contaminated levels in drinking water for the consumer safety on the announcement of the Guideline for Drink Water Quality (WHO 2006), which the contaminated levels are listed in Table 1-4.

Table 1-4 The acceptance level of heavy metals contamination in drinking water

Metals	Level (μg g^{-1})
Cadmium (Cd)	3
Copper (Cu)	2000
Lead (Pb)	10
Mercury (Hg)	6
Arsenic (As)	10
Manganese (Mn)	400
Chromium (Cr)	50
Nickel (Ni)	70

Source: (WHO, 2006).

Lead was potentially accumulated in water and transferred to human through the water consumption. The study of lead contamination in tap water is an intensive point due to the highly toxicity of metals. Because even low concentration of lead can cause serious toxic effects to human, the analytical method becomes significant and then the awareness amount of the lead concentration has been emphasized.

1.1.4 Instrumentation analysis method of determining lead in tap water

The contamination of lead in tap water was found to be at the trace levels (Spataru, 2006), so the sensitive instrument techniques were required. Electrothermal atomic absorption spectrometry, atomic absorption spectroscopy and inductively coupled plasma mass spectrometry usually have enough sensitivity to allow the determination of this element in these samples. Anodic stripping voltammetry (ASV) is one of the most suitable methods for the determination of lead at low concentrations in water samples owing to its inherent high sensitivity, specificity and favorable detection limits, minimum need for sample preparation (Acar, 2001).

In this research, a AUTOLAB PGSTAT 100 (Metrohm, Switzerland), 663 VA stand (Metrohm, Switzerland), and a GPES-μAutolab software were used. The electrochemical cell containing BDD electrodes was used as working electrode. Ag/AgCl and Platinum wire (Metrohm, 6.1204.120) were used as the reference and counter electrodes, respectively, for lead determination.

1.2 Basic knowledge of votammetry

Votammetric techniques are based on the recording of the current, i, which flows between the working electrode and an auxiliary electrode, due to the reduction or oxidation of the test element, as function of the potential, E, imposed on the working electrode and expressed with respect to that of a reference electrode. In potentiometry, E = f(t) curves are recorded under controlled current. Working electrode and reference electrode are key components of the voltammetric cells (Buffle, 2005).

1.2.1 Electrode

In all electrochemical experiments, the reactions of interest occur at the surface of the working electrode. Therefore, we are interested in controlling the potential drop across the interface between the surface of the working electrode and the solution (i.e., the interfacial potential). However, it is impossible to control or measure this interfacial potential without placing another electrode in the solution. Thus, two interfacial potentials must be considered, neither of which can be measured independently. Hence, one requirement for this counter electrode is that its interfacial potential remains constant, so that any changes in the cell potential produce identical changes in the working electrode interfacial potential.

An electrode whose potential does not vary with current is referred to an ideal non-polarizable electrode, and is characterized by a vertical region on a current vs. potential plot. However, there is no electrode that behaves in this way (although some approach ideal non-polarizable behavior at low currents). Consequently, the interfacial potential of the counter electrode in the two-electrode system varies as current is passed through the cell. This problem is overcome by using a three-electrode system, in which the functions of the counter electrode are divided into two electrodes; reference and auxiliary electrodes. That is, the potential between the

working and reference electrodes is controlled and the current passes between the working and auxiliary electrodes. The current passing through the reference electrode is further diminished by using a high-input-impedance operational amplifier for the reference electrode input.

The requirements for the counter electrode of the two-electrode system include a high exchange current (fast electron transfer kinetics), very large surface area (to lower the current density) and a high concentration of the species involved in the redox reaction, such that the concentrations are not significantly changed by the passage of a current. One previously widely used reference electrode that fulfills these criteria is the saturated calomel electrode (with a large surface area mercury pool). However, the current passing through the reference electrode in the three-electrode system is many orders of magnitude which is lower than the current that passes through the two-electrode system, the requirements for the reference electrode are less demanding; hence, smaller, more polarizable electrodes can be used.

One aspect that is often overlooked is the variation of the reference electrode potential with temperature. Ideally, the potential should be temperature independent; however, it typically changes by 0.5-1.0 mV per degree Celsius. Consequently, precise potential measurements require the use of a constant temperature apparatus. In addition, the temperature at which the measurements were carried should always be reported. The absence of any temperature control limits the accuracy of the measurements to about 5-10 mV (although this level of precision may be acceptable for some experiments). Two widely used aqueous reference electrodes are the silver/silver chloride electrode and the saturated calomel electrode. For Silver/Silver Chloride Reference Electrode, the redox process for this electrode is

$$AgCl + e^- <=> Ag + Cl^- \qquad \text{……(1.1)}$$

This electrode consists of a silver wire, coated with silver chloride, which is immersed in a solution containing chloride ions. The electrode uses an aqueous solution containing 3 M sodium chloride (or potassium chloride); a fritz porous is used for the junction between the reference electrode solution and the sample solution. The potential (E) for any electrode is determined by the Nernst equation, which relates E to the standard potential (E^0) and the activities of the redox components (the standard potential is the potential of the electrode at

unit activity under standard conditions). The Nernst equation for the silver/silver chloride electrode is expressed as follows:

$$E = E^0 + \frac{RT}{nF} \ln \frac{1}{a_{cl^-}} \qquad \text{……(1.2)}$$

(The activities of the solid silver and silver chloride under standard conditions are unity). It is generally more convenient to consider concentrations rather than activities.

These parameters are related by the activity coefficient of the solution, γ:

$$a_{cl^-} = \gamma_{cl^-}[Cl^-] \qquad \text{……(1.3)}$$

The Nernst equation can therefore be rewritten as follows:

$$E = E^{0'} + \frac{RT}{nF} \ln \frac{1}{[Cl^-]} \qquad \text{…… (1.4)}$$

Where $E^{0'}$ is the formal potential and is related to the standard potential by the equation:

$$E^{0'} = E^0 + \frac{RT}{nF} \ln \frac{1}{\gamma_{cl^-}} \qquad \text{…… (1.5)}$$

When quoting a redox potential, it is important to be specific. For example, the standard redox potential (E^0) for the silver/silver chloride redox reaction at 25 ^oC is +0.222 V (vs. NHE), whereas the redox potential (E) for the silver/silver chloride reference electrode at this temperature is +0.196 V (vs. NHE).

The above equations show that variations in the chloride ion concentration in the electrode change the redox potential. Since there is generally a large chloride concentration gradient across the reference electrode porous membrane, there is slow diffusion of chloride ions from the reference electrode solution into the sample solution; that is, the reference potential will gradually change when it is used. There are some precautions that can be taken to minimize this potential drift (BAS Epsilon, 2000).

1.2.2 Electrolyte

The medium must be conducting. This can be achieved using either a molten salt or an electrolyte solution. An electrolyte solution is made by adding an ionic salt to an appropriate solvent. The salt must become fully dissociated in the solvent in order to generate a conducting (i.e., ionic) solution. The electrolyte solution must be able to dissolve the analyte, must be electrochemically inert over a wide potential range (i.e., no current due to electrolyte solution oxidation/reduction), and must also be pure (e.g., the presence of water decreases the size of the potential range). It must also be chemically inert, so that it will not react with any reactive species generated in the experiment (e.g., acetonitrile is nucleophilic, so can react with electrogenerated cations). If the temperature is to be varied, the electrolyte solution must have an appropriate liquid range. Electrolyte solutions can be aqueous or non-aqueous. A wide range of salts can be used for aqueous electrolyte solutions. Since the redox potentials of some compounds are pH sensitive. Therefore the buffered solutions should be used for these compounds. Suitable non-aqueous solvents include acetonitrile, DMF, DMSO, THF, methylene chloride and propylene carbonate. Salts for non-aqueous electrolyte solutions typically consist of a large cation (e.g., tetraalkylammonium cations) and large anions (e.g., hexafluorophosphate, tetrafluoroborate and perchlorate) to ensure full dissociation. Nile blue Perchlorate salts must be handled with care, since they are potentially explosive. Although the addition of fully dissociated salts improves the conductivity of the electrolyte solution, many electrolyte solutions (particularly those based on non-aqueous solvents) have a significant resistance (hundreds of ohms). This leads to a potential drop between the electrodes [termed iR drop - potential = current (i) x solution resistance (R)]. Some of this iR drop can be compensated by a potentiostat and a three-electrode system. However, some resistances (between the working and reference electrodes) remain uncompensated. This uncompensated resistance can be decreased or eliminated by careful cell design (including use of a Luggin capillary), positive feedback iR compensation, or post-run data correction (BAS Epsilon, 2008).

1.2.3 Voltammetric techniques

A large number of voltammetric techniques with variable imposed modulations of potential has been developed, in particular to increase sensitivity. The most important features for environmental applications are shown in the Table 1-5.

Linear sweep voltammetry is a simple technique for stripping the electrode. The potential-time waveform is a linear ramp (Table 1-5a). The potential scan is initiated at the deposition potential in ether a positive direction for ASV or a negative direction for CSV. Then the resulting peak current is measured.

The differential pulse voltammetric waveform (Table 1-5b) consists of a slow linear potential ramp (5-10 mV s^{-1}) upon which small fixed-height potential pulses (5-100 mV) are superimposed every 0.5 to 5 s. A second advantage of the differential pulse technique is the redeposition of metal ion analyte during the rest period between the pulses. As the potential is pulsed through that at which the metal is stripped, the oxidized metal does not have time to diffuse from the electrode surface. At the end of the potential pulse the stripped metal is redeposited into the electrode to be stripped again during the next pulse cycle (as long as the potential ramp is negative of the reduction potential for the metal ion). Shot waiting periods between the pulses result in decreased peak currents from increasing pulsing frequencies and in decreased redeposition. Overall, differential pulse stripping voltammetry is more sensitive than linear sweep stripping voltammetry. The tradeoff is a slower analysis. Used for routine analysis at relatively high concentration (μg L^{-1})

The square wave voltammetry (Table 1-5c) utilizes a square wave potential pulse superimposed upon a staircase ramp. The current is sampled each time the square wave changes polarity. A net current is obtained from the difference between the forward and reverse pulses of a square wave period and it is plotted versus the potential. The high frequency of the square wave requires a high concentration supporting electrode solution to allow the capacitive to decay rapidly. Detection limits of square wave stripping are comparable to differential pulse stripping (Vanysek, 1996).

Anodic (ASV) or Adsorptive stripping techniques (AdSV) as shown in the Table 1-5d and e. In ASV, the metal is preconcentrated at working electrode surface, in a first step, by reduction of its free ion (M^{n+}), at constant potential and the reoxidation peak is measured in a

second step. In AdSV, a ligand is added to complex with M^{n+}, which the M^{n+} is preconcentrated by adsorption at the electrode surface. The reduction peak of this adsorbed complex is measured in a second step (Howard and Stratham, 1993).

Table 1-5 The major voltammetric techniques used for trace-metal analysis and their typical concentration ranges. v = Potential scan rate; ΔE = Pulse amplitude; f = Frequency; t_d = Preconcentration time; i_p = Peak current; E_p = Peak potential

Technique	Imposed function	Recorded function	Conc. range (mole L)
(a) **Linear sweep voltammetry (LSV) (cyclic voltammetry dotted line)**	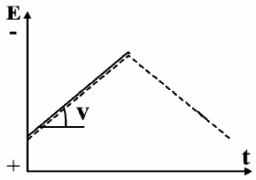	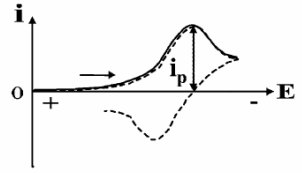	$10^{-2} - 10^{-6}$
(b) **Differential pulse voltammetry (DPV)**	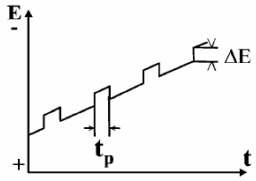	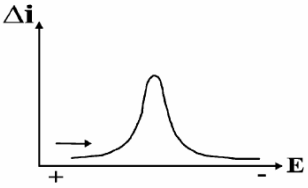	$10^{-4} - 10^{-7}$
(c) **Square wave voltammetry (SWV)**	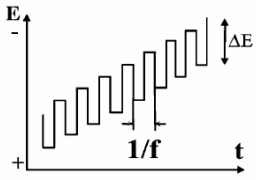	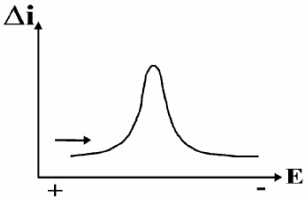	$10^{-4} - 10^{-8}$
(d) **Anodic Stripping Voltammetry (ASV) with linear scan (full line) or modulations (e.g. DP → DPASV or SW → SWASV; dotted line)**	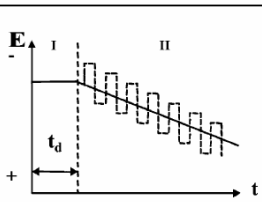	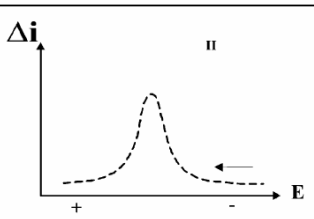	$10^{-6} - 10^{-11}$
(e) **Adsorptive stripping voltammetry (AdSV) (with or without modulation)**	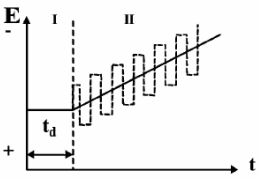	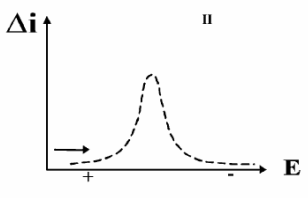	$10^{-6} - 10^{-12}$

reduction at the electrode surface. The capacitive or charging current component, due to electrical charging of electrode double layer, is largely eliminated. This increases the signal to noise ratio

(versus comparable DC methods). Trace analyses of metallic ions and of organic pharmaceutical compounds are common applications for these pulse techniques. The difference in the two techniques is in the detail of the applied potential pulsed waveform as shown in the Table 1-5b and c (www.cypresssystems.com).

Traditionally, voltammograms, in which currents are plotted as a function of applied potential, have been used to describe an electrode reaction at the electrode/electrolyte interface, because the currents are a measure of the electrode reaction kinetics for its activational parameter, overpotential. The current has two components, Faradaic and non-Faradaic, of which the non-Faradaic component is not related to the electrode reaction and is often regarded as noise.

A non-faradaic process involves the accumulation of charges at the metal/solution interface. The structure formed in this process is called the electrical double layer as shown in the Figure 1-1.

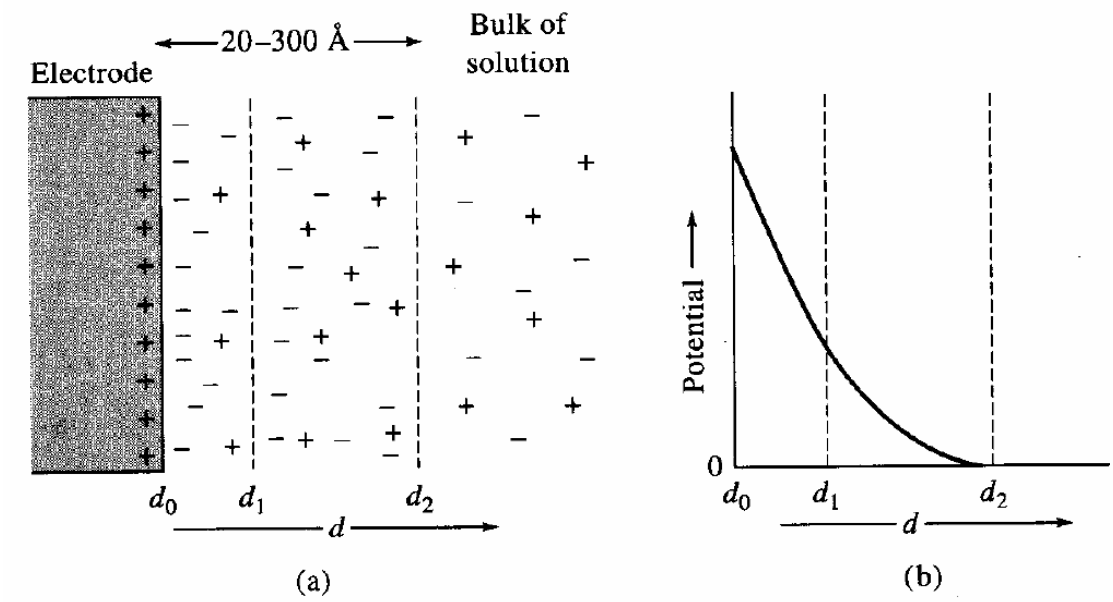

Figure 1-1 Electrical double layer formed at electrode surface as a result of an applied potential

The double layer resembles a capacitor. The double layer capacitance depends on the solution composition of and also depends somewhat on potential applied to the electrode. The specific capacitance of typical electrodes is usually in the range of 5 to 50 μF cm^{-2}. Non-faradaic processes occurring at electrodes cause a flow of non-faradaic currents (also called charging currents). The non-faradaic currents value (i_{nf}) can be calculated from the equation below:

$$i_{nf} = \frac{dQ}{dt} = \frac{d(C_{dl} A \cdot E)}{dt} = C_{dl} E \frac{dA}{dt} + C_{dl} A \frac{dE}{dt} \qquad \text{……(1.6)}$$

Where;

Q = the electrical charge

t = time

A = electrode surface area

E = the electrode potential

C_{dl} = specific double layer capacitance (in above equation we assume that C_{dl} doesn't change significantly with time).

Since all species present in solution may affect the double layer capacitance, the non-faradaic currents are usually non-specific and they are rarely used to provide analytical signals; however, non-faradaic currents contribute to the background noise (i_{nf} ↑, noise ↑, analytical sensitivity ↓). Non-faradaic currents are particularly large when surface of the electrode changes with time (e.g. in the case of the dropping mercury electrode).

Faradaic processes are associated with electron transfer across the interface as shown in the Figure 1-2.

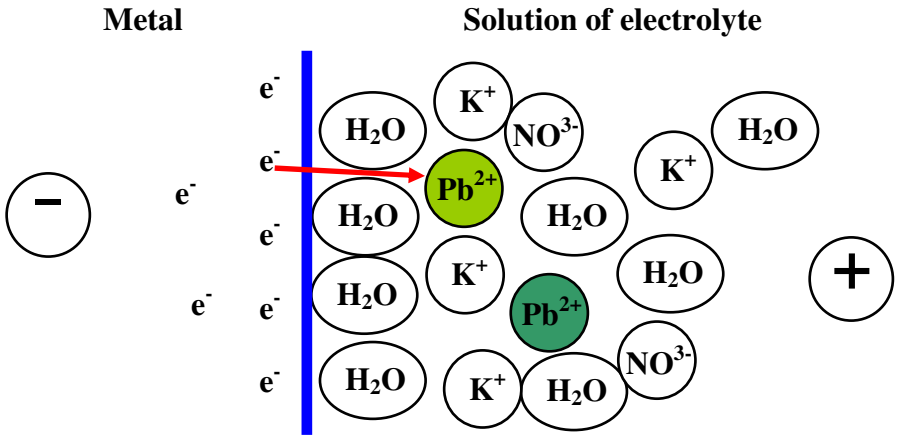

Figure 1-2 A faradaic process leads to reduction or oxidation of species present at the interface

The faradaic currents value (i_f) can be calculated from the equation below:

$$i_f = nFAk \cdot C_{Pb^{2+}} \qquad \text{.....(1.7)}$$

Where;

F = faraday constant

A = interfacial area

k = rate constant

$C_{Pb^{2+}}$ = the concentration of Pb^{2+}

n = valance of the complexes which across the interface (n = 1 in the present analysis)

Electron transfer may occur via overlapping of orbitals (in the case of adsorption), via bridging ligands or via electron tunneling; in any case, a molecule undergoing the electron transfer process must be in near proximity of the electrode surface (usually < 1 nm). Species present in bulk solution may be reduced or oxidized only if they are brought to the electrode surface via a mass transport process. The mass transport was contributions from the diffusion, migration and convection, respectively (http://electrochem.usask.ca).

The word “conventional” in describing approaches to voltammetry is used here to designate well-established techniques or devices, in contrast to more recent developments. With respect to environmental applications, conventional approaches include, in particular, the use of:

- Macro (typically >100 μm) working electrode is widely used rather than micro-working electrode. They mostly include Hg working electrodes (i.e. dropping mercury electrode (DME), hanging mercury-drop electrodes (HMDE), and thin-mercury film electrodes (TMFE) on Pt or glassy carbon), and, in a few cases, solid or chemically modified working electrode.

- Batch cells; although flow-through cells tend to be used more and more. Batch cells are still used routinely; and,

- Potentiostats, designed for laboratory measurements, which have limitations for field applications. As far as techniques are concerned (Table 1-5), cyclic voltammetry is not sensitive enough for environmental analysis but it is useful to optimize analytical conditions. Direct reduction methods, such as differential pulse polarography, differential pulse voltammetry or square wave voltammetry, have been used both in the laboratory and/or on field to measure Mn^{2+}, Fe^{2+} and S^{2-} in anoxic freshwater (Davison, 1993) and in marine sediment pore waters (Rickard *et al.,* 1999 and Taillefert *et al.,* 2000) However, for most trace metals, direct reduction methods are not sensitive enough and techniques with a preconcentration step are required. ASV or AdSV techniques with various modulations (usually differential pulse or square wave; Table 1-5) have been used most widely. AdSV has enabled the application range of voltammetry to be broadened to a large number of elements. However, more works are still needed to evaluate their reliability for routine and multi-element analysis. In contrast, ASV techniques have been used over 30 years for laboratory trace-metal measurements in waters, and routine instruments have been developed.

Although the range of inorganic and organic substances that can be monitored by voltammetry in environmental samples is very broad, analysis of metal ions is still the major type of application. The aforementioned techniques have been applied in the laboratory to the analysis of all the environmentally relevant trace elements [i.e., Pb, Cd, As, Hg, Cr, Al, Cu, Zn, Ni, Co, Se, Bi in waters (Buffle and Tercier-Waeber, 2000 and Van Loon and Barejoot, 1992), Cu, Pb, Cd, Zn, Se, As, Hg in sediments (Locatelli and Torsi, 2002 and Ugo *et al.,* 2002) and Cu, Pb, Cd, Zn, Cr in soils (Kosakova *et al.,* 1996)]. Generally, measurements of total metal concentrations,

usually after sample acidification or pre-treatments of the samples were performed by these conventional approaches. As for all trace-metal analysises, they require strictly clean working practice (Howard and Stratham, 1993).

1.3 Review of literatures

Anodic stripping voltammetry (ASV) is an established method for trace metal ion analysis in contaminated water samples. ASV involves a two-step measurement sequences: (i) electroreducing the ions at a negative potential to form metal deposits on the electrode surface, thereby preconcentrating the analytes, and (ii) selectively electrooxidizing each metal during a slow potential scan toward positive potentials (Swain, 2004). The method, when coupled with an appropriate electrode material, generally provides low detection limits for many metal ions with a wide linear dynamic range and good response precision. Additionally, the method possesses multi-element detection capability and requires instrumentation of low cost and low maintenance. The instrumentation or analysis method is field deployable and requires low power without the need for cooling or ventilation (Swain, 2004).

Carapuca and co-worker (Carapuca *et al.,* 2004) studied on the sensitivity of the anodic stripping voltammetry (ASV) method for the determination of lead at in situ and at ex situ formed thin mercury films (TMFEs). It was concluded that, in acidic solutions (pH 2.5-5.7) and fairly negative deposition potentials, e.g. -1.3 to -1.5V, thiocyanate ion promotes the formation of the mercury film, in respect both to the amount of deposited mercury and to the mercury deposition rate. Also, the mercury coatings produced in thiocyanate solutions are more homogeneous, as depicted by microscopic examinations. In the presence of thiocyanate, there is no obvious advantage of using high concentrations of mercury and/or high deposition times for the in situ and ex situ preparation of the mercury film electrodes. The optimized thin mercury film electrode ex situ prepared in a 5.0 mM thiocyanate solution of pH 3.4 was successfully applied to the ASV determination of lead and copper in acidified seawater (pH 2). The limit of detections (3σ) obtained were 6×10^{-11} M for lead and 2×10^{-10} M for copper for a deposition time of 5 min. Relative standard deviations (RSD)$<$1.2% were obtained for the determinations at nanomolar of concentration level.

Sherigara and co-worker (Sherigara *et al.,* 2007) studied on the deposition and stripping processes of lead, copper and cadmium ions over the wide concentrations range of 1×10^{-5} to 5×10^{-9} M, at mercury film deposited on wax impregnated carbon paste electrode, using cyclic voltammetry, linear sweep anodic stripping voltammetry and differential pulse anodic stripping voltammetry. The carbon paste electrode modified with the mercury film was characterized for its physical and electrochemical properties. The parameters of deposition and stripping processes of the analytes have been investigated using standard solution of the metal ions at various concentrations and different supporting electrolytes and different pH values. The linear sweep anodic stripping has been adopted for the determination of analytes at higher concentrations whereas the analytes at lower concentrations were determined using DPASV. The DPASV behavior for the ions studied dependent on concentrations of the analyte as well as on the time used in the pre-concentration step. The method developed using standard solutions have been successfully applied for the determination of Cu^{2+}, Pb^{2+} and Cd^{2+} in Fin Fish muscles and water samples.

Hg and Hg-coated electrodes are often used for ASV; however, there is a need to develop alternate electrodes that possess the same attractive properties as Hg because of toxicity, stability and volatility issues. For instance, some of the alternate electrodes that have been investigated are Ir, Ag, Bi, Au and graphite.

Kounaves and co-worker (Kounaves *et al.,* 1999) studied on the characterization and separate electrochemical determinations of Cu^{2+} and Hg^{2+} directly on a microlithographically fabricated array of iridium ultramicroelectrodes (Ir-UMEA). Square wave anodic stripping voltammetry was used to optimize experimental parameters such as supporting electrolyte, square-wave frequency, and deposition time and potential. Reproducible stripping peaks were obtained for solutions containing low parts per billion ($\mu g\ L^{-1}$) concentrations of either metal. Excellent linearity was obtained for Cu^{2+} in the range of 20-100 $\mu g\ L^{-1}$ and for Hg^{2+} in the range of 1-10 $\mu g\ L^{-1}$ when the bare iridium substrate was used. Detection limits were calculated to be 1 $\mu g\ L^{-1}$ (0.1 M KNO_3 and 0.1 M $HClO_4$, deposition time 180 s) and 5 $\mu g\ L^{-1}$ (0.1 M H_2SO_4, deposition time 120 s) for Cu^{2+} (S/N) = 3) and 85 ng L^{-1} for Hg^{2+} (deposition time 600 s). The experimental detection limits were determined to be 5 $\mu g\ L^{-1}$ for Cu^{2+} (deposition time 180 s) and 100 ng L^{-1} for Hg^{2+} (deposition time 600 s). Interference studies were performed, and it was

determined that Pb, Zn, and Cd had little or no influence on the copper signal. Tap water and spring water samples were analyzed for copper, and the results were in good agreement with conventional methods.

Kirowa-Eisner and co-worker (Kirowa-Eisner *et al.,* 1999) studied on the determination of sub-nanomolar concentrations of lead by anodic-stripping voltammetry at the silver electrode. The detection limit has been lowered with the use of a method of differences (SWASV) to 0.05 nM (10 ng L^{-1}) at 60 s electrodeposition. Measurements at the sub-nanomolar concentration level by the option of the GPES-μAutolab software. The repeatability of consecutive SWASV runs is good (0.5% at 4 mg L^{-1} for 30 s electrolysis; 2% at 0.4 mg L^{-1} for 60 s electrolysis; 5% at 0.06 mg L^{-1} for 60 s electrolysis). The high stability is attributed to a process that takes place during the electrodeposition step in a two-electrode cell: the silver counter/quasi-reference electrode generates silver ions that codeposit with lead at the Ag-RDE, thus ensuring a continuously renewed surface of the latter. The analysis of lead in rivers and drinking water has been performed. Surfactants distort the SWASV. In order to ensure surfactant-free solutions, the pretreatment of the samples included digestion with HNO_3 and H_2SO_4, evaporation to dryness and heating at 650^{o}C. The detection limit is about 0.5 nM (0.1 mg L^{-1}) and is limited by the purity of the reagents used in the digestion procedure.

Wang and co-worker (Wang *et al.,* 2000) studied on the bismuth-coated carbon electrodes for Anodic Stripping Voltammetry. The bismuth-film electrodes were prepared by adding 400 μg L^{-1} bismuth (Bi^{3+}) directly to the sample solution and simultaneously depositing the bismuth and target metals on the glassy-carbon or carbon-fiber substrate. Stripping voltammetric measurements of microgram per liter levels of cadmium, lead, thallium, and zinc in nondeaerated solutions yielded well-defined peaks, along with a low background, following short deposition periods. Detection limit of 1.1 and 0.3 μg L^{-1} lead were obtained following 2 and 10 min deposition, respectively. Changes in the peak potentials (compared to those observed at mercury electrodes) offer new selectivity dimensions. Scanning electron microscopy sheds useful insights into the different morphologies of the bismuth deposits on the carbon substrates. The in situ bismuth plated electrodes exhibit a wide accessible potential window (-1.2 to -0.2 V) that permits quantitation of most metals measured at mercury electrodes (except of copper, antimony, and bismuth itself). Numerous key experimental variables have been characterized and optimized.

High reproducibility was indicated from the relative standard deviations (2.4 and 4.4%) for 22 repetitive measurements of 80 μg L^{-1} cadmium and lead, respectively. Moreover, Wang and co-worker (Wang *et al.,* 2001) studied the limitations of bismuth film electrodes and concluded that into the attractive stripping voltammetric performance. The results confirm that the stripping performance of the bismuth electrode compares favorably with that of its mercury counterparts. Measurements of trace copper were feasible despite of its positive stripping potential (versus bismuth). Thallium and indium display well-defined peaks over the 20-100 μg L^{-1} range following a 2 min deposition. Most metals, with the exception of copper, (e.g., Pb, Cd, Tl, In) form binary alloys with bismuth, and hence, display well-defined and undistorted peaks. Such sharp peaks result in high resolution (of neighboring signals) and permit convenient multi-elemental measurements down to the low μg L^{-1} level. The bismuth-coated electrode is shown to be prone to errors caused by the formation of Cu-Zn intermetallic compound, that can be circumvented by the addition of gallium, in a manner analogous to mercury film electrodes.

Bonfil and co-worker (Bonfil *et al.,* 1999) studied on a rotating disc gold electrode for the determination of copper in mg L^{-1} and sub-mg L^{-1} concentrations without removal of oxygen by the method of subtractive anodic stripping voltammetry (SASV). The detection limit for a 90 s electrodeposition is 0.2 nM. The reduction and stripping of copper on gold under the SASV conditions were underpotential deposition/dissolution phenomena. A uniformly distributed submonolayer of copper, occupying 0.01±5% of the real surface of the electrode, was formed. Linearity in calibration plot was obtained up to 5% electrode coverage; in terms of the experimental parameters of the deposition step (rate of rotation and time of electrolysis). The bulk and underpotential deposition of Cu^{2+} have been characterized in the supporting electrolyte used (10 mM HNO_3 and 10 mM NaCl). The analysis of copper in drinking and in sea waters has been performed. In addition, Liawruangrath and co-worker (Liawruangrath *et al.,* 2003) studied on the flow injection measurement of lead using mercury-free disposable gold-sputtered screen-printed carbon electrodes (SPCE). Screen-printed sensors are promising devices for disposable, cheap and reliable environmental monitoring. A disposable sputtered gold sensor which allows underpotential analyte preconcentration and avoids the environmental contamination associated with mercury-based sensors. It was used in combination with a specially fabricated thin-layer flow cell for stripping analysis. The sensor consists of a screen-printed strip with three electrodes;

gold coated over carbon-silver ink as the working electrode, silver-silver chloride ink as the pseudo reference electrode, and a carbon-silver ink as the counter electrode. The optimized flow injection (FI) system allows the convenient monitoring of micrograms per litre lead concentrations following short deposition times (detection limit 0.8 mg L^{-1} at 120 s deposition). The method was evaluated by determining lead in spiked drinking and tap water samples; the recoveries of Pb^{2+} were 103% (RSD 2.8%) and 97.9% (RSD 7.1%), n = 5, respectively.

Compton and co-worker (Compton *et al.,* 2004) studied on the Edge Plane Pyrolytic Graphite Electrodes for Stripping Voltammetry comparison with other carbon based electrodes The first examples of using edge plane pyrolytic graphite electrodes for anodic and cathodic stripping voltammetry (ASV and CSV) were presented. Detection limits for silver (based on 3σ) of 8.1 nM and 0.185 nM for 120 s and 300 s accumulation time, respectively, were achievable using the edge plane electrode, which was superior to those observed on glassy carbon, basal plane pyrolytic graphite and boron-doped diamond electrodes. In the second example, a detection limit for manganese of 0.3 μM was possible which was comparable with that achievable with a boron-doped diamond electrode but with an increased sensitivity. The detection limits and sensitivities of the edge plane pyrolytic graphite electrode and boron-doped diamond electrodes were compared. It was found that a lower signal to noise ratio and large potential window for the trace analysis using with boron-doped diamond electrodes were revealed. Thus, the boron-doped diamond electrode was able to replace the edge plane pyrolytic graphite electrode.

The deposition of a metal adlayer on bare solid electrodes is a more complicated process than in the case of forming an Hg amalgam (i.e., deposition of the metal within a volume of Hg). The activity of a deposit depends on the amount deposited, the interaction of the deposit with the electrode, and the distribution on the surface (Swain, 2004). The practical utility of any electrode depends on its effectiveness for detecting metal ions in water samples. For example, Kounaves and Feeney reported on the use of microfabricated Au ultramicroelectrode arrays for the on-site analysis of As^{3+} in groundwater (Kounaves, 2000). The same group reported on the use of a microfabricated array of Ir disks for Cu^{2+} analysis in tap and spring water (Kounaves *et al.*, 1999). Wang et al. reported on the use of Bi-coated, screen-printed carbon electrodes for the determination of Pb^{2+} in drinking water samples (Wang *et al.*, 2000). The working potential

window for Bi is between -1.2 and -0.2 V, and this limits the detection of metal ions to those with more negative redox potentials than -0.2 V.

Several types of carbon electrodes have also been investigated for this assay. The first example is the screen-printed carbon powder electrode as mentioned above. Another example is the determination of Pb^{2+} at a glassy carbon electrode, modified with multi-wall carbon nanotubes (Hu *et al.*, 2003). With the comparison of bare glassy carbon, the modified electrode exhibited increased sensitivity for Pb^{2+}. The linear dynamic range for the detection of Pb^{2+} was from 2×10^{-8} to 1×10^{-5} mol L^{-1} (4.1 μg L^{-1} to 2.1 mg L^{-1}) for deposition (i.e., preconcentration) time of 5 min. These figures of merit were comparable to those obtained with boron-doped diamond thin films using a 3 min deposition time (no stirring) (Swain *et al.*, 2004). Diamond exhibits a background current density that is about one order of magnitude lower than glassy carbon, leading to improved S/B ratios. The use of nitrogen-doped, diamond-like carbon film electrodes for the analysis of Pb^{2+}, Cu^{2+}, and Cd^{2+} was also reported (Zeng *et al.*, 2002). A linear dependence of the Pb^{2+} stripping peak current with concentration from 5×10^{-7} to 2×10^{-6} M (100-400 μg L^{-1}) was observed for a 2 min deposition time (with stirring).

Diamond is an alternate electrode that possesses many of the same attributes as Hg and, therefore, appears to be a viable material for this electroanalytical measurement. The diamond electrodes have been used for both anodic and cathodic stripping voltammetry. For example, high-quality diamond exhibits: (i) large overpotentials for hydrogen evolution and oxygen reduction, (ii) a large overpotential for oxygen evolution (large positive window), (iii) low background current, (iv) resistance to electrode fouling, (v) rapid electrode reaction kinetics for metal deposition and stripping reactions, and (vi) no chemical interaction with metal deposits. The unique properties of diamond make it ideally suited for the ASV analysis of Hg^{2+}, Pb^{2+}, Cd^{2+}, Cu^{2+} and Ag^{+}. Boron-doped diamond has been employed for the detection of Pb^{2+} in river sediments via cathodic stripping voltammetry (Compton *et al.*, 1999). The electrode has also been successfully employed for the detection of Mn^{2+} in tea samples via anodic stripping voltammetry (Farre *et al.*, 2003). Babyak and Smart studies on the electrochemical detection of trace concentrations of Cadmium and Lead with a Boron-Doped Diamond Electrode. The studies including the effect of KCl and KNO_3 electrolytes, interferences and the measurement at parts-per-billion levels of cadmium and lead in river water using square-wave anodic stripping

voltammetry with a boron-doped diamond electrode. Preferred electrolyte was found to be KCl for cadmium, while lead could be measured in either electrolyte. The lowest concentrations included in the linear portion of the calibration plot (5 min deposition time) for cadmium were 10 μg L^{-1} and 50 μg L^{-1} in KCl and KNO_3, respectively, and 10 μg L^{-1} for lead in KNO_3. The presence of either lead or copper suppressed the cadmium stripping peak, but the lead stripping peak was unaffected by cadmium, and enhanced by the addition of copper (Babyak and Smart, 2004). Kruusma and co-worker (Kruusma *et al.*, 2004) studied on the electroanalytical determination of lead by anodic stripping voltammetry at in-situ-formed, bismuth-film-modified, boron-doped diamond electrodes. Detection limits in 0.1 mol L^{-1} nitric acid solution of $9.6x10^{-8}$ mol L^{-1} (0.2 μg L^{-1}) and $1.1x10^{-8}$ mol L^{-1} (2.3 μg L^{-1}) were obtained after 60 and 300 s deposition times, respectively. An acoustically assisted deposition procedure was also investigated and found to result in improved limits of detection of 2.6×10^{-8} mol L^{-1} (5.4 μg L^{-1}) and 8.5×10^{-10} mol L^{-1} (0.18 μg L^{-1}) for 60 and 300 s accumulation times, respectively. Boron-doped nanocrystalline diamond thin-film electrodes were employed for the detection and quantification of Ag^{+}, Cu^{2+}, Pb^{2+}, Cd^{2+} and Zn^{2+} in several contaminated water samples using anodic stripping voltammetric (ASV). Differential pulse voltammetry (DPASV) was used to detect these metal ions in lake water, well water, tap water, wastewater treatment sludge and soil. The electrochemical results were compared with data from inductively coupled plasma mass spectrometric (ICP-MS) and/or atomic absorption spectrometric (AAS) measurements of the same samples. Diamond is shown to function well in this electroanalytical application, providing a wide linear dynamic range, a low limit of quantitation, excellent response precision, and good response accuracy. For the analysis of Pb^{2+}, bare diamond provided a response nearly identical to that obtained with a Hg-coated glassy carbon electrode (Swain *et al.*, 2004). Manivannan studied on the interaction of Pb and Cd during anodic stripping voltammetric analysis at boron-doped diamond electrodes. Highly boron-doped diamond (BDD) films were utilized for simultaneous electrochemical measurement of micromolar-level concentrations of Pb and Cd for the examination of their interactions. Differential pulse anodic stripping voltammetry (DPASV) was used for this detection. This approach can help to understand the possible detection of trace metals at BDD electrodes without the aid of mercury. These metals were found to strip at their characteristic potentials, in solutions containing Cd or Pb alone, and in those containing these metals together. The mixed solutions

(concentration range: 1-5 μM) yielded well-separated stripping peaks for Pb and Cd and the differential stripping peak currents for the respective metals increased linearly with increasing metal concentration. There were mutual interferences due to Pb-Cd interactions, but these can be taken into account with the aid of three-dimensional calibration plots (Manivannan *et al.*, 2004). Compton studied on the cadmium detection via boron-doped diamond electrodes: surfactant inhibited stripping voltammetry. The deposition of cadmium on boron-doped diamond is investigated with square-wave anodic stripping voltammetry. The system was investigated in quiescent conditions, in the presence of an acoustic field and then in the presence of the neutral surfactant Triton® X-100. The effect of optimised insonation was to increase the sensitivity from 0.63 (under silent conditions) to 3.78 μA μM^{-1} and to reduce the limit of detection by an order of magnitude from 10^{-8} to 10^{-9} M. More recently (Compton *et al.*, 2004). Compton and co-worker was studied the detection of lead in a river sediment sample at Boron-doped diamond electrode employing microwave-enhanced anodic stripping voltammetry. The deposition and anodic stripping detection by square-wave voltammetry of Pb^{2+} in a 0.1 M HNO_3 solution is shown to be strongly enhanced by microwave activation at boron-doped diamond electrode. The temperature at the electrode-solution interface is calibrated with reversible redox couple Fe^{3+}/Fe^{2+} (4 mM Fe^{3+}, 4 mM Fe^{2+}) in 0.1 M HNO_3 and a standard addition procedure is developed for the sensitive detection of Pb^{2+} concentrations from 1 μM to 5 μM. The limit of detection by square-wave voltammetry after 20 s deposition time was found to be 0.1 μM and 1.0 μM with microwave activation and without microwave activation, respectively (Compton *et al.*, 2000).

We report presently the analysis of Pb^{2+} in contaminated natural and processed water samples by SWASV, using a polycrystalline boron-doped diamond electrode. This work is our first report on the use of diamond for metal ion analysis in contaminated samples. Good analytical detection figures of merit were observed with limits of quantitation (the minimum actual concentration measured and detected) in the low μg L^{-1} range, good sensitivity, and excellent response precision, and stability. Data for the detection of these metal ions in eleven different tap water samples are presented. The goals of this research were to (i) investigate the feasibility of detecting trace metal ions in contaminated water samples using boron-doped diamond electrode, (ii) obtain a complete set of detection figures of merit for the metal ions

presented in the different contaminated samples, and (iii) validate the method through comparison measurements using standard reference material and or ICP-OES.

1.4 Objectives

1.4.1 To study the optimum condition for determination of trace levels of Pb^{2+} in tap water by stripping voltammetry with BDD electrode.

1.4.2 To determine lead concentration of tap water in Hatyai city.

1.4.3 To assess the Hatyai city tap water quality for consumption in the term of lead concentration.

CHAPTER 2

EXPERIMENTAL

2.1 Chemicals and materials

2.1.1 Standard chemicals

- Cadmium nitrate stock standard solution (1,000 g L^{-1}) (Carlo Erba, Italy)
- Cobalt nitrate stock standard solution (1,000 g L^{-1}) (J.T. Baker, USA)
- Copper nitrate stock standard solution (1,000 g L^{-1}) (Carlo Erba, Italy)
- Iron nitrate stock standard solution (1,000 g L^{-1}) (J.T. Baker, USA)
- Lead nitrate stock standard solution (1,000 g L^{-1}) (Fluka, Switzerland)
- Mercury nitrate stock standard solution (1,000 g L^{-1}) (Merck, Germany)
- Nickel nitrate stock standard solution (1,000 g L^{-1}) (J.T. Baker, USA)
- Zinc nitrate stock standard solution (1,000 g L^{-1}) (J.T. Baker, USA)

2.1.2 NIST reference solution

A reference material® (1640, henceforth referred to as SRM 1640) was procured for testing from the National Institute of Standards and Technology (NIST). The standard contained certified amounts of metals (Table 2-1, 2-2, 2-3).

Table 2-1 Certified Mass Fractions

Element	µg kg^{-1}	Element	µg kg^{-1}
Aluminum	52.0 ± 1.5	Iron	34.3 ± 1.6
Antimony	13.79 ± 0.42	Lead	27.89 ± 0.14
Arsenic	26.67 ± 0.41	Manganese	121.5 ± 1.1
Barium	148.0 ± 2.2	Molybdenum	46.75 ± 0.26
Beryllium	34.94 ± 0.41	Selenium	21.96 ± 0.51
Boron	301.1 ± 6.1	Silver	7.62 ± 0.25

Cadmium	22.79 ± 0.96	Strontium	124.2 ± 0.7
Chromium	38.6 ± 1.6	Vanadium	12.99 ± 0.37
Cobalt	20.28 ± 0.31		

Source: (Taylor, 1995).

Table 2-2 Reference Mass Fractions

Element	**µg kg^{-1}**	**Element**	**mg kg^{-1}**
Copper	85.2 ± 1.2	Calcium	7.045 ± 0.089
Lithium	50.7 ± 1.4	Magnesium	5.819 ± 0.056
Nickel	27.4 ± 0.8	Silicon	4.73 ± 0.12
Potassium	994 ± 27	Sodium	29.35 ± 0.31
Rubidium	2.00 ± 0.02		
Zinc	53.2 ± 1.1		

Source: (Taylor, 1995).

Table 2-3 Information Mass Fraction

Element	**µg kg^{-1}**
Thallium	<0.1

Source: (Taylor, 1995).

According to the supplier, the sample was prepared in the following manner. A sample of about 3500 L of natural (fresh) water was obtained from the United States Geological Survey (USGS) at Clear Creek County Offices in Colorado, USA. It was passed through a 0.1 µm ultrafilter and acidified with nitric acid. Analysis of the water by ICP-MS, before and after the stabilization process, revealed that arsenic, beryllium, cobalt, selenium, and zinc decreased in concentration during the stabilization process. These elements were adjusted to their original

concentrations by the addition of the appropriate salts. The stabilized solution was then pumped through an ultrafilter, past a UV light source (for sterilization purposes), and then to a bottling station. At the bottling station, the containers were first rinsed with the sample and then filled with it for storage (Taylor, 1995). A unit of this SRM consists of approximately 250 mL of natural fresh water, which has been filtered and stabilized with nitric acid at a concentration of 0.5 mol L^{-1}. The solution is preserved in a polyethylene bottle sealed in an aluminized plastic bag to maintain stability (Cellarosi, 2003).

2.1.3 General chemicals and solvents

- Aluminium nitrate (Assay 98.0% min), AR grade (ASP, Australia)
- Ammonium acetate (Assay 97.0% min), AR grade (Ajax Finechem, Australia)
- Calcium nitrate (Assay 99.0% min), AR grade (Ajax Finechem, Australia)
- Manganese chloride (Assay 99.0% min), AR grade (Carlo Erba, Italy)
- Magnesium chloride (Assay 99.0% min), AR grade (Carlo Erba, Italy)
- Nitric acid 69-70% (w /v), AR grade (J.T. Baker, USA.)
- Potassium chloride (Assay 99.8% min), AR grade (Ajax Finechem, Australia)
- Potassium nitrate (Assay 99.5% min), AR grade (Ajax Finechem, Australia)
- Sodium acetate (Assay 99.8% min), AR grade (Ajax Finechem, Australia)
- Sodium chloride (Assay 99.5% min), AR grade (Merck, Germany)
- Sodium nitrate (Assay 99.0% min), AR grade (Ajax Finechem, Australia)
- Ultra pure water resistivity 18 MΩ obtained by passing deionized water through a ELGA water purification system (ELGA, England)

2.1.4 Samples

Tap water samples (Hatyai city, in the South of Thailand, approximately 30 km. from Songkhla province; in February 2008). The samples were collected from eleven regions at Hatyai city (Appendix D).

2.2 Instruments and apparatus

2.2.1 Autolab potentiostat

- AUTOLAB PGSTAT 100 (Metrohm, Switzerland) with GPES-μAutolab software as shown in Figure 2-1.
- Computer system
- IME663 interface (Metrohm, Switzerland)
- Nitrogen gas, High purity 99.99%, (TIG, Thailand)
- 663 VA stand (Metrohm, Switzerland)

2.2.2 Inductively couple plasma optical emission spectrometer

- Inductively couple plasma optical emission spectrometer, Optima 4300 DV (Perkin-Elmer, USA)

2.2.3 Electrochemical cell and electrodes (Figure 2-2).

- Ag/AgCl (3 M KCl) served as the reference electrodes (Metrohm, Switzerland)
- Boron-doped diamond electrode (3 mm diameter) as a working electrode (Windsor Scientific Ltd., UK)
- Platinum wire as an auxiliary electrodes (Number 6.1204.120, Metrohm, Switzerland)
- 50 mL of Electrochemical cell (Metrohm, Switzerland)

2.2.4 Apparatus

- General glassware such as volumetric flasks 10, 25, 50, 100, 250, 500, 1000 mL; Beakers 50, 100, 500, 1000 mL
- Hotplate EGO Model 14.12871.301 (CDR Technical Services Limited, Germany)
- Microbalance Model TC-254 (Denver Instrument, USA)
- Microlitre pipette model: SL200 (20-200 μL) (Rainin, USA)
- Microlitre pipette model: SL1000 (100-1000 μL) (Rainin, USA)
- pH meter Model 225 (Denver Instrument, USA)
- pH meter Model pHscan3 (Eutech Instrument, Netherlands)

- Polyethylene bottles
- Polypropylene bottles
- Tissue paper (Kimberly-Clark, Thailand)

2.2.5 Materials

- Alumina powder 0.05 micron diameter (Buehler, USA)
- Refill Black Ink for Hewlett Packard HPc8727/6656 (NEOINK, USA)
- Solder Wire Alloy Tin/Lead (60/40) 1.2 mm diameter (Ultracore, USA)

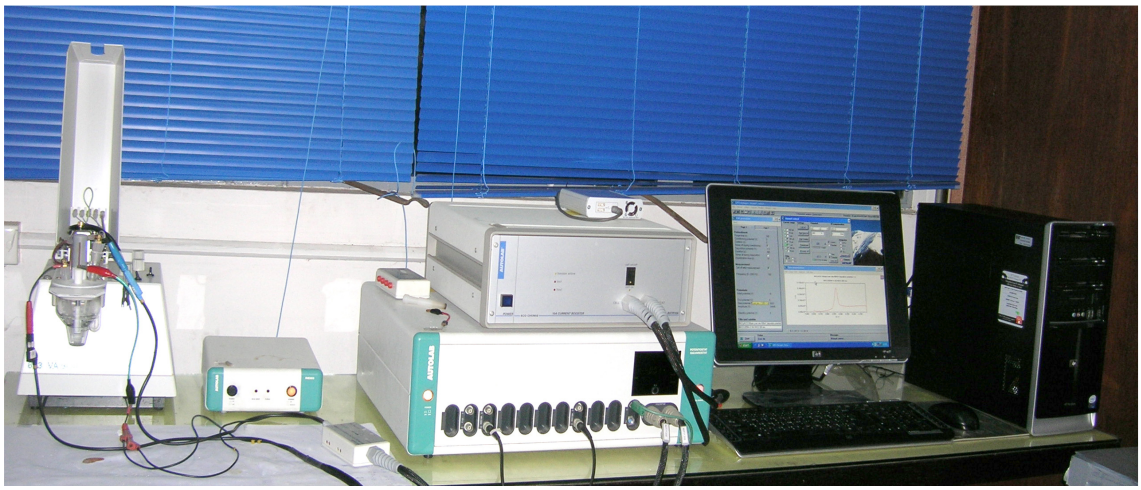

Figure 2-1 AUTOLAB PGSTAT 100 (Metrohm, Switzerland)

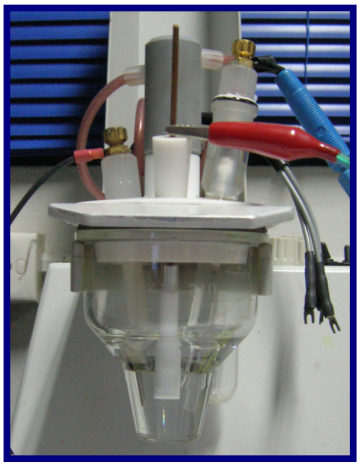

BDD (Working electrode)	Platinum wire (Auxiliary electrode)	Ag/AgCl (3 M KCl) (Reference electrode)

Figure 2-2 Electrochemical cell and electrodes

2.3 Methodology

2.3.1 Preparation of stock standard solutions

Stock standard solution of 1,000 µg L^{-1} Pb was prepared by using 1,000 mg L^{-1} Pb standard solution and diluted for the corresponding stock solutions.

2.3.2 Preparation of glassware and plasticware

The glassware and plasticware were soaked in 10% (v/v) nitric acid for overnight, and then rinsed at least three times with ultra pure water (Farghaly, 2003).

2.3.3 Working electrode preparation

The BDD electrode was polished at the beginning of the experiments with 0.05 micron diameter alumina powder (Buehler, USA) and was rinsed thoroughly with ultra pure water to obtain a clean, renewed electrode surface. The electrode was connected to the potentiostat and placed in ultra pure water; a constant potential of 600 mV for 120s after completion of the anodic sweep to fully oxidize all metal deposits prior to the next measurement. The electrochemical pre-treatment was repeated daily. The polishing was reformed only when the contamination of the

electrode surface was suspected (Swain, 2004). However, an electrode used in untreated tap waters may need frequent polishing. Whenever the proper functioning of the electrode deteriorated, the treatment with the alumina was repeated. In previous work (Kirowa-Eisner, 1997), a stable background and a stable response were obtained after a series of about 20 anodic stripping runs in the supporting electrolyte that was carry out under conditions typical for the determination of lead with 30 s deposition time.

2.3.4 Reference electrode

The porous position should be immersed in a 3 M aqueous sodium chloride solution (or potassium chloride). The reference electrode should also be removed from the electrochemical cell and stored in this solution between experiments (this is particularly important when using non-aqueous solvent systems). Occasionally, air bubbles will form in the solution next to the porous point; these should be removed by gently flicking the end of the electrode (BAS Epsilon, 2000).

2.3.5 Optimization of operating conditions

The optimization was carried out by varying the required parameters and keeping other parameters constant. The optimum value was then used for all experiments. The optimization tests were carried out by using 20.0 μg L^{-1} Lead stock solution. The following parameters for AUTOLAB PGSTAT 100 with GPES-μAutolab software were summarized in Table 2-4.

Table 2-4 Optimized operating conditions for AUTOLAB PGSTAT 100

Parameters	Optimum conditions
Signal	SWASV
Purge times (s)	≥300
Stirring	2000 rpm
Nitric concentration (M)	0.05

Electrolyte Type	KNO_3
Electrolyte concentration (M)	0.2
Deposition potential (V)	-1.3
Deposition time (s)	600
Equilibration time (s)	10
Frequency (Hz)	160
Scan rate (mV s^{-1})	1000
Amplitude (mV)	50

2.3.5.1 Signal

Square wave anodic stripping voltammetry (SWASV) was optimized for the determination of Pb in tap water samples. Optimum voltammograms were obtained by applying 7 min of a deposition potential at -1.3 V (vs. Ag/AgCl, 3 M KCl). Voltammetric scan parameters were optimized to obtain maximum sensitivity, retaining good peak resolution, and well discrimination from background. Optimal parameters were: frequency 160 Hz, pulse amplitude 50 mV and scan rate 1000 mV

s^{-1}. The sensitivity of optimized SWASV proved to be more than that of differential pulse anodic stripping voltammetry (DPASV). Samples containing around 5.0 µg L^{-1} Pb^{2+} can be analyzed using 7 min deposition time and the total analysis time using three standard additions is about 2 hr.

2.3.5.2 Purge time

The purgation with inert gas can reduce oxygen on analyte. Oxygen is electroactive, and can be reduced quite easily. Therefore, it must be removed from the solution if the system under study is reducible. Oxygen is typically removed by bubbling an inert gas (e.g., nitrogen or argon) through the solution for about 5 min. If a stationary solution experiment is to be performed, it is important that the stirring is stopped and the solution is allowed to become quiescent before the experiment is started although a blanketing layer of inert gas over the

solution can be maintained during the experiment. The purge time in this study was varied from 60 to 360 s.

2.3.5.3 Stirring

Stirring the solution on the accumulation stage has a significant effect on the current response, since it affects the rate at which electroactive molecules are brought from the bulk solution to the electrode surface (this process is referred to as mass transport). In many voltammetric experiments, there is no stirring, and the only formation of mass transport is diffusion (this gives rise to the tailed peak shape observed in cyclic voltammetry). These are referred to as stationary solution techniques. In other experiments, the solution is stirred. The studies of stirring speed on the accumulation stage were examined in the rage of 0-3000 rpm, in the present of 20.0 μg L^{-1} lead was also investigated.

2.3.5.4 Nitric concentration

Throughout the process, the pH of solution plays an important role because of its effectiveness on electrode surface interaction. This important variable value was studied with 0.2 M KNO_3 (optimum electrolyte) solution with the pH range of 0.89-4.50 (adjusted with nitric acid concentrations from 0.0-0.2 M) with the concentration of 20.0 μg L^{-1} Pb^{2+}. Three replicates were performed for each.

2.3.5.5 Electrolyte

(a) Type of electrolyte solution

The effect of various types of electrolyte on the current of 20.0 μg L^{-1} Pb^{2+} was performed. The operating parameters at the optimum conditions obtained from section 2.3.5 were applied with various types of ionic salt as shown in Table 2-5. The electrolyte yielding high current and good peak shape was selected.

Table 2-5 Electrolytes in the investigation to select the suitable one

No.	Electrolyte
1	KNO_3
2	$NaNO_3$
3	KCl
4	NaCl
5	CH_3COONH_4
6	CH_3COONa

(b) Electrolyte concentration

The concentration of electrolyte was investigated in the range of 0.0 to 0.6 M for KNO_3 with the same procedure and parameters above. The experiment was run three times for each concentration.

2.3.5.6 Deposition potential

To achieve maximum sensitivity in the voltammetric response, first of all instrumental parameters for the deposition potential were examined with standard solution containing 20.0 µg L^{-1} Pb^{2+} and suitable electrolyte solutions. Then the deposition potential was varied from -0.9 to -1.4 V (-0.9, -1.0, -1.1, -1.2, -1.3, -1.4 V) versus silver/silver chloride reference electrode in stirred solution. The stripping voltammogram was recorded in the square wave mode with the same conditions and same parameters in section 2.3.5. Three replicates of square wave mode were performed for each potential.

2.3.5.7 Deposition time

To increase peak current and to improve the sensitivity of the method, the influence of deposition time was investigated. For Pb^{2+} concentration of 20.0 µg L^{-1} and selected electrolyte concentration, deposition time periods between 5-11 min (5, 6, 7, 8, 9, 10, 11 min) were tried with the deposition potential of -1.3 V in stirred solution versus silver/silver chloride

reference electrode. The stripping voltammogram was recorded in the square wave mode with the same conditions and same parameters in section 2.3.5 and three replicates were performed for each time period.

2.3.5.8 Scan rate and step potential

The scan rate is related to step potential of square wave mode. Therefore, when increasing step potential, the scan rate is increased automatically. Then the effects of scan rate and step potential on peak current were studied by varying scan rates the range of 200-1400 mV s^{-1} (the step potential in the range of 1.20-8.85 mV). The concentration of Pb^{2+} used was 20.0 µg L^{-1} in 0.2 M KNO_3 (pH 1.93). The stripping was performed with the optimum conditions as described in section 2.3.5 and three replicates were performed for each.

2.3.5.9 Amplitude

The effect of amplitude on peak current was studied by varying amplitudes in the range of 25-150 mV with 25 mV increment (25, 50, 75, 100, 125, 150 mV). The concentration of Pb^{2+} used was 20.0 µg L^{-1} in 0.2 M KNO_3 (pH 1.26). The stripping peak was performed with the optimum condition in section 2.3.5 and three replicates were performed for each.

2.3.5.10 Equilibration time

The dependence of the anodic peak current on the equilibration time for Pb^{2+} concentrations was studied. The peak current was found to increase with increasing equilibration time, indicating an enhancement of Pb^{2+} uptake at the electrode surface. Normally, the increase in the response current continues to a maximum signal level (presumably corresponding to either saturation or an equilibrium surface coverage).

The influence of equilibration time on peak current was carried out by varying equilibration time in a range of 0-40 s. The dependence of deposition efficiency upon equilibration time was studied with 20.0 µg L^{-1} Pb^{2+} in 0.2 M KNO_3 (pH 1.26). The stripping peak was performed with the optimum condition in section 2.3.5 and three replicates were performed for each.

2.3.6 Analytical performances of ASV methods

2.3.6.1 Linear range

The stock standard solution of Pb^{2+} was diluted with ultra pure water to obtain various concentrations with the range from 2.0 to 40.0 µg L^{-1}. The 25.0 mL of each concentration was analyzed by AUTOLAB PGSTAT 100 at the optimum conditions taken from section 2.3.5. The linear dynamic range was obtained by plotting the current versus the concentration. The linearity of response was evaluated from the correlative coefficient of the linear curve.

2.3.6.2 Limit of detection (LOD)

The limit of detection is defined by IUPAC as the smallest concentration that can be detected with a certainty of more than 95%. Limit of detection for ASV techniques was determined based on $3\sigma/m$ (Coelho *et al.,* 2002) where;

σ = the standard deviation of 10 measurements of blank signal*

m = the slope of the calibration graphs

*Blank signal obtained was the signal of 2.0 µg L^{-1} Pb^{2+} adding in blank solution, due to the fact that no peak appeared at blank solution.

2.3.6.3 Limit of quantification (LOQ)

The limit of quantification is expressed as the smallest concentration that can be quantified with suitable precision and accuracy. Usually the limit of quantification is evaluated as the signal to noise ratio (S/N) that is equivalent to 10 times of the standard deviation of the noise ($S/N=10\sigma$). The determination of the limit of quantification for ASV techniques was studied based on $10\sigma/m$ (Coelho *et al.,* 2002) where;

σ = the standard deviation of 10 measurements of blank signal*

m = the slope of the calibration graphs

* Blank signal obtained was the signal of 2.0 µg L^{-1} Pb^{2+} adding in blank solution, due to the fact that no peak appeared at blank solution.

2.3.6.4 Accuracy

The accuracy of analytical method was assessed from certified reference material. The accuracy of the studied method was performed by analysizing the Standard Reference Material (SRM), Trace Elements in Natural Water (SRM 1640) from the USA. 20.0 mL of standard was diluted to 100.0 mL by using ultra pure water and added 2.02 g KNO_3 electrolyte solution. The stripping peak was performed with the optimum conditions in section 2.3.5 and three replicates were performed for each. The concentration of Pb^{2+} was evaluated by standard addition method using AUTOLAB PGSTAT 100. The results from experimental and certified values were compared and then the percent of the error was examined.

The accuracy term is the measurement of exact value of the analyte concentration or agreement between measured value and certified value or an accepted reference value. Normally, the accuracy value is expressed in terms of relative percent error as follows:

$$\% \text{ Error} = \frac{\left(\text{Measured value} - \text{Real value}\right)}{\text{Real value}} \times 100 \qquad \text{……(2.2)}$$

2.3.6.5 Precision

Precision is the measure of the degree of repeatability of an analytical method under the same condition. Normally it is expressed as a percentage of the relative standard deviation (%RSD) for a statistically significant number of samples. The calculation of %RSD is given as:

$$\%\text{RSD} = \frac{\text{SD}}{\overline{\text{X}}} \times 100 \quad ; \quad \text{SD} = \sqrt{\sum_{i=1}^{n} \frac{\left(x_i - \bar{x}\right)^2}{\left(n-1\right)}} \qquad \text{……(2.1)}$$

Where;

SD = standard deviation

n = total number of values

x_i = each individual value to calculate the mean

$\bar{x}$ = the mean of *n* values

In this study, the precisions were investigated by measuring the degree of repeatability for analyses of lead standard solutions in the concentration of 2.0, 10.0 and 30.0 µg L^{-1}. The experiments for the lead standard solutions were repeated 10 times.

2.3.6.6 Recovery

The terms recovery (R) is used to indicate the yield of an analyte in a extraction stage in an analytical method. Generally, the recovery value is presented as a percent recovery (% R) and can be calculated from the equation below:

$$\% \text{ Recovery} = \frac{\text{Measured value}}{\text{Real value}} \times 100 \qquad \text{……(2.3)}$$

In this study, the % recovery was obtained from tap water sample spiked with 2.0, 5.0, 10.0 and 20.0 µg L^{-1} of Pb^{2+}. The stripping peak was performed with the optimum conditions in section 2.3.5 and three replicates were performed for each.

2.3.7 General procedure for determination of lead

The measurements were carried out in a conventional three-electrode cell, at the room temperature. All SWASV experiments were carried out with an AUTOLAB PGSTAT 100 (Metrohm, Switzerland), 663 VA stand (Metrohm, Switzerland), IME663 interface (Metrohm, Switzerland) and a GPES-µAutolab software. The electrochemical cell containing a BDD electrode as working electrode, Ag/AgCl (3 M KCl) and Platinum wire (Metrohm, Switzerland) as the reference and auxiliary electrodes, respectively was used. For all the stripping voltammetric measurements, a 25 ml aliquot of the analyte was transferred to 50 ml cell. A Denver pH-meter (model 225) was used for the pH measurements and pH was adjusted to ca. 1.26 by adding appropriate amounts of concentrated HNO_3 solution to an electrochemical cell. A certain volume of supporting electrolyte and standard solution of Pb^{2+} were added into the cell. The solution was stirred and deaerated for 5 min and kept quiet for 10 s. The stripping voltammograms in the range of -0.80 to -0.00 V were recorded in the square wave mode, for which the scan rate was 1 V s^{-1},

the pulse amplitude was 50 mV and the duration time was 10 min. The stripping peaks were observed at -0.460 V. All measurements were made at the room temperature (ca. 25-35 ^{o}C).

2.4 Effect of interferences

The effect of various common ions was evaluated with respect to their interferences with the stripping peak of Pb^{2+} by adding foreign ions to 25 mL solution containing 20.0 μg L^{-1} of Pb^{2+}. The chemicals used as interference include $Zn(NO_3)_2$, $Ni(NO_3)_2$, $Fe(NO_3)_2$, $Co(NO_3)_2$, $Cu(NO_3)_2$, $Cd(NO_3)_2$, $Ca(NO_3)_2 \cdot 4H_2O$, $Al(NO_3)_3 \cdot 9H_2O$, $MgCl_2 \cdot 6H_2O$ and $MnCl_2 \cdot 4H_2O$. The stripping was performed with the optimum conditions in section 2.3.5 and three replicates were performed for each.

2.5 Application of this investigation method to tap water samples

2.5.1 Sampling

Tap water samples (Hatyai city, in the South of Thailand, approximately 30 km. from Songkhla; in February 2008) were collected in polyethylene bottles (the polyethylene bottles was cleaned by soaking with a 10% HNO_3 solution overnight, and then rinsing at least three times with ultra pure water). The water samples were taken from the sampling sites around Hatyai city (Appendix D-3) by means of polyethylene bottles with the volume between 1 and 1.5 L. Prior to the actual sampling, the bottle was filled with the tap water and emptied several times. Then, it was left full for about half an hour before being emptied and refilled with a fresh sample. The tap water samples were collected from eleven regions at Hatyai city after 15 min from the opening of the taps (Farghaly, 2003).

2.5.2 Sample pretreatment

The suspended matter was separated from water samples by filtration through Whatman No. 42 filter paper. The filtrate is then acidified to pH 1.26 by the addition of nitric acid. This prevents the adsorption of analyte ions on the walls of the container, and causes dissociation of metal ions from some of the complexes, thereby making these ions available for the analysis. The acidified samples were stored at -4 ^{o}C before being experimented. The digestion step is not

necessary because the tap water samples usually do not have any particulate matter or significant organic content (Farghaly, 2003).

2.5.3 Tap water contaminated with ink preparation

The tap water contaminated with ink was prepared by using 1 ml of refill black Ink for Hewlett Packard diluted with tap water samples from 4th regions at Hatyai city to a final volume of 1L. The water sample was then acidified to pH 1.26 with nitric acid before being analyzed by SWASV.

2.5.4 Tap water contaminated with solder wire preparation

The tap water contaminated with solder wire was prepared by using 10 g of solder wire alloy tin/lead (60/40) 1.2 mm diameter submerged in 1L of tap water samples from 4th regions at Hatyai city for 24 hours (without being acidified with nitric acid). The supernatant was decanted and diluted 5000 fold. The water sample was then acidified to pH 1.26 with nitric acid before being analyzed by SWASV.

CHAPTER 3

RESULTS AND DISCUSSION

The results from the determination of Pb^{2+} in tap water samples carried out by stripping voltammetry with boron-doped diamond (BDD) electrode are as follows:

3.1 Optimization of ASV parameters

3.1.1 Cyclic voltammetry of blank solution at boron-doped diamond (BDD) electrode

Cyclic voltammogram in 0.01 M HNO_3 solution (pH 1.93), as blank solution, was recorded in the potential range from -0.800 to 0.800 V vs Ag/AgCl (3 M KCl) with the scan rate of 50 mV s^{-1}. No significant peak was found, indicating that there were no significant impurities as shown in Figure 3-1.

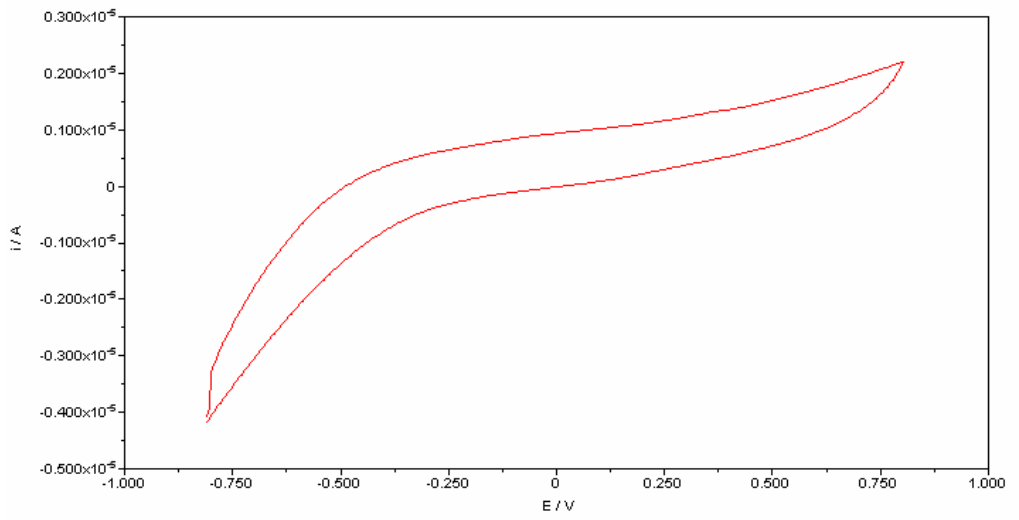

Figure 3-1 Cyclic voltammogram of blank solution recorded with the potential range from -0.800 to 0.800 V vs Ag/AgCl (3 M KCl) with the scan rate of 50 mV s^{-1}

3.1.2 Cyclic voltammetry of Pb^{2+} at boron-doped diamond (BDD) electrode

The cyclic voltammogram of 50.0 mg L^{-1} Pb^{2+} in 0.01 M HNO_3 solution (pH 1.93) as a supporting electrolyte was recorded in the potential range from -0.900 to 0.000 V vs Ag/AgCl (3 M KCl) with the scan rate of 50 mV s^{-1}. The cyclic voltammogram obtained is shown in Figure 3-2. Reduction/oxidation processes were clearly exhibited. The reduction peak appears at -0.659 V vs Ag/AgCl (3 M KCl) with Ipc = 6.526×10^{-6} A. When the scan was reversed, the oxidation peak occurred at -0.420 V vs Ag/AgCl (3 M KCl) with Ipa = 4.082×10^{-5} A. The scan was intended to start from 0.000 V which was high enough to drive the reduction of Pb^{2+} [$Pb^{2+}(aq) + 2e^- \rightarrow Pb^{2+}(s)$]. Lead ion in the solution takes an electron and becomes elemental form (Pb metal) at the surface of working electrode. After that, the oxidation reaction [$Pb(s) \rightarrow Pb^{2+}(aq) + 2e^-$] occurs, i.e. lead atom loses electron and become to $Pb^{2+}(aq)$ back into the solution.

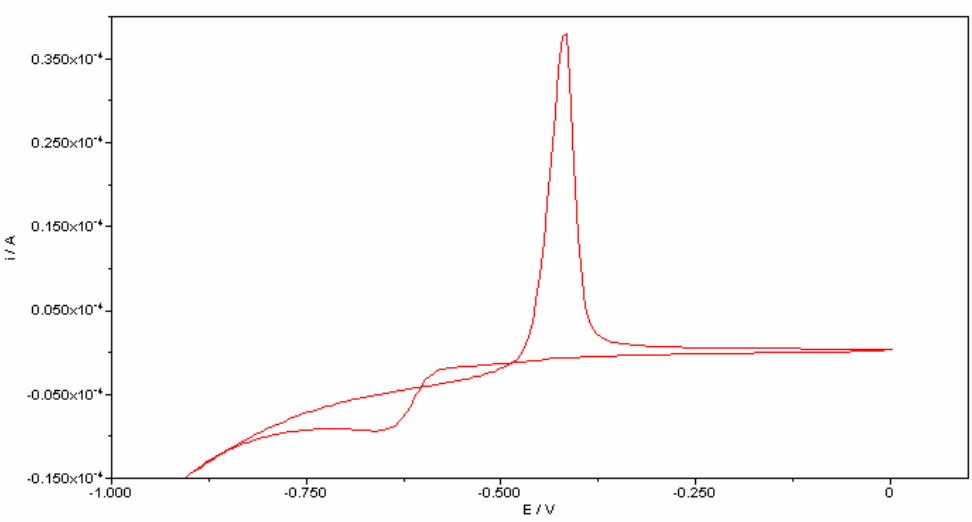

Figure 3-2 Cyclic voltammogram of 50.0 mg L^{-1} Pb^{2+} in 25 mL 0.01 M HNO_3 (pH 1.93), recorded with the potential range from -0.900 to 0.000 V vs Ag/AgCl (3 M KCl) with the scan rate of 50 mV s^{-1}

3.1.3 Operational principle of stripping voltammetric determination of lead ions at the electrode

In the preconcentration step, the accumulated Pb^{2+} is reduced at -1.30 V, i.e. the lead ion is electro-chemically deposited at the electrode surface. The stripping step was then performed with square wave voltammetry. The deposited lead is oxidized, electrochemically stripped off. And the peak current was measured. The mechanism can be represented as follows:

The accumulation stage;

(Pb^{2+})solution + (BDD)surface $\longrightarrow$ $(Pb^{2+}$ - BDD)adsorption

The reduction stage;

$(Pb^{2+}$ - BDD)adsorption + $2e^-$ $\longrightarrow$ (Pb - BDD)adsorption

The stripping stage;

(Pb - BDD)adsorption $\longrightarrow$ (Pb^{2+})solution + (BDD)surface + $2e^-$

3.1.4 Comparison of Pb^{2+} stripping voltammogram between differential pulse and square wave modes

At the beginning, a comparison of Pb^{2+} stripping voltammogram between differential pulse (DPASV) and square wave (SWASV) modes was performed. The stripping peak for 20.0 μg L^{-1} Pb^{2+} in differential pulse mode at boron-doped diamond (BDD) electrode occurs at -0.460 V. It displays 5.27×10^{-7} A of current peak. For the square wave mode, the current of the stripping peak for 20.0 μg L^{-1} Pb^{2+} at -0.425 V is 5.65×10^{-6} A. As shown in Figure 3-3, the current from SWASV is higher than that of DPASV. Consequently, the square wave mode was chosen for all experiments.

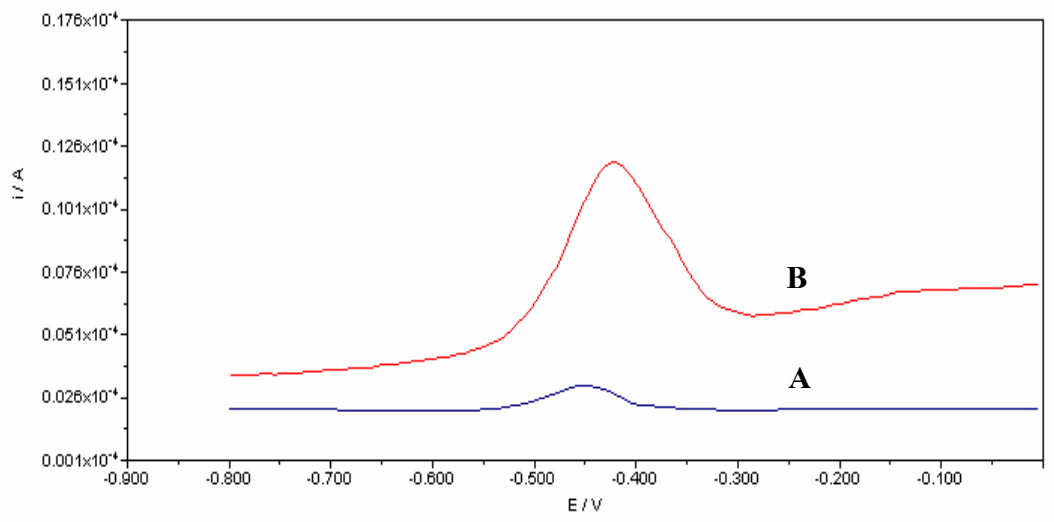

Figure 3-3 Stripping voltammogram of Pb^{2+} in differential pulse mode (**A**) and square wave mode (**B**) of 20.0 µg L^{-1} Pb^{2+} in 25 mL 0.01 M HNO_3 (pH 1.93) and 0.2 M KNO_3 (electrolyte) after deposition time of 7 min at deposition Potential -1.3 V vs Ag/AgCl (3 M KCl)

A comparison of current peak between differential pulse (DPASV) and square wave (SWASV) modes with various lead concentrations was shown in Figure 3-4.

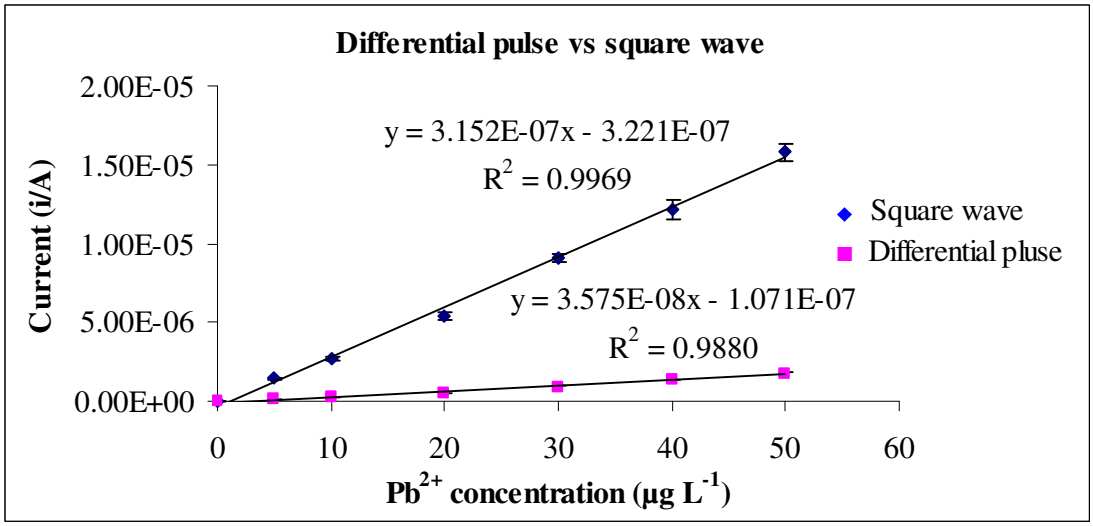

Figure 3-4 A comparison of current peak between differential pulse (DPASV) and square wave (SWASV) modes in various lead concentrations in 25 mL 0.01 M HNO_3 (pH 1.93) and 0.2 M KNO_3 (electrolyte) after deposition

time of 7 min at deposition potential of -1.3 V vs Ag/AgCl (3 M KCl)

Moreover, the sensitivity of peak height is higher than that of the peak area about 10 times (Figure 3-5). As a result, the peak height was chosen for quantifying instrumental response in all experiments.

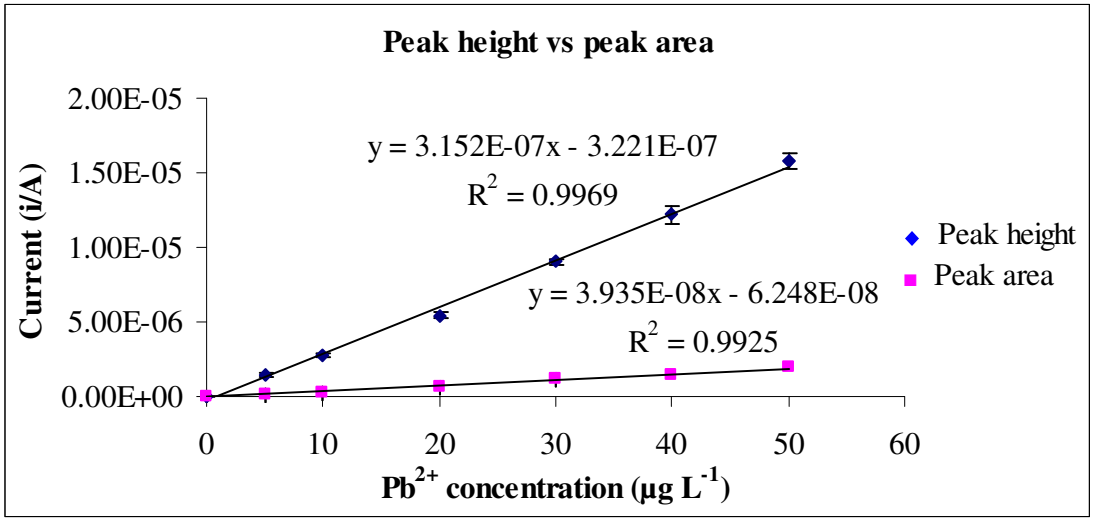

Figure 3-5 A comparison of current peak between peak height and peak area of square wave (SWASV) mode in various lead concentrations in 25 mL 0.01 M HNO_3 (pH 1.93) and 0.2 M KNO_3 (electrolyte) after deposition time of 7 min at deposition potential -1.3 V vs Ag/AgCl (3 M KCl)

3.1.5 Type of electrolyte solutions

Electrolyte solutions are required in controlled potential experiments to decrease the resistance of solution, to eliminate electromigration effects and to maintain a constant ionic strength. An electrolyte solution is made by adding an ionic salt to an appropriate solvent. Pb^{2+} has different electrochemical behaviors in different electrolytes. In the studies, various electrolytes with the concentration of 0.2 M were evaluated for their suitabilities for the Pb^{2+} determination at the electrode surface as shown in Table 3-1 and Figure 3-6. Among the tested ones, 0.2 M KNO_3 was found to provide the best current and peak shape.

Table 3-1 Electrochemical response of lead in various electrolytes

Electrolyte solution (0.2 M)	Current (µA)			Average	SD	%RSD
	I	II	III			
KNO_3	4.960	5.401	5.401	5.254	0.312	5.933
$NaNO_3$	2.714	3.051	3.569	3.111	0.238	7.650
KCl	3.136	2.948	3.958	3.347	0.132	3.957
NaCl	2.474	2.678	2.582	2.578	0.144	5.606
CH_3COONH_4	3.052	2.651	2.970	2.891	0.284	9.811
CH_3COONa	1.376	1.551	1.903	1.610	0.124	7.673

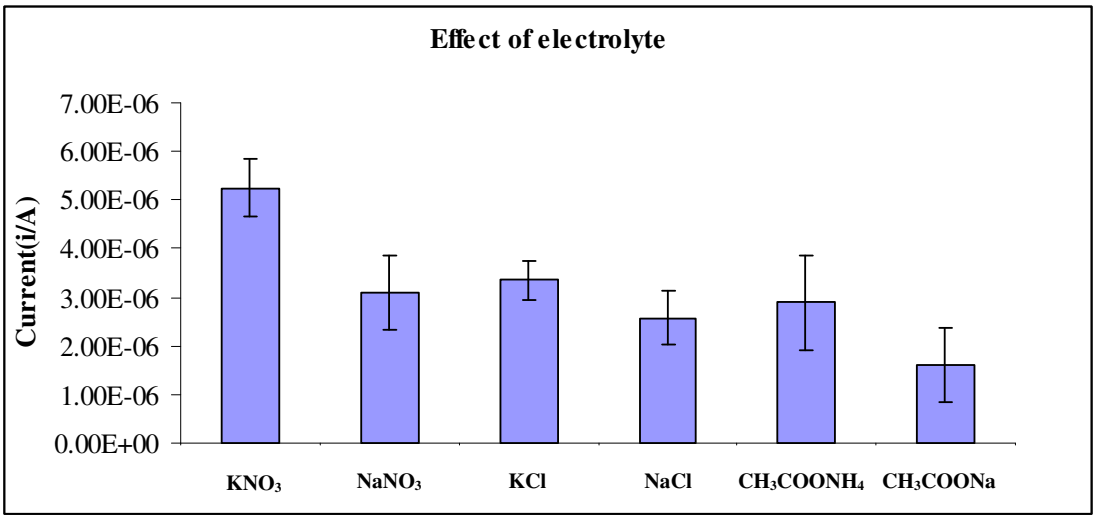

Figure 3-6 Effect of various electrolytes at 0.2 M concentration on the SWASV peak current. Conditions: 20.0 µg L^{-1} Pb^{2+} in 25 mL 0.01 M HNO_3 (pH 1.93); Deposition potential, -1.3 V vs Ag/AgCl; Deposition time, 7 min; pulse amplitude, 75 mV

3.1.6 Electrolyte concentration

Various concentrations were investigated in the range of 0.0 to 0.6 M for KNO_3 with the same procedure and parameters above. The lead detection was accomplished by increasing the concentration of KNO_3 solution from 0.0 to 0.3 M which significantly improves the sensitivity of lead detection. Although 0.3 M KNO_3 electrolyte solution resulted the highest peak current, in this study 0.2 M KNO_3 electrolyte solution was selected because the lower relative standard deviation was yielded at this point, as shown in Table 3-2 and Figure 3-7.

Table 3-2 Electrochemical response of lead in various electrolyte concentrations

KNO_3 Concentration (M)	**Current (μA)**			**Average**	**SD**	**%RSD**
	I	**II**	**III**			
0.0	3.656	3.376	3.422	3.485	0.150	4.309
0.1	4.385	4.313	4.775	4.349	0.051	1.171
0.2	5.377	5.561	5.535	5.491	0.100	1.813
0.3	5.365	5.830	5.658	5.618	0.235	4.185
0.4	4.774	4.936	5.175	4.962	0.202	4.066
0.5	4.708	4.791	5.191	4.750	0.059	1.236
0.6	4.884	4.385	4.543	4.604	0.255	5.539

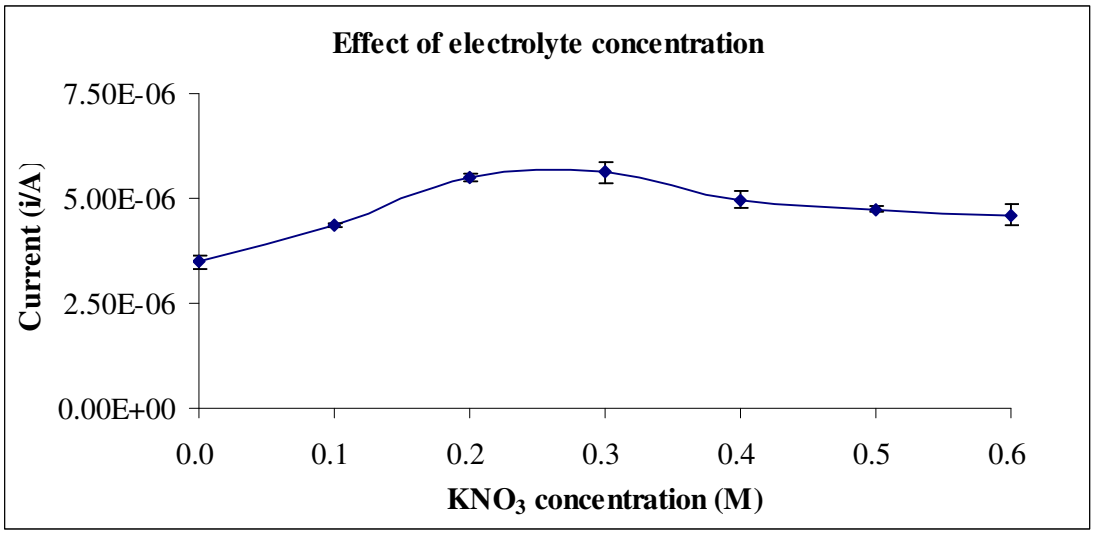

Figure 3-7 Effect of electrolyte (KNO_3) concentrations on the SWASV peak current. Conditions: 20.0 µg L^{-1} Pb^{2+} in 25 mL 0.01 M HNO_3 (pH 1.93); Deposition potential, -1.3 V vs Ag/AgCl; Deposition time, 7 min; pulse amplitude, 75 mV

3.1.7 Effect of scan rate and step potential

The scan rate was varied from 200 to 1400 mV s^{-1}. The scan rate is related with step potential. When the step potential is changed, the scan rate is also altered automatically by the instrument. The scan rate from 200 to 1400 mV s^{-1} is corresponding with the step potential of 1.20-8.85 mV. The peak current increases up to a scan rate of 1000 mV s^{-1}, after which the peak becomes a solid angle with lower stability (greater %RSD value) as shown in Table 3-3 and Figure 3-8, 3-9. Therefore, a scan rate of 1000 mV s^{-1} was chosen for further studies.

Table 3-3 Electrochemical response of lead at various scan rates

Scan rate ($mV\ s^{-1}$)	Step potential (mV)	Current (µA)			Average	SD	%RSD
		I	II	III			
200	1.20	2.353	2.524	2.533	2.470	0.101	4.106
400	2.55	3.450	3.740	3.538	3.576	0.149	4.158
600	3.75	4.832	4.404	4.596	4.611	0.214	4.650
800	4.95	5.084	5.553	5.528	5.388	0.264	4.897
1000	6.30	6.434	5.902	5.957	6.098	0.293	4.798
1200	7.50	7.655	7.382	8.251	7.763	0.444	5.725
1400	8.85	9.426	9.698	10.670	9.931	0.654	6.585

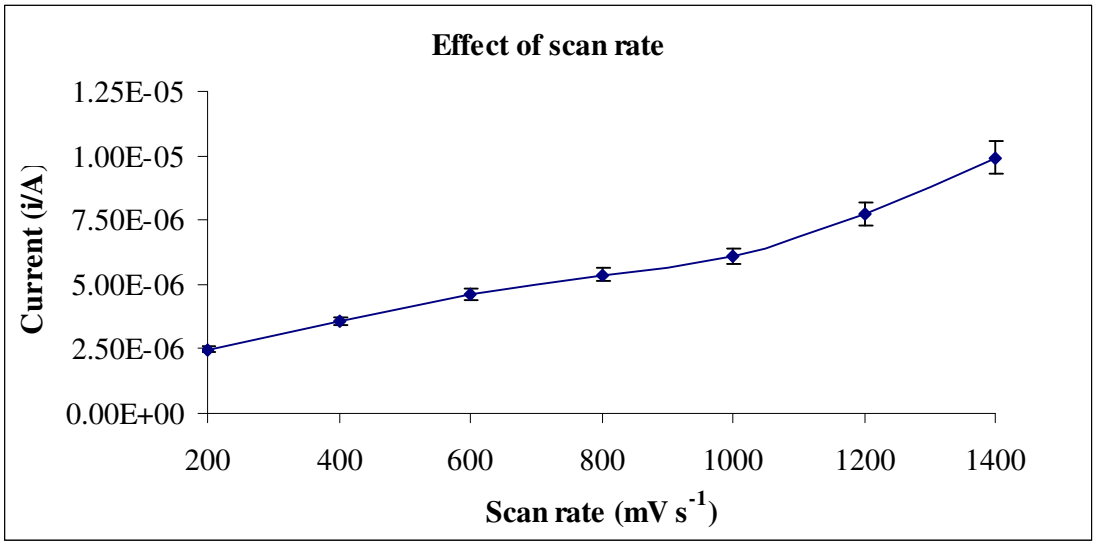

Figure 3-8 Effect of scan rates on the SWASV peak current. Conditions: 20.0 µg L^{-1} Pb^{2+} in 25 mL 0.01 M HNO_3 (pH 1.93) and 0.2 M KNO_3; Deposition potential, -1.3 V vs Ag/AgCl; Deposition time, 7 min; pulse amplitude, 75 mV

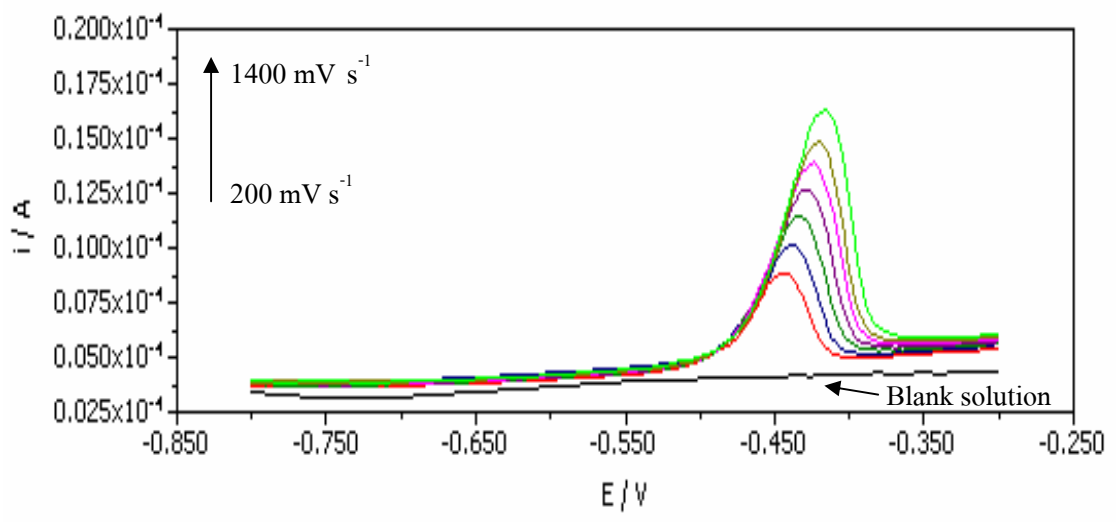

Figure 3-9 Effect of scan rates on the stripping voltammograms. Conditions: 20.0 µg L^{-1} Pb^{2+} in 25 mL 0.01 M HNO_3 (pH 1.93) and 0.2 M KNO_3; Deposition potential, -1.3 V vs Ag/AgCl; Deposition time, 7 min; pulse amplitude, 75 mV

3.1.8 Effect of nitric acid concentration

The influence of pH on determination of Pb^{2+} was also investigated. As the pH values was varied between 0.89 to 4.50 because the concentrations of HNO_3 were adjusted between 0.0 and 0.2 M. It can be seen that the maximum peak current was observed at 0.1 M HNO_3 as shown in Table 3-4 and Figure 3-10. However, 0.05 M HNO_3 was found to yield higher peak current and lower relative standard deviation. Therefore, a 0.05 M nitric solution was used for the preconcentration and voltammetric measurements of Pb^{2+} ions for all subsequent work.

Table 3-4 Electrochemical response of lead in various nitric acid concentrations

Nitric concentration (M)	pH	Current (µA)			Average	SD	%RSD
		I	II	III			
0.000	4.50	2.654	2.872	2.923	2.816	0.143	5.073
0.001	2.71	3.449	3.387	3.735	3.524	0.186	5.268
0.005	2.17	4.550	4.138	4.182	4.290	0.226	5.274
0.010	1.94	4.982	5.261	5.501	5.248	0.260	4.949
0.050	1.26	6.850	6.645	6.342	6.612	2.556	3.865
0.100	1.00	7.148	6.617	6.810	6.858	2.688	3.919
0.150	0.95	4.764	4.856	5.242	4.954	2.536	5.120
0.200	0.89	3.740	3.856	3.431	3.676	2.197	5.977

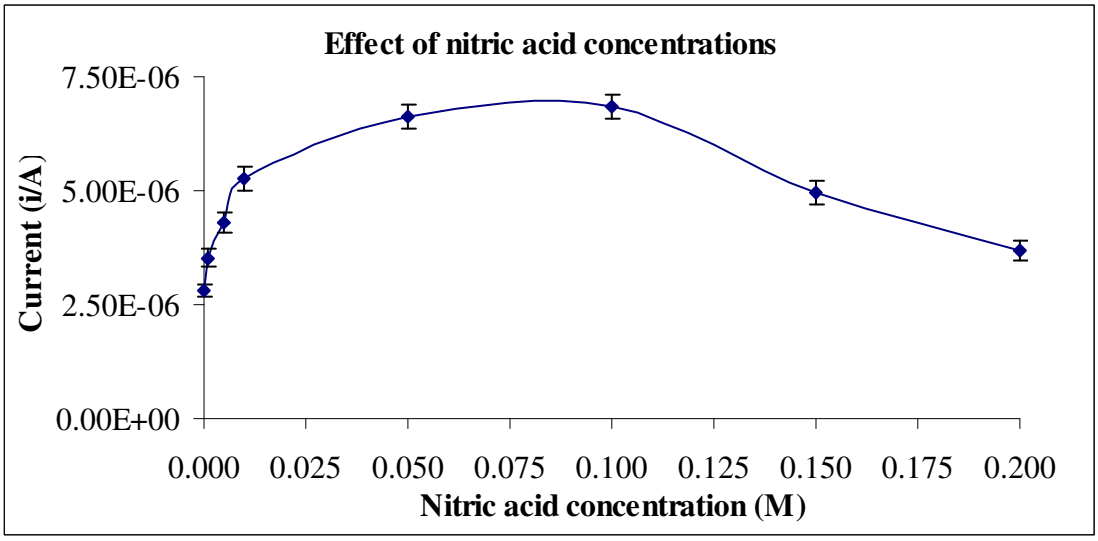

Figure 3-10 Effect of nitric acid concentrations on the SWASV peak currents. Conditions: 20.0 µg L^{-1} Pb^{2+} in 25 mL 0.2 M KNO_3; Deposition potential, -1.3 V vs Ag/AgCl; Deposition time, 7 min; pulse amplitude, 75 mV

3.1.9 Effect of amplitude

Peak currents were obtained with increasing pulse amplitudes (from 25 to 150 mV). A pulse amplitude of 50 mV was chosen for further studies because the current is the most stable at this point, and when the pulse amplitude was increased up to over 50 mV, the shape of stripping peak became apparently asymmetry, as shown in Table 3-5 and Figure 3-11 and 3-12.

Table 3-5 Electrochemical response of lead with various amplitudes

Amplitude (mV)	Current (μA)			Average	SD	%RSD
	I	II	III			
25	5.167	5.000	5.055	5.074	0.085	1.677
50	5.983	5.889	6.060	5.977	0.086	1.433
75	5.708	6.187	6.041	5.979	0.246	4.106
100	6.905	6.418	6.365	6.563	0.298	4.536
125	8.796	9.131	8.687	8.871	0.231	2.608
150	11.580	11.850	12.340	11.923	0.385	3.231

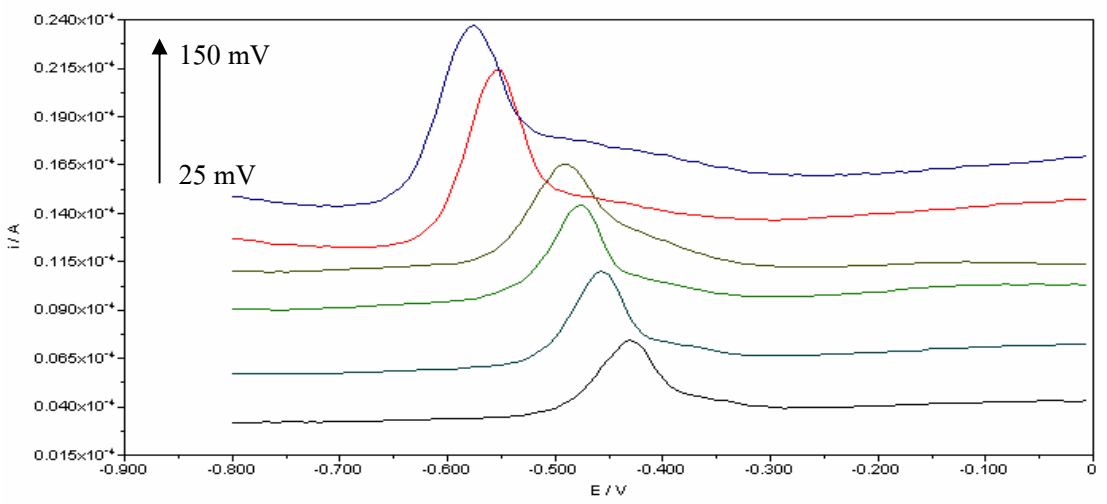

Figure 3-11 Effect of pulse amplitudes on the stripping voltammograms. Conditions: 20.0 µg L^{-1} Pb^{2+} in 25 mL 0.05 M HNO_3 (pH 1.26) and 0.2 M KNO_3; Deposition potential, -1.3 V vs Ag/AgCl; Deposition time, 7 min

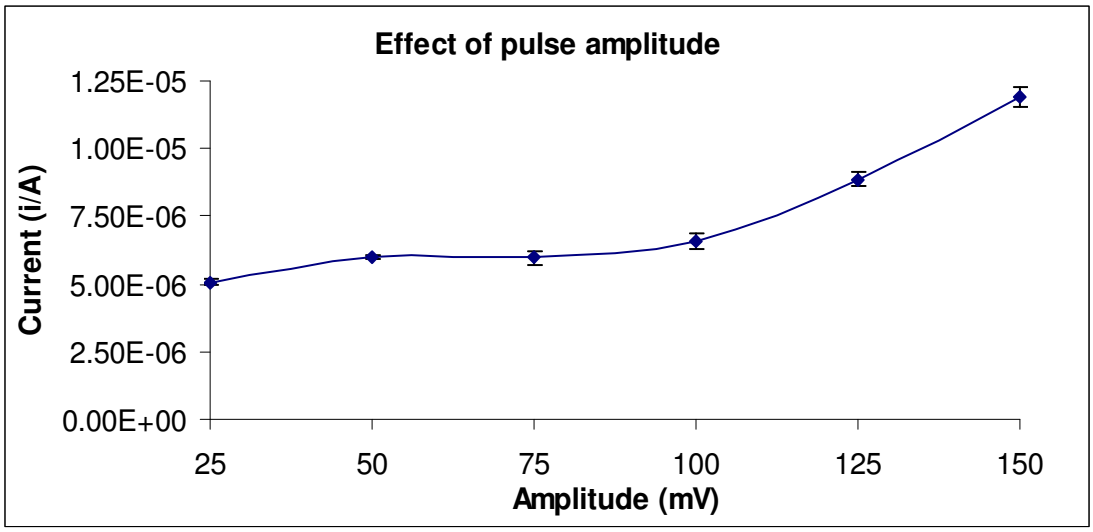

Figure 3-12 Effect of pulse amplitudes on the SWASV peak currents. Conditions: 20.0 µg L^{-1} Pb^{2+} in 25 mL 0.05 M HNO_3 (pH 1.26) and 0.2 M KNO_3; Deposition potential, -1.3 V vs Ag/AgCl; Deposition time, 7 min; pulse amplitude, 75 mV

3.1.10 Effect of nitrogen purge time

Oxygen was removed by bubbling nitrogen gas through the solution for 5 min before the experiment started. After that, the solution needed to have a blanketing layer of inert gas over the solution during the determination. Purge time periods were varied from 60 to 360 s. The optimum peak current was observed 300 s with the highest stability (lower %RSD given). When increasing purged time to over 300 s the peak current was slightly increased, as shown in Table 3-6 and Figure 3-13.

Table 3-6 Electrochemical response of lead with various nitrogen purge time periods

Purge Nitrogen (s)	Current (µA)			Average	SD	%RSD
	I	II	III			
60	0.653	0.592	0.615	0.620	0.031	4.934
120	4.563	4.993	4.640	4.732	0.229	4.845
180	5.666	6.087	6.068	5.940	0.239	4.003
240	6.303	5.924	5.854	6.027	0.242	4.008
300	6.179	6.592	6.646	6.472	0.256	3.947
360	6.180	6.688	6.702	6.523	0.297	4.559

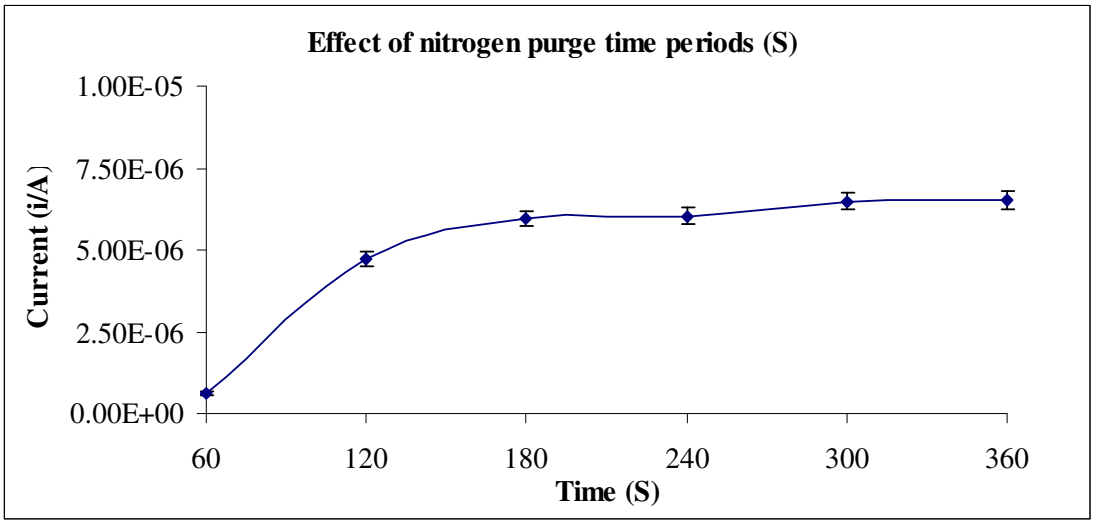

Figure 3-13 Effect of nitrogen purge time periods on the SWASV peak currents. Conditions: 20.0 µg L^{-1} Pb^{2+} in 25 mL 0.05 M HNO_3 (pH 1.26) and 0.2 M KNO_3; Deposition potential, -1.3 V vs Ag/AgCl; Deposition time, 7 min; pulse amplitude, 50 mV

3.1.11 Effect of Stirring speeds

The stirring at the accumulation stage was examined in the range of 0-3000 rpm, with 20.0 µg L^{-1} lead. The results are shown in Table 3-7 and Figure 3-14. The peak current increased slightly with increasing stirring speed. In experiments, therefore, it was established that the stirring speed is not essentially significant for lead detection within the range of lead concentrations under study. Nevertheless the stirring speed to be necessary when determine at low concentration of lead. A 2000 rpm stirring speed was found to yield high peak current and lower relative standard deviation. Therefore, this speed was employed in all subsequent experiments.

Table 3-7 Electrochemical response of lead in various stirring speeds

Stirrer speed (rpm)	Current (μA)			Average	SD	%RSD
	I	II	III			
0	7.099	6.459	6.719	6.759	0.322	4.375
1000	7.096	6.860	6.414	6.790	0.346	3.882
2000	7.423	6.890	7.078	7.130	0.270	3.342
3000	7.731	7.175	7.194	7.367	0.316	4.077

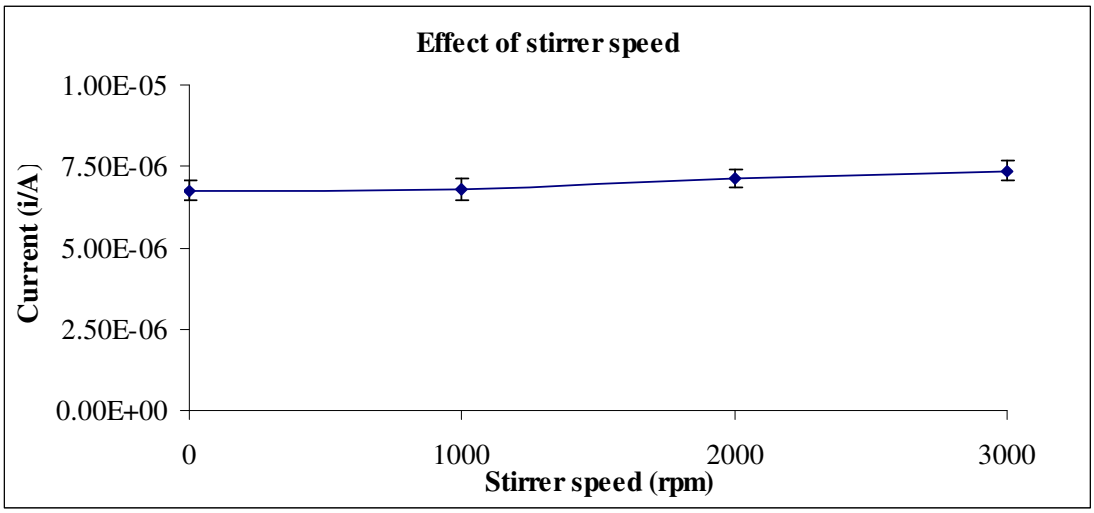

Figure 3-14 Effect of stirring speeds on the SWASV peak currents. Conditions: 20.0 μg L^{-1} Pb^{2+} in 25 mL 0.05 M HNO_3 (pH 1.26) and 0.2 M KNO_3; Deposition potential, -1.3 V vs Ag/AgCl; Deposition time, 7 min; pulse amplitude, 50 mV

3.1.12 Effect of deposition potential

Deposition potential is an important parameter for stripping techniques and it has substantial influence on the sensitivity of the determination. The effect of deposition potentials on the stripping peak currents of Pb^{2+} is shown in Table 3-8 and Figure 3-15. The deposition potential was varied from -0.9 to -1.4 V with a constant deposition time of 420 s. It is obvious

that the negative shifts of electrode potential can improve the oxidation of Pb^{2+} on the surface of electrode and increase the peak current that was increased up to the potential of -1.3 V. Beyond that point the intensity go down. Therefore, the optimum value of the deposition potential used in this work is -1.3 V.

Table 3-8 Electrochemical response of lead in various deposition potentials

Deposition potential (V)	Current (µA)			Average	SD	%RSD
	I	II	III			
-1.4	4.813	4.437	4.504	4.585	0.201	4.375
-1.3	5.831	5.651	6.103	5.862	0.228	3.882
-1.2	4.280	4.434	4.576	4.430	0.148	3.342
-1.1	1.785	1.921	1.799	1.835	0.075	4.077
-1.0	0.239	0.210	0.222	0.224	0.014	6.346
-0.9	ND	ND	ND	-	-	-

ND : non detectable**.**

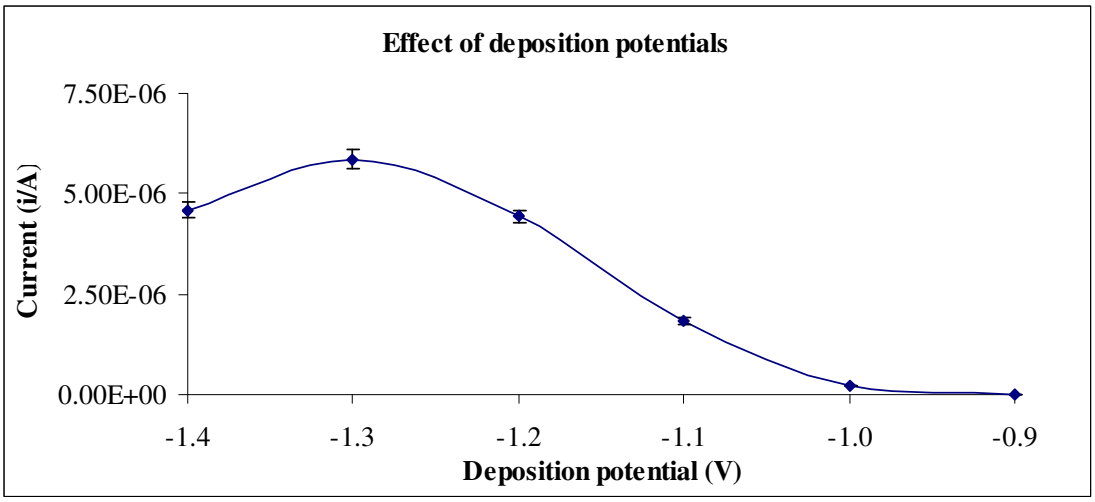

Figure 3-15 Effect of deposition potentials on the SWASV peak currents. Conditions: 20.0 μg L^{-1} Pb^{2+} in 25 mL 0.05 M HNO_3 (pH 1.26) and 0.2 M KNO_3; Deposition potential, -1.3 V vs Ag/AgCl; Deposition time, 7 min; pulse amplitude, 50 mV

3.1.13 Effect of deposition time

The deposition time dependence of the peak heights for lead ion was examined in the range from 300 to 660 s, in the present of 20.0 μg L^{-1} Pb^{2+}. As in Table 3-9 and Figure 3-16, the peak current increased almost linearly with the deposition time. The sensitivity for low levels of this metal can be increased by using a longer deposition time. Hence, a 600 s deposition time was employed in all subsequent experiments. Due to at this deposition time can be evaluating the sufficiently lead concentration for tap water lead contamination assessable. Therefore, is much more than the drinking water contamination standard limited level (10.0 μg L^{-1}), source by World Health Organization (WHO). Then a 600 s deposition time was conduced to be enough for clearly assessable.

Table 3-9 Electrochemical response of lead at various deposition time periods

Deposition time (s)	Current (µA)			Average	SD	%RSD
	I	II	III			
300	1.148	1.107	1.223	1.159	0.059	5.074
360	2.850	3.107	2.924	2.960	0.132	4.469
420	4.252	4.556	4.621	4.476	0.197	4.400
480	5.256	5.306	5.024	5.195	0.150	2.896
540	5.617	5.759	5.998	5.791	0.192	3.325
600	6.085	6.537	6.189	6.270	0.237	3.775
660	6.514	6.608	6.922	6.681	0.214	3.200

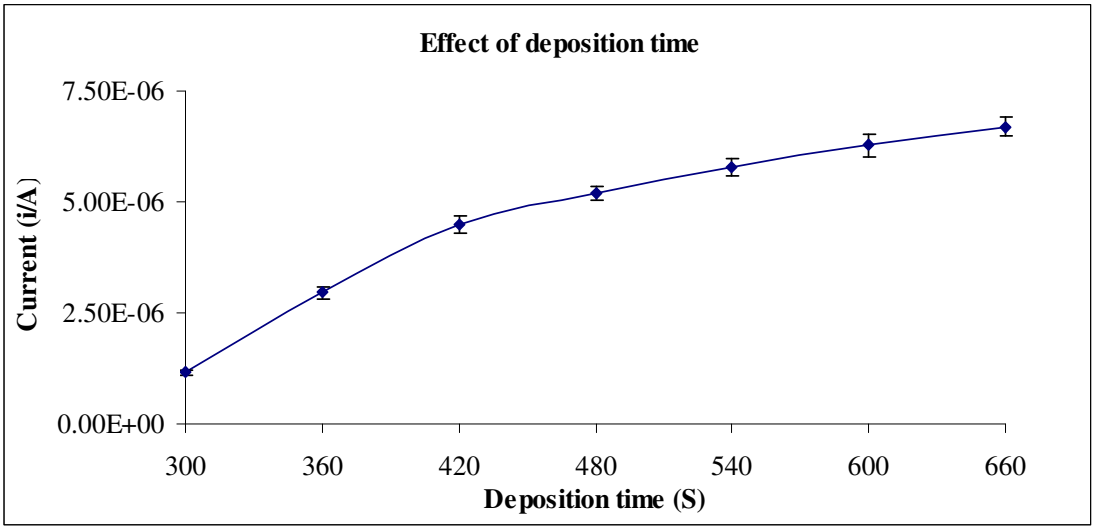

Figure 3-16 Effect of deposition time on the SWASV peak currents. Conditions: 20.0 µg L^{-1} Pb^{2+} in 25 mL 0.05 M HNO_3 (pH 1.26) and 0.2 M KNO_3; Deposition potential, -1.3 V vs Ag/AgCl; pulse amplitude, 50 mV

3.1.14 Effect of equilibration time

It was desirable to employ the shortest equilibration time, compromising with the completion of reaction and the efficiency of deposition. The dependence of deposition efficiency upon equilibration time was studied within a range of 0-40 s as shown in Table 3-10 and Figure 3-17, 3-18. An equilibration time of 10 s was chosen as this is the best time to obtain quantitative extraction. It was found that a equilibration time of 10 s is adequate for lead analysis and was employed in all subsequent experiments.

Table 3-10 Electrochemical response of lead at various equilibration time periods

Equilibration time (s)	Current (μA)			Average	SD	%RSD
	I	II	III			
0	12.320	12.820	13.210	12.783	0.446	3.490
10	12.520	12.670	13.330	12.840	0.431	3.356
20	13.630	15.020	14.020	14.223	0.717	5.041
30	15.510	17.290	16.030	16.277	0.915	5.623
40	17.930	17.290	19.410	18.210	1.087	5.971

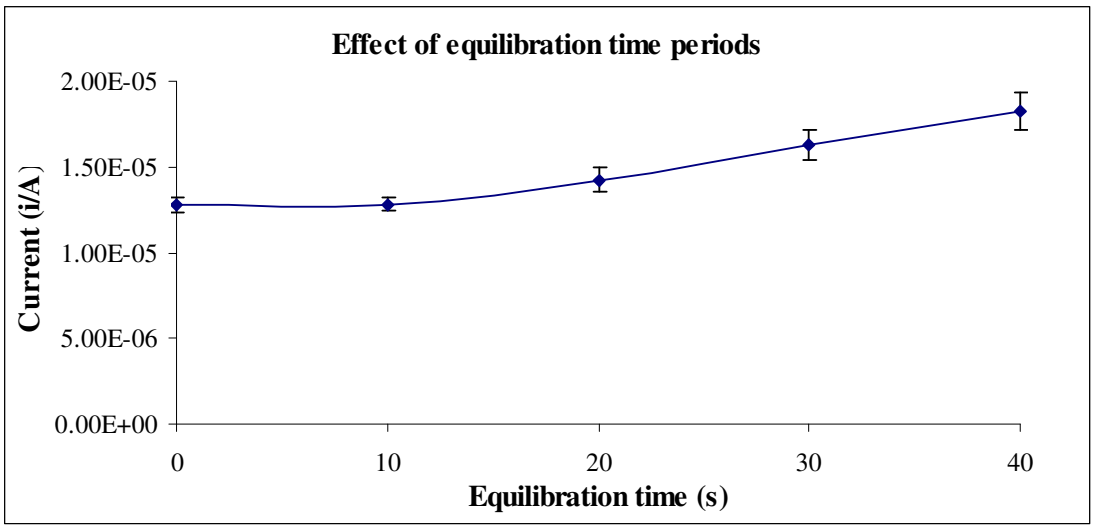

Figure 3-17 Effect of equilibration time periods on the SWASV peak currents. Conditions: 20.0 µg L^{-1} Pb^{2+} in 25 mL 0.05 M HNO_3 (pH 1.26) and 0.2 M KNO_3; Deposition potential, -1.3 V vs Ag/AgCl; pulse amplitude, 50 mV

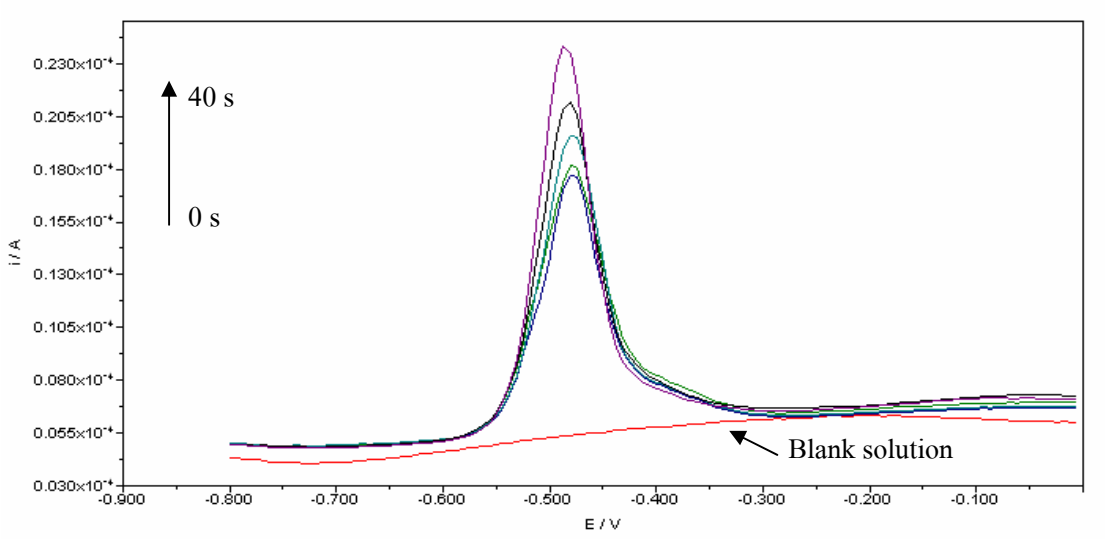

Figure 3-18 Effect of equilibration time periods on the stripping voltammograms. Conditions: 20.0 µg L^{-1} Pb^{2+} in 25 mL 0.05 M HNO_3 (pH 1.26) and 0.2 M KNO_3; Deposition potential, -1.3 V vs Ag/AgCl; pulse amplitude, 50 mV

3.1.15 Linear range

The linear range was determined the ultra pure water containing 25 mL 0.05 M HNO_3 (pH 1.26) and 0.2 M KNO_3 with the deposition potential of -1.3 V and 600 s deposition time (optimum conditions). The linear range is determined by plotting the current versus the concentration of standard solution.

The calibration graphs of lead at various concentrations are shown in Table 3-11 and Figure 3-19, 3-20 and 3-21. It was found that the linear dynamic range was obtained in the concentration range 2.0-30.0 µg L^{-1} Pb^{2+} with the correlation coefficient of 0.9994. At the low lead concentration found to be increase relative standard deviation (%RSD) value, due to the low concentration of lead ions the stirring speed was became importance for efficiency of lead deposition on electrode.

Table 3-11 The current of lead stripping at the different concentrations

Concentration (µg L^{-1})	**Current (µA)**			**Average**	**SD**	**%RSD**
	I	**II**	**III**			
0.0	0	0	0	0	0	0
2.0	1.378	1.250	1.2580	1.295	0.072	5.535
5.0	7.429	7.395	6.835	7.220	0.334	4.620
10.0	18.700	17.570	19.640	18.637	1.036	5.561
20.0	41.250	44.330	45.250	43.610	2.095	4.804
30.0	69.220	70.150	64.260	67.877	3.166	4.665
40.0	112.000	104.200	103.200	106.470	4.818	4.525

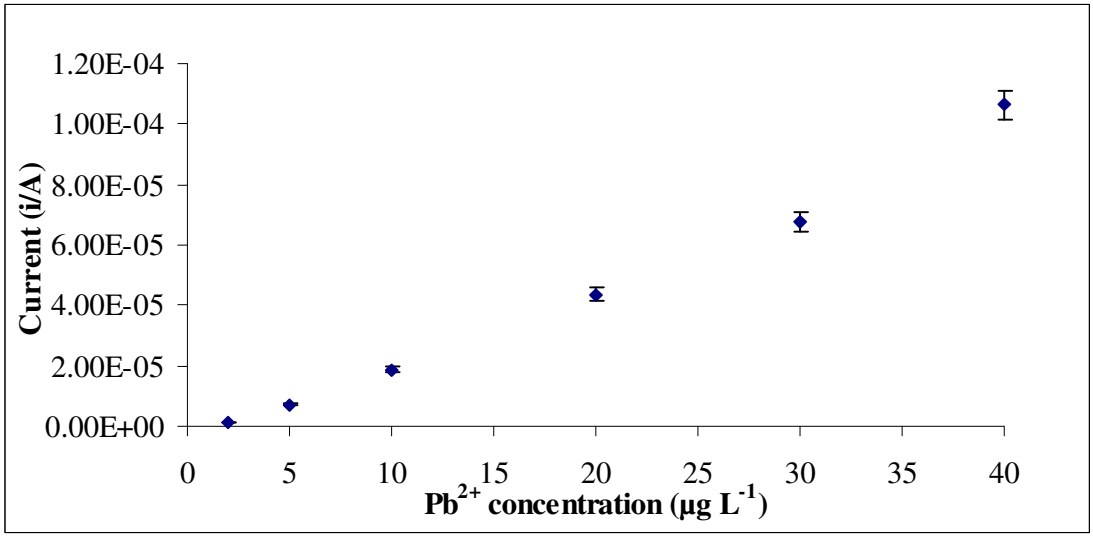

Figure 3-19 The SWASV peak currents at the concentration range from 2.0 to 40.0 µg L^{-1} Pb^{2+}

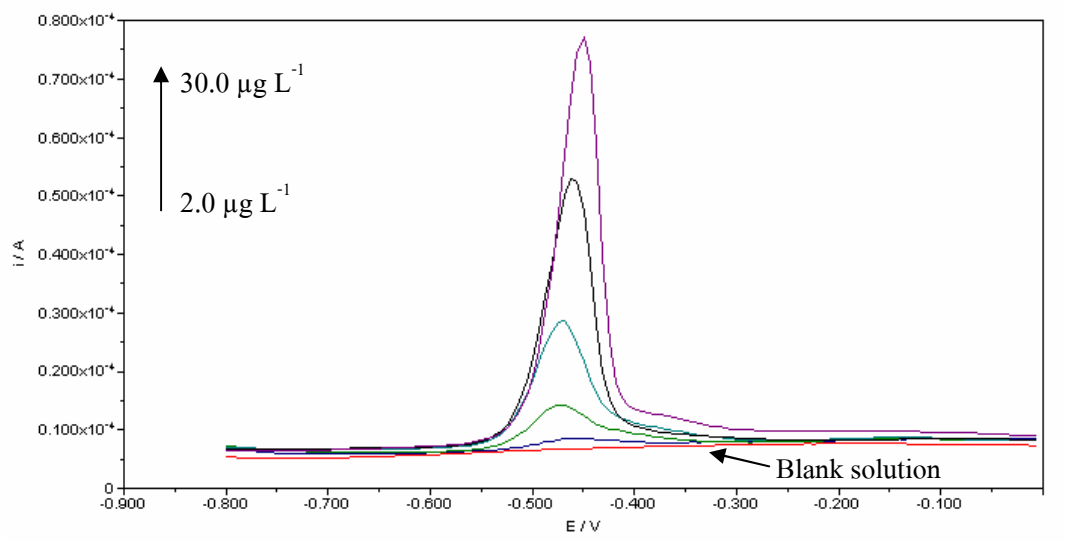

Figure 3-20 The voltammetric curves of 2.0, 5.0, 10.0, 20.0 and 30.0 µg L^{-1} Pb^{2+} for plotting the linear dynamic range

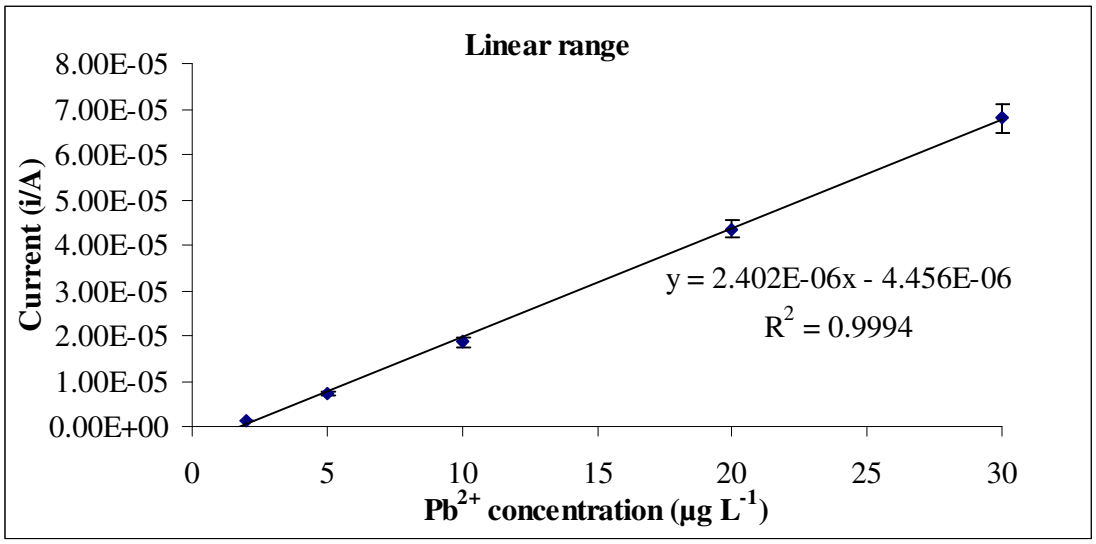

Figure 3-21 The linear dynamic range graph of lead at the different concentrations; 2.0-30.0 µg L^{-1}

3.1.16 Limit of detection (LOD) and limit of quantification (LOQ)

The limit of detection (LOD) and limit of quantification (LOQ) of lead were studied by measuring the current of ten replications of 2.0 µg L^{-1} Pb^{2+}. The limit of detection and limit of quantification were calculated following section 2.3.6.2 and 2.3.6.3, respectively (Coelho *et al.,* 2002).

The current of 2.0 µg L^{-1} Pb^{2+} was carried out for evaluating limit of detection and limit of quantification of lead. When the signal to noise ratio (S/N) is 3, the limit of detection is 0.3 µg L^{-1} and when the signal to noise ratio (S/N) is 10, the limit of quantification is 1.0 µg L^{-1} at the deposition time of 10 min. The slope from calibration graph was obtained as shown in Figure 3-22, and the results are shown in Table 3-12.

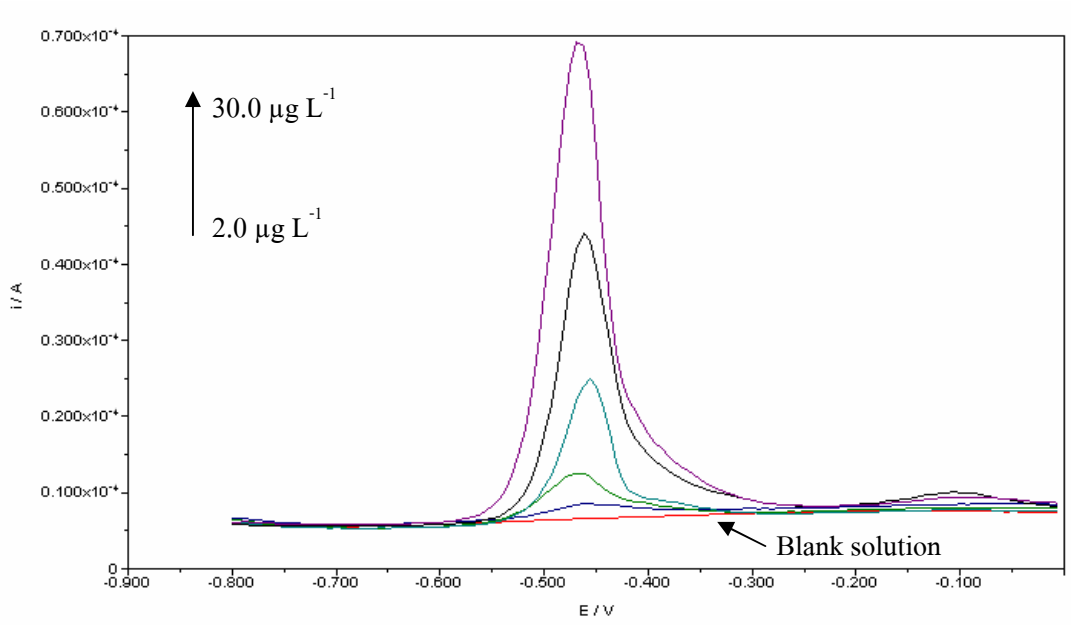

Figure 3-22 The voltammetric curves of 2.0, 5.0, 10.0, 20.0 and 30.0 µg L^{-1} Pb^{2+} for plotting the calibration curve

Table 3-12 Current from 10 replicates of 2.0 µg L^{-1} lead (n = 10)

Replicate	Current (µA)	
1	0.578	
2	0.543	
3	0.547	
4	0.525	
5	0.526	
6	0.533	
7	0.564	
8	0.605	
9	0.598	
10	0.592	
Average	0.561	
SD (σ)	0.030	
%RSD	5.441	
Calibration Slope (m)	0.300	
LOD (3σ/m)	0.3	µg L^{-1}
LOQ (10σ/m)	1.0	µg L^{-1}

3.1.17 Accuracy and precision

The method set up in aqueous reference solutions was applied to standard reference material, natural water SRM 1640 (from the National Institute of Standards and Technology, USA), in order to confirm and verify the applicability of the analytical procedure and to evaluate its accuracy and precision. The determined and certified values were compared by the principle as mentioned in section 2.3.6.4 and 2.3.6.5. The results are shown in Table 3-13, and the voltammograms are shown in Appendix B-1.

Table 3-13 The comparison of the experimental and certified values for lead determination in certified reference materials (n = 3) by the method under investigation

Sample	Concentration of Pb ($\mu g\ kg^{-1}$)		%Error	%Recovery
	Certified value	Determined value		
SRM 1640 (Trace elements in natural water)	27.89 ± 0.14	27.57 ± 0.27 (% RSD = 4.970)	1.16	98.84

Mean ± S.D. (n = 3)

From the results in Table 3-13, the determined concentrations of lead in SRM 1640 from the proposed method were in good agreement with the certified values. The recovery of lead was 98.85%.

In addition, the precision of the proposed method was also evaluated as %RSD of ten replication measurements. The %RSD values obtained from this method were 5.441, 4.576 and 4.238% for lead concentration of 2.0, 10.0 and 30.0 $\mu g\ L^{-1}$, respectively. The results are shown in Table 3-14.

Table 3-14 The currents for evaluating the precision

Replicate	Current (µA)		
	2.0 µg L^{-1}	**10.0 µg L^{-1}**	**30.0 µg L^{-1}**
1	0.578	2.515	7.530
2	0.543	2.708	8.031
3	0.547	2.263	7.556
4	0.525	2.570	8.168
5	0.526	2.604	8.152
6	0.533	2.533	7.905
7	0.564	2.442	8.239
8	0.605	2.573	8.576
9	0.598	2.547	8.437
10	0.592	2.553	8.269
Average	0.561	2.531	8.086
SD	0.030	0.116	0.343
%RSD	5.441	4.576	4.238

3.2 Interferences of some coexisting ions with the determination of lead

The effect of some metal ions was studied following section 2.3.6.6. The results are shown in Table 3-15 and Figure in Appendix A-1 to A-10.

The influence of other ions present in the analyte solution on the current response of Pb^{2+} is shown in Table 3-15 and Figure in Appendix A-1 to A-10. At the coexisting ion concentration that affected on the stripping peak current of Pb^{2+}, there was 5% of peak current allowed to change. Several ions such as Mg^{2+}, Ca^{2+}, Ni^{2+}, Fe^{2+}, Zn^{2+}, Cd^{2+} and Mn^{2+} have only negligible effect on the determination of Pb^{2+}. However, A 20.0 µg L^{-1} of Co^{2+} and Al^{3+} was found

to decrease the determination response significantly. A 20.0 μg L^{-1} of Cu^{2+} interferes significantly by decreasing the Pb^{2+} signal, due to strong competition of copper with lead in the deposition at the electrode. However, the interfering effect of Cu^{2+} can be eliminated by the addition of 0.001 M KCN as the masking reagent (Holgado *et al*., 1995). Furthermore, the influence of weakly interfering ions can easily be eliminated by applying the standard addition method for the evaluation of the concentration of Pb^{2+}.

Table 3-15 Interferences of some metal ions with the determination of 20.0 μg L^{-1} Pb^{2+}

Interfering ions	**Concentration (μg L^{-1})**	**WHO, 1993 recommendation (μg L^{-1})**	**Peak current change (%)**
Ca^{2+}	3000	-	-5.09
Mg^{2+}	1000	-	-6.25
Mn^{2+}	500	100	-5.50
Al^{3+}	20	200	-4.93
Zn^{2+}	100	3000	-5.77
Fe^{2+}	200	300	+5.15
Cu^{2+}	20	1000	-5.80
Co^{2+}	20	-	-5.20
Ni^{2+}	50	20	-5.36
Cd^{2+}	50	3	-5.50

In the general tap water condition, the current of lead with and without coexist ions was no significant difference at the 95% confidential level ($P>0.05$) then the interference of coexist ions does not affect the stripping peak current from the studied method.

3.3 The comparison of the calibration and standard addition method for determination of Pb^{2+} in tap water samples

The experiment was performed to compare the standard methods of calibration and standard addition for determination of Pb^{2+} in tap water samples after 10 min deposition. The results are shown in Table 3-16 and Figure 3-23.

Table 3-16 The comparison of stripping peak current between calibration and standard addition method for Pb^{2+} determination in tap water samples

Pb^{2+} conc. ($\mu g\ L^{-1}$)	Current (µA)							
	Calibration				Standard addition			
	Rep.1	Rep.2	Rep.3	Average	Rep.1	Rep.2	Rep.3	Average
0.0	BDL	BDL	BDL	-	BDL	BDL	BDL	-
2.0	1.428	1.492	1.498	1.473	1.958	1.986	1.845	1.930
5.0	2.744	2.994	2.815	2.851	3.756	3.989	4.026	3.924
10.0	5.777	5.521	5.965	5.754	6.821	7.051	7.268	7.047
20.0	11.870	12.590	12.010	12.160	13.820	14.540	13.830	14.060

BDL: below the detection limit. [compared with the limit of detection (LOD)]

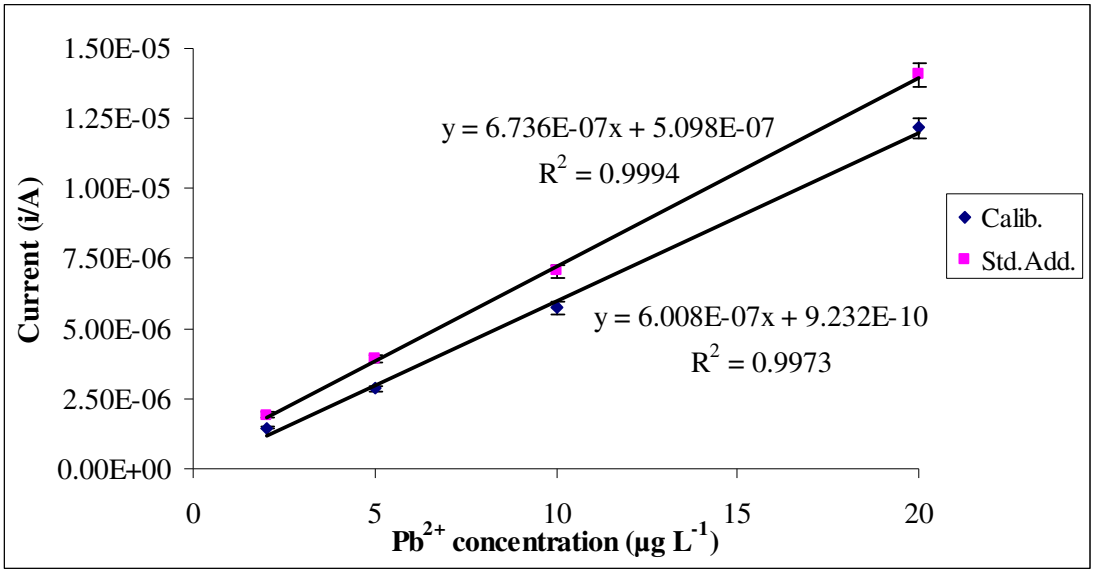

Figure 3-23 The comparison of calibration curve and standard addition curve for Pb^{2+} determination in tap water samples

From the results in Figure 3-23, it can be concluded that the calibration curve and the standard addition curve for Pb^{2+} were not parallel. The slopes of standard addition and calibration curve for Pb^{2+} were compared using two-way ANOVA. From the statistical evaluation in Appendix C-1, it was found that the slopes of both methods were significant difference at the 95% confidence level ($P<0.05$). It suggests that the matrix effect can affect the analysis. Therefore, the standard addition was considered to be more suitable method for Pb^{2+} determination in tap water samples.

3.4 The study of percent recovery of Pb^{2+} in tap water samples

The percent recovery of Pb^{2+} in tap water samples was studied as described in section 2.3.6.6 and the results are shown in Table 3-17. The studied method was applied to the determination of Pb^{2+} in three tap water samples with random selected by SWASV under the optimized conditions using standard addition method. The three samples used were the water from different places in Hatyai city including tap water at 9^{th}, 10^{th} and 11^{th} regions as shown in Appendix D-3. The concentrations of Pb^{2+} in sample were deduced from the stretched range of the regression equation. All of the samples were measured without any further treatment. The

results are listed in Table 3-17. The excellent average recoveries of three water samples suggest that the studied method developed in this work has practical significance and is able to satisfactorily determine of Pb^{2+} in tap water samples.

Table 3-17 Recovery test for the studied method using tap water samples (n = 3) spiked with 2.0, 10.0 and 20.0 µg L^{-1} of Pb^{2+}

Sample	Added Pb^{2+} (µg L^{-1})	Expected Pb^{2+} (µg L^{-1})	Measured Pb^{2+} (µg L^{-1})	%Recovery
Tap water 9th regions	0.0	-	BDL	-
	2.0	-	2.84±0.13	-
	10.0	10.84	10.51±0.35	96.97
	20.0	20.84	20.17±0.28	96.77
Tap water 10th regions	0.0	-	BDL	-
	2.0	-	2.68±0.17	-
	10.0	10.68	10.26±0.62	96.08
	20.0	20.68	21.10±0.67	102.03
Tap water 11th regions	0.0	-	BDL	-
	2.0	-	2.59±0.14	-
	10.0	10.59	10.57±0.44	99.85
	20.0	20.59	20.05±0.42	97.36

Mean ± S.D. (n = 3)

BDL: below the detection limit. [compared with the limit of detection (LOD)]

3.5 Application of the studied method to tap water samples

3.5.1 Determination of Pb^{2+} in tap water samples using the studied method (ASV)

The studied method was applied to the determination of Pb^{2+} in tap water sample from eleven regions at Hatyai city, in the South of Thailand, approx. 30 km. from Songkhla province; in February 2008**.**

The real samples examined here had the pH values summarized in Table 3-18. The displayed natural pH values of tap water samples are higher than 6 thus these samples were analyzed after acidification to pH 1.26 with HNO_3.

Table 3-18 pH values of the tap water sample investigated

Sample	pH
1st regions	6.23
2nd regions	5.90
3rd regions	6.26
4th regions	6.29
5th regions	6.28
6th regions	5.98
7th regions	6.24
8th regions	6.14
9th regions	6.40
10th regions	6.31
11th regions	6.61

A typical stripping voltammogram obtained in tap water sample is shown in Fig. 3-24. The voltammogram shows the oxidation process of Pb^{2+}, the stripping peaks of lead are well shaped and are characterized by stripping peak potential values of -0.460 V.

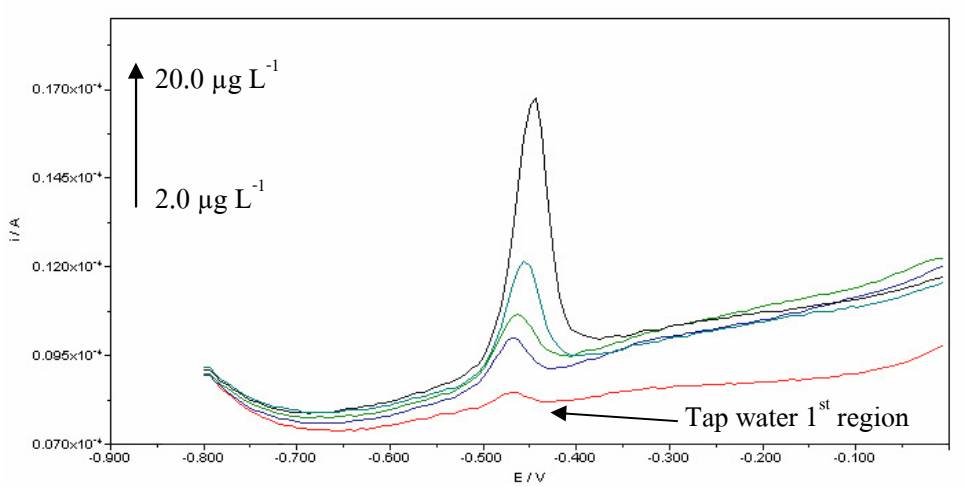

Figure 3-24 SWASV voltammogram (1000 mV s^{-1}) for a tap water sample 1st region and for standard solution of Pb^{2+} ranging in concentration from 2.0 to 20.0 µg L^{-1} acidified to pH l.26. Conditions: 0.2 M KNO_3 electrolyte; Deposition potential, -1.3 V vs Ag/AgCl; Deposition time, 10 min; pulse amplitude, 50 mV

The SWASV voltammogram of Pb^{2+} determination in tap water samples from 1st region at Hatyai city as shown in Figure 3-24 and the standard addition calibration curve of Pb^{2+} in tap water sample are shown Table 3-19 and Figure 3-25.

Table 3-19 The results of standard addition calibration curve of Pb^{2+} in tap water sample from the 1st region

Pb^{2+} conc. (µg L^{-1})	Current (µA)				SD	%RSD
	Rep.1	Rep.2	Rep.3	Average		
Sample 1st	0.462 (BDL)	0.438 (BDL)	0.485 (BDL)	0.462 (BDL)	0.024	5.12
Sample 1st+2.0 µg L^{-1}	1.131	1.136	1.185	1.151	0.030	2.593
Sample 1st+5.0 µg L^{-1}	1.956	1.951	1.796	1.901	0.091	4.785
Sample 1st+10.0 µg L^{-1}	3.741	3.551	3.568	3.620	0.105	2.904
Sample 1st+20.0 µg L^{-1}	7.382	7.254	7.415	7.350	0.085	1.157

BDL: below the detection limit. [compared with the limit of detection (LOD)]

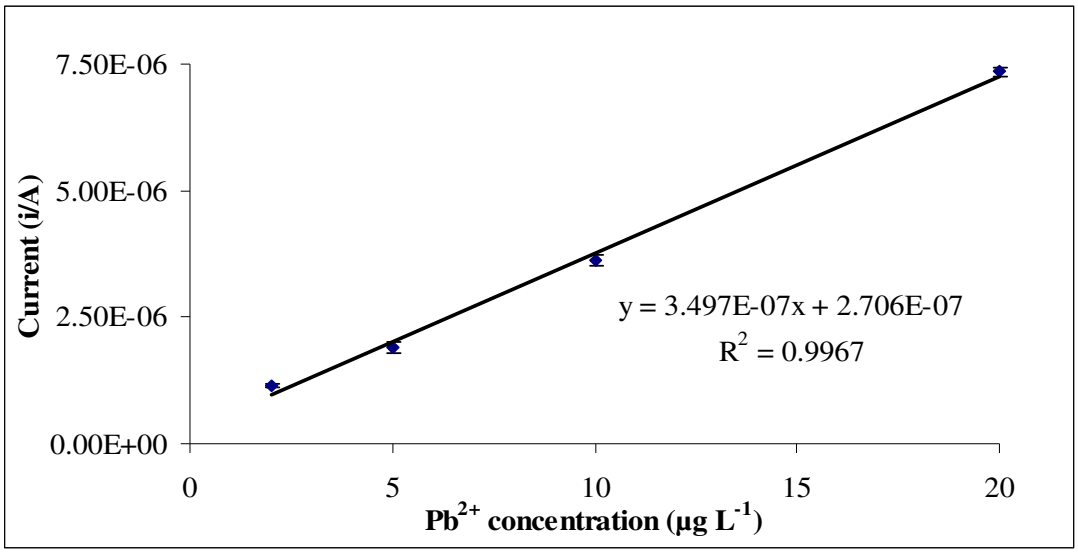

Figure 3-25 Standard addition calibration curve of Pb^{2+} in tap water sample from the 1st region, Pb^{2+} ranging in concentration from 2.0 to 20.0 µg L^{-1}

The results of Pb^{2+} determination in tap water samples from eleven regions at Hatyai city are shown in Table 3-20 and Figure 3-26. The results suggested that the concentrations of Pb^{2+} in tap water samples were at the trace levels.

Table 3-20 The concentration of Pb^{2+} in tap water sample from eleven regions at Hatyai city in the South of Thailand

Regions	**Pb^{2+} concentration ($\mu g\ L^{-1}$)**
1	0.6
2	BDL
3	BDL
4	BDL
5	BDL
6	BDL
7	BDL
8	BDL
9	0.8
10	BDL
11	BDL

BDL: below the detection limit. [compared with the limit of detection (LOD)]

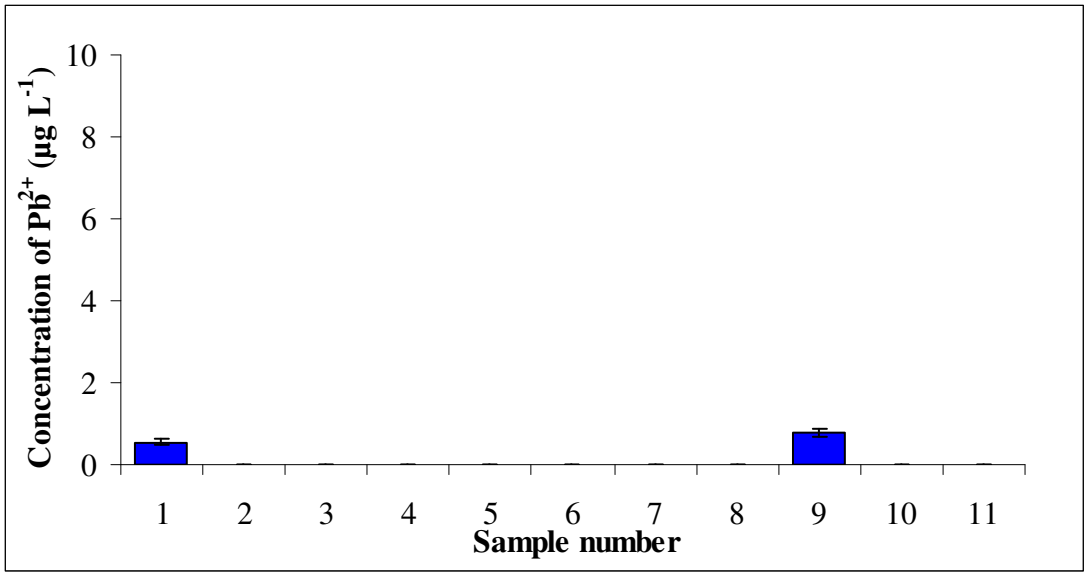

Figure 3-26 The concentration of Pb^{2+} in tap water sample from eleven regions at Hatyai city in the South of Thailand

The concentrations of Pb^{2+} in various tap water samples were found in the range of 0.0-0.8 µg L^{-1} which are within the range of the standard in water by World Health Organization, which established the maximum allowable contaminant lead levels in the drink water recommendation (WHO 1993) to be less than 10.0 µg L^{-1}. Therefore, the lead concentration in tap water samples under the investigation is safety for public health.

3.5.2 Comparison between the studied method and ICP-OES for Pb^{2+} determination in tap water samples

To further assay the reliability of the method, the results of the SWASV analysis of tap water sample were compared with those provided by ICP-OES. Due to the small metal amount to be detected, an instrument equipped with an electrothermal atomizer was used. In order to achieve a satisfactory signal to noise ratio (S/N), tap water samples used in the SWASV analysis were prepared, using the sampling method as described in section 2.5.1. After the SWASV analysis, the same solutions were analysed by ICP-OES.

The results from determination of Pb^{2+} using the studied method (ASV) and ICP-OES are presented in Table 3-21. The means of Pb^{2+} concentration in tap water sample determined by using the studied method (ASV) and ICP-OES were compared.

From the statistical evaluation, it was found that the amount of Pb^{2+} by using the two methods was not detected in almost every sample. The results provided by the studied method (ASV) and ICP-OES were in a good agreement [The limit of detection (LOD) of ICP-OES is 5.0 μg L^{-1}].

Table 3-21 The concentration of Pb^{2+} in tap water sample determined by the studied method under investigation and ICP-OES

Regions	**Pb Concentration (μg L^{-1})**	
	ASV	**ICP-OES**
1	0.6	BDL
2	BDL	BDL
3	BDL	BDL
4	BDL	BDL
5	BDL	BDL
6	BDL	BDL
7	BDL	BDL
8	BDL	BDL
9	0.8	BDL
10	BDL	BDL
11	BDL	BDL
Mean	0.7	-
P-Value	-	

BDL: below the detection limit. [compared with the limit of detection (LOD)]

It can be concluded that the investigated method in this study is effective to be used for Pb^{2+} determination in tap water samples.

3.5.3 Contaminated ink analysis

Figure 3-28 shows SWASV i-E curve for a tap water contaminated ink sample, as well as the curves for standard addition calibration curve of Pb^{2+} in tap water sample ranging in concentration from 2.0 to 20.0 µg L^{-1}. Pb^{2+} and Cu^{2+} were the two metal ions detected in the tap water contaminated ink sample. The sample preparation is explained in section 2.5.3. Stripping peaks for Cu^{2+} (ca. -275 mV) and Pb^{2+} (ca. -460 mV) are present in the voltammogram. The standard addition curve of the peak current versus the Pb^{2+} concentration was linear over two orders of magnitude from 2.0 to 20.0 µg L^{-1}, with a correlation coefficient 0.9972 as shown in Figure 3-27. The concentrations of Pb^{2+} were determined by SWASV to be 3.1±0.2 µg L^{-1}. At least three measurements were made to evaluate the precision of the SWASV technique.

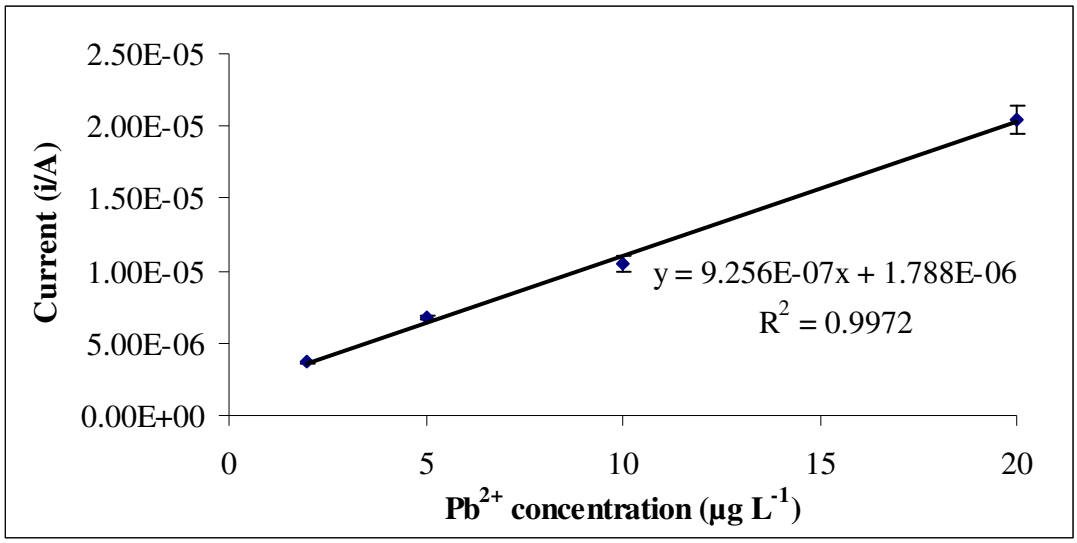

Figure 3-27 Standard addition calibration curve of Pb^{2+} in tap water sample from the 1st region, Pb^{2+} ranging in concentration from 2.0 to 20.0 µg L^{-1}

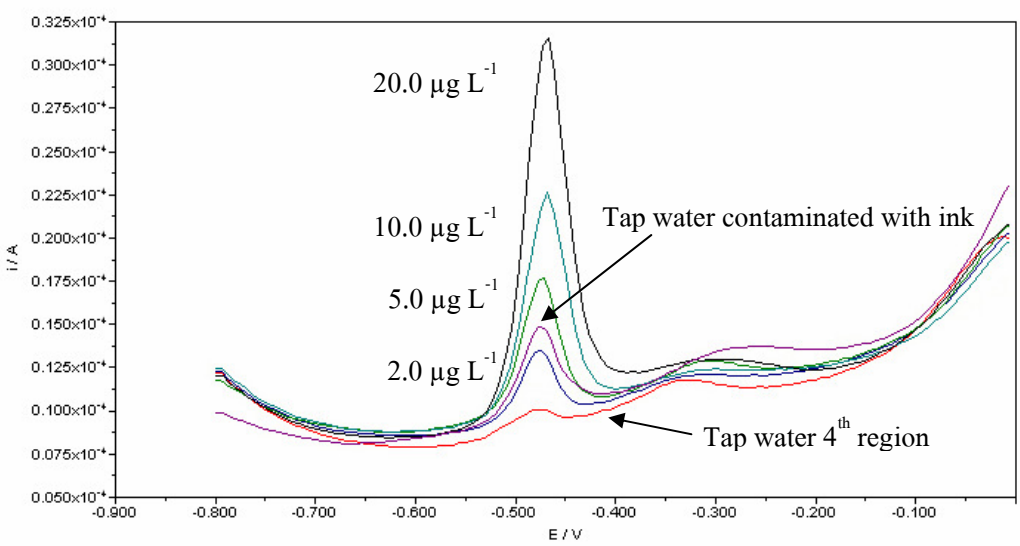

Figure 3-28 Square wave anodic stripping voltammetry (SWASV) *i-E* curve for a tap water contaminated ink sample overlaid with curves for standard addition calibration curve of Pb^{2+} in tap water sample ranging in concentration from 2.0 to 20.0 µg L^{-1}. The supporting electrolyte was 0.2 M KNO_3, pH 1.26. Deposition potential = -1.3 V vs. Ag/AgCl. Deposition time = 10 min. Other SWASV conditions are described in section 2.3.7

3.5.4 Contaminated solder wire analysis

Figure 3-29 shows SWASV i-E curve for a tap water contaminated with solder wire sample, as well as the curves for standard addition calibration curve of Pb^{2+} in tap water sample ranging in concentration from 2.0 to 20.0 µg L^{-1}. The sample preparation is described in section 2.5.4. The Pb^{2+} was the only metal ion found at detectable concentrations in both water samples. Figure 3-25. The curves show the peak currents which increase proportionally with the Pb^{2+} concentration. The peak current was used for quantitation via the standard addition method. The standard addition curve of the peak current versus the Pb^{2+} concentration was linear over two orders of magnitude from 2.0 to 20.0 µg L^{-1}, with a correlation coefficient 0.9972 as shown in Figure 3-27. The Pb^{2+} concentration in a tap water contaminated solder wire was determined by SWASV to be 18.9±0.9 µg L^{-1}. At least three measurements were made to evaluate the precision of the SWASV technique.

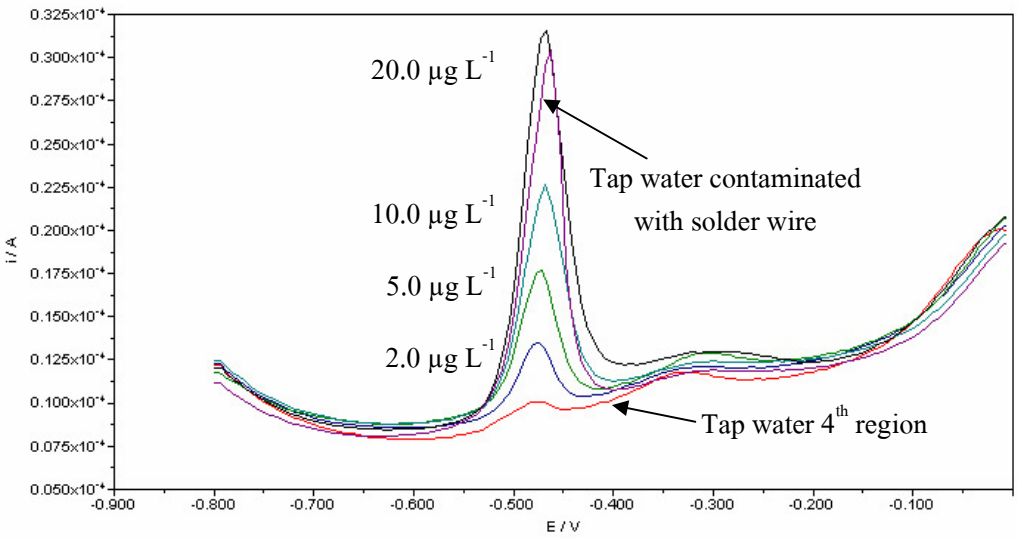

Figure 3-29 Square wave anodic stripping voltammetry (SWASV) *i-E* curve for a tap water contaminated solder wire sample overlaid with curves for standard addition calibration curve of Pb^{2+} in tap water sample ranging in concentration from 2.0 to 20.0 µg L^{-1}. The supporting electrolyte was 0.2 M KNO_3, pH 1.26. Deposition potential = -1.3 V vs. Ag/AgCl. Deposition time = 10 min. Other SWASV conditions are described in section 2.3.7

CHAPTER 4

CONCLUSION

Lead is the most common of the heavy elements and is widely distributed throughout the environment. It is used in the production of lead acid storage batteries, tetraethyl lead (a gasoline additive), pigments, chemicals and solder. From a drinking water perspective, the almost universal use of lead compounds is in plumbing fittings and as solder in water distribution systems. Older distribution systems and plumbing may also be made from lead pipe. Lead is present in tap water as a result of dissolution from natural sources or from household plumbing systems containing lead in pipes, solder or service connections to homes (Health Canada, 1996). Then the exposure of lead can increase the number of adverse health effects due to their toxicity after accumulation in the multiple organs in human body. Therefore, the sensitive instrument techniques for lead determination are more important.

This research presents the investigation method for lead determination in tap water samples, using ASV (SWASV) for quantitative analysis. ASV conditions were optimized such as effect of the pH and supporting electrolyte. The optimum pH was ca. 1.26 by adding appropriate amounts of concentrated HNO_3 and potassium chloride solution (0.2 M) which was generally used as the supporting electrolyte. The deposition potential was -1.3 V vs. Ag/AgCl and the deposition time was 600 s. The optimum conditions were provided the response that was found to more sensitive than that of the previous methods. The linearity range for lead determination was found to be 2.0-30.0 µg L^{-1} with correlation coefficient (R^2) of 0.9994. In order to test the reliability of the proposed methodology suitable for the assaying of lead, the proposed method and its procedures were verified by considering the analytical performance. The accuracy of the method was obtained by the analysis of certified reference material (SRM-1640). The recoveries of lead were 98.84% with the relative standard deviation (%RSD) of 4.970. The limits of detection and limits of quantification of lead determination were 0.3 µg L^{-1} and 1.0 respectively. In the general tap water condition, the various ions had no significant effect on the analysis of lead by the developed method. For the quantitative analysis of lead in tap water, the samples were collected from the eleven regions at Hatyai city, in the South of Thailand, approximately 30 km. from Songkhla province; in February 2008.

The concentration of lead in various tap water samples were found in range of 0.0-0.8 μg L^{-1}. However, the concentrations of Pb^{2+} ion in tap water samples were lower than the drinking water contamination standard limited level (< 10.0 μg L^{-1}) issued by the World Health Organization (WHO).

Table 4-1 Comparison of the proposed method and previous studied for anodic stripping voltammetry (water determination using Boron-doped diamond (BDD) electrodes)

	The previous studied		**The proposed studied**
	(Manivannan, 2004)	(Spataru, 2006)	
Limit of detection	72.5 μg L^{-1}	0.4 μg L^{-1}	0.3 μg L^{-1}
Deposition time	2 min	15 min	10 min
Linear range	0-1.0 mg L^{-1}	0.4-20.7 μg L^{-1}	2.0-30.0 μg L^{-1}

The proposed sample preparation method in this research was satisfactory due to simplicity, speed and efficiency compare with the previous studied as shown in Table 4-1. It can be successfully applied to determination of lead in tap water samples. The results were in good agreement with those obtained by ICP-OES, demonstrating the practical analytical utility of the method. Tap water samples, that have been kept in contact for several hours with a solder wire and ink contaminate, were analyzed for the lead content by ASV at the diamond electrode.

For further study, various chemically modified electrodes can be introduced to improve effect of the obtaining conditions of the polycrystalline diamond films on the analytical performance characteristics for lead detection by ASV.

REFERENCES

Acar, O. 2001. Determination of Cadmium and Lead in Biological Samples by Zeeman ETAAS Using Various Chemical Modifiers. *Talanta* **55**, 613-622.

Aikamphon, K. 1978. Adsorption and Distribution of Lead and Zinc in Certain Vegetable Plants. Chulalongkorn University, Bangkok, Thailand.

ATSDR (Agency for Toxic Substance and Disease Registry). 1993d. Toxicology Profile for Lead, Agency for Toxic Substance and Disease Registry, U.S. Public Health Service, Atlanta, GA.

ATSDR (Agency for Toxic Substance and Disease Registry). 2005. Lead, Agency for Toxic Substance and Disease Registry, U.S. Public Health Service, Atlanta, GA.

Babyak, C., and Smart, R.B. 2004. Electrochemical Detection of Trace Concentrations of Cadmium and Lead with a Boron-doped Diamond Electrode: Effect of KCl and KNO_3 Electrolytes, Interferences and Measurement in River Water. *Electroanalysis* **16**, 175-182.

Banks, C.E., Hyde, M.E., Tomcik, P., Jacobs, R., and Compton, R.G. 2004. Cadmium Detection via Boron-doped Diamond Electrodes: Surfactant Inhibited Stripping Voltammetry. *Talanta* **62**, 279-286.

BAS EPSILON. 2000. Instruction Manual for Bas Epsilon for Electrochemistry Version 1.60.70. Bioanalytical Systems, Inc.

BAS EPSILON. 2008. Instruction Manual for Bas Epsilon for Electrochemistry Version 2.00.71. Bioanalytical Systems, Inc.

Bonfil, Y., Brand. M., and Kirowa-Eisner, E. 1999. Determination of Sub-µg l^{-1} Concentrations of Copper by Anodic Stripping Voltammetry at the Gold Electrode. *Analytica Chimica Acta* **387**, 85-95.

Boyd, G.R., Tarbert, N.K., Oliphant, R.J., Kirmeyer ,G.J., Murphy, B.M., and Serpente, R.F. 2000. Lead Pipe Rehabilitation and Replacement Techniques for Drinking Water Service-survey of Utilities. *Tunnelling and Underground Space Technology* **15**, 13-24.

Buffle, J., and Tercier-Waeber, M.L. 2000. In situ Monitoring of Aquatic Systems; Chemical Analysis and Speciation, IUPAC series. *Analytical and Physical Chemistry of Environmental Systems* **6**, 279.

Buffle, J., and Tercier-Waeber, M.L. 2005. Voltammetric Environmental Tracemetal Analysis and Speciation: From Laboratory to In situ Measurements. *Trends in Analytical Chemistry* **24**, 3.

Carapuca, H.M., Monterroso, S.C.C., Simao, J.E.J., and Duarte, A.C. 2004. Optimisation of Mercury Film Deposition on Glassy Carbon Electrodes: Evaluation of the Combined Effects of pH, Thiocyanate ion and Deposition Potential. *Analytica Chimica Acta* **503**, 203-212.

Cellarosi, M.J. 2004. MSDS nitric acid. MDL Information Systems, Inc.,

Coelho, N.M.M., Cosmen da Silva, A., and Moraes da Silva, C. 2002. Determination of As(III) and Total Inorganic Arsenic by Flow Injection Hydride Generation Atomic Absorption Spectrometry. *Analytica Chimica Acta* **460**, 227-233.

Cordon, F., Ramirez, S.A., and Gordillo, G.J. 2002. Adsorption and Electrochemical Reduction of Co(II)-Dimethylglyoxime on Mercury. *Journal of Electroanalytical Chemistry* **534**, 131-141.

Compton, R.G., Foord, J.S., and Saterlay, A.J.1999. Sono-cathodic Stripping Voltammetry of Manganese at a Polished Boron-doped Diamond Electrode: Application to the Determination of Manganese in Instant Tea. *Analyst* **124**, 1791-1796.

Compton, R.G., Coles, B.A., Holt, K., Foord, J.S., Markenk, F., and Tsai, Y.C. 2001. Microwave-enhanced Anodic Stripping Detection of Lead in a River Sediment Sample. A mercury-free Procedure Employing a Boron-doped Diamond Electrode. *Electroanalysis* **13**, 831-835.

Compton, R.G., Banks, C.E., Hyde, M.E., Tomcık, P., and Jacobs, R. 2004. Cadmium Detection via Boron-doped Diamond Electrodes: Surfactant Inhibited Stripping Voltammetry. Talanta **62,** 279-286.

Compton, R.G., Wantz, F., and Banks, C.E. 2004. Edge Plane Pyrolytic Graphite Electrodes for Stripping Voltammetry: a Comparison with Other Carbon Based Electrodes. *Electroanalysis* **17**, 655-661.

Daecharat, S. 2002. Contamination of lead and cadmium in Tapi-Phumduang River Sludge. Master of Science Thesis in Environment Management, Prince of Songkla University, Songkhla, Thailand.

Davison, W. 1993. Iron and Manganese in Lakes. *Earth-Science Rev*iews **34**, 119-163.

Demars, R.D., and Shain, I. 1957. Anodic Stripping Voltammetry using the Hanging Mercury Drop Electrode. *Analytical Chemistry* **29**, 1825-1827.

EPA. 2005. 3Ts For Reducing Lead in Drinking Water in Schools. http://www.epa.gov/OGWDW/schools/pdfs/lead/toolkit_leadschools_fs_3ts_main.pdf (accessed 5/05/2007).

Farghaly., and Othman, A. 2003. Direct and Simultaneous Voltammetric Analysis of Heavy Metals in Tap Water Samples at Assiut city: an Approach to Improve

Theanalysis Time for Nickel and Cobalt Determination at Mercury Film Electrode. *Microchemical* **75**, 119-131.

Farre, M., and Barcelo, D. 2003. Toxicity Testing of Wastewater and Sewage Sludge by Biosensors, Bioassays and Chemical Analysis. *Trends in Analytical Chemistry* **22**, 229-310.

Flechsig, G.U., Korbout, O., Hocevar, S.B., Thongngamdee, S., Ogorevc, B., Grundler P., Wang, J., and Chemie, F. 2002. Electrically Heated Bismuth-film Electrode for Voltammetric Stripping Measurements of Trace Metals. *Electroanalysis* **14**, 192-196.

Fischer, E., and Berg, C.M.G. 1999. Anodic Stripping Voltammetry of Lead and Cadmium using a Mercury Film Electrode and Thiocyanate. *Analytica Chimica Acta* **385**, 273-280.

Fujishima, A., Rao, T.N., Yagi, I., Miwa, T., and Tryk, D.A. 1999. Electrochemical Oxidation of NADH at Highly Boron-doped Diamond Electrodes. *Analytical Chemistry* **71**, 2506-2511.

Gazy, A.A., Mahgoub, H., Khamis, E. F., Youssef, R. M., and El-Sayed, M. A. 2006. Differential Pulse, Square Wave and Adsorptive Stripping Voltammetric Quantification of Tianeptine in Tablets. *Journal of Pharmaceutical and Biomedical Analysis* **41,** 1157-1163.

Geater, A., Chompikul, J., Chongsuvivalwong, V., and Mcneil, D. 1996. Lead Contamination Among School Children Living in the Pattani River Basin. Songkla : Epidemiology Unit, Prince of Songkla University, Songkhla, Thailand.

Goyer, R. 1995. Toxic effect of metal: Casarett and doult's toxicology. the Basic Science of Poisons. Klaassen CD Eds. 5th Ed, Mc Graw-Hill, New York, pp 691-736.

Guide to the Expression of Uncertainty in Measurement, 1993. ISBN 92-67-10188-9, 1st ed. International Organization for Standardization: Geneva, Switzerland.

Guilarte, T.R., and Toscano, C.D. 2005. Lead Neurotoxicity: From Exposure to Molecular Effects. *Brain Research Reviews* **49**, 529-554.

Holgado T.M., Macias, J.M.P., and Hernandez, L.H. 1995. Voltammetric Determination of Lead with a Chemically Modified Carbon Paste Electrode with Diphenylthiocarbazone**.** *Analytica Chimica Acta* **309**, 117-122.

Health Canada. 1996. *Guidelines for Canadian Drinking Water Quality* **6**, 52-54.

Herdan, J., Feeney, R., and Kounaves, S.P. 1998. Field Evaluation of an Electrochemical Probe for In situ Screening of Heavy Metals in Groundwater. *Environmental Science & Technology* **32**, 131-136.

Hill, S. 1995. Lead. *Encyclopedia of Analytical Science* **4**, 2506-2511.

Howard, A.G., and Stratham, P.J. 1993. Inorganic Trace Analysis: *Philosophy and Practice, Wiley, Chichester, West Sussex, UK,*

Hu, S., Wu, K., Fei, J., and Bai, W. 2003. Mercury-free Simultaneous Determination of Cadmium and Lead at a Glassy Carbon Electrode Modified with Multi-wall Carbon Nanotubes. *Analytica Chimica Acta* **489**, 215-221.

Kosakova, E., Spankova, M., Kandrac, J., and Mikus, P. 1996. Forms of Binding of Copper, Lead, and Cadmium in Carbonate Type Soil Studied by Differential Pulse Anodic Stripping Voltammetry. *Chemical Papers-Chemicke Zvesti* **50**, 334-340.

Kirowa-Eisner, E., Brand, M., and Eshkenazi, I. 1997. the Silver Electrode in Square-wave Anodic Stripping Voltammetry. Determination of Pb^{2+} Without Removal of Oxygen. *Analytical Chemistry* **69**, 4660-4664.

Kirowa-Eisner, E., Brand, M., and Tzur, D. 1999. Determination of Sub-nanomolar Concentrations of Lead by Anodic-stripping Voltammetry at the Silver Electrode. *Analytica Chimica Acta* **385**, 325-335.

Korolczuk, M. 2000. Voltammetric Method for Direct Determination of Nickel in Natural Waters in the Presence of Surfactants. *Talanta* **53**, 679-686.

Kounaves, S.P., and Nolan, M.A. 1999. Microfabricated Array of Iridium Microdisks as a Substrate for Direct Determination of Cu^{2+} or Hg^{2+} using Square-wave Anodic Stripping Voltammetry. *Analytical Chemistry* **71**, 3567-3573.

Kounaves, S.P., and Feeney, R. 2000. On-site Analysis of Arsenic in Groundwater using a Microfabricated Gold Ultramicroelectrode Array. *Analytical Chemistry* **72**, 2222-2228.

Kruusma, J., Banks, C.E., and Compton, R.G. 2004. Mercury-free Sono-Electroanalytical Detection of Lead in Human Blood by use of Bismuth-film-modified Boron-doped Diamond Electrodes. *Analytical and Bioanalytical Chemistry* **379,** 700-706.

Lead in Drinking Water, http://www.epa.gov/safewater/lead/leadfacts.html, (accessed 5/05/2007).

Liawruangrath, S. Masawat, P., and Slater J.M. 2003. Flow Injection Measurement of Lead using Mercury-free Disposable Gold-sputtered Screen-printed Carbon Electrodes (SPCE). *Sensors and Actuators B* **91**, 52-59.

Locatelli, C., and Torsi, G. 2002. A New Voltammetric Method for the Simultaneous Monitoring of Heavy Metals in Sea Water, Sediments, Algae and Clams: Application to the Goro Bay Ecosystem. *Environmental Monitoring and Assessment* **75**, 281-292.

Manivannan, A., Kawasaki, R., Tryk, D.A., and Fujishima A. 2004. Interaction of Pb and Cd During Anodic Stripping Voltammetric Analysis at Boron-doped Diamond Electrodes. *Electrochimica Acta* **49**, 3313-3318.

Manivannan, A., Seehra, M.S., and Fujishima, A. 2004. Detection of Mercury at the ppb Level in Solution using Boron-doped Diamond Electrode. *Fuel Process. Technol* **85**, 513-519.

Pochareng, C., and Kamnurtpriwul, T. 2004. http://www.khlong-u-taphao.com/doc/khlong_u_taphao_info_water_use.pdf (accessed 5/05/2007).

Prado, C., Wilkins, S.J., Marken, F., and Compton, R.G. 2002. Simultaneous Electrochemical Detection and Determination of Lead and Copper at Boron-doped Diamond Film Electrodes. *Electroanalysis* **14**, 262-272.

Rickard, D., Oldroyd, A., and Clamp, A. 1999. Voltammetric Evidence for Soluble FeS Complexes in Anoxic Estuarine Muds. *Estuaries* **22**, 693-701.

Rojanapaiwong, S. 1999. State of the Thai Environment 1997-1998. Green world foundation. Bangkok, Thailand.

Ross, J.W., Demars, R.D., and Shain, I. 1956. Analytical Applications of the Hanging Mercury Drop Electrode. *Analytical Chemistry* **28**, 1768-1771.

Saito, M.A., and Moffett, J.W. 2001. Complexation of Cobalt by Natural Organic Ligands in the Sargasso Sea as Determined by a New High-sensitivity Electrochemical Cobalt Speciation Method Suitable for Open Ocean Work. *Marine Chemistry* **75**, 49-68.

Saterlay, A.J., Marken, F., Foord, J.S., and Compton, R.G. 2000. Sonoelectrochemical Investigation of Silver Analysis at a Highly Boron-doped Diamond Electrode. *Talanta* **53**, 403-415.

Saterlay, A.J., Tibbetts, D.F., and Compton, R.G. 2000. Comparative Study to Evaluate the Feasibility of Sono-anodic and Sono-cathodic Stripping Voltammetry for the Determination of Pb in a Cu-Pb Alloy. *Analytical Sciences* **16**, 1055-1060.

Sherigara, B.S., Shivaraj, Y., Mascarenhas, R.J., and Satpati, A.K. 2007. Simultaneous Determination of Lead, Copper and Cadmium onto Mercury Film Supported on Wax Impregnated Carbon Paste Electrode Assessment of Quantification Procedures by Anodic Stripping Voltammetry. *Electrochimica Acta* **52**, 3137-3142.

Spataru, N., Dragoe, D., Kawasaki, R., Manivannan, A., Spataru, T., Tryk, D.A., and Fujishima, A. 2006. Detection of Trace Levels of Pb^{2+} in Tap Water at Boron-doped Diamond Electrodes with Anodic Stripping Voltammetry. *Electrochimica Acta* **51**, 2437-2441.

Suwannarath, G. 1995. Level of some Heavy Metals in Klong Wat Basin, Changwat Songkhla. Master of Science Thesis in Environmental Management, Prince of Songkla University, Songkhla, Thailand.

Swain, G.M., Sonthalia, P., McGaw, E., and Show, Y. 2004. Metal Ion Analysis in Contaminated Water Samples using Anodic Stripping Voltammetry and a Nanocrystalline Diamond Thin-film Electrode. *Analytica Chimica Acta* **522**, 35-44.

Swain, G.M., and McGaw, E.A. 2006. A Comparison of Boron-doped Diamond Thin-film and Hg-coated Glassy Carbon Electrodes for Anodic Stripping Voltammetric Determination of Heavy Metal Ions in Aqueous Media. *Analytica Chimica Acta* ***575,*** 180-189.

Taillefert, M., Bono, A.B., and Luther, G.W. 2000. Reactivity of Freshly Formed Fe(III) in Synthetic Solutions and Marine (pore)Waters: Voltammetric Evidence of an Aging Process. *Environmental Science and Technology* **34**, 2169-2177.

Taylor, B.N. 1995. *Guide for the Use of the International System of Units (SI)*; NIST Special Publication 811, U.S. Government Printing Office: Washington, DC (1995).

Ugo, P., Sperni, L., and Mazzocchin, G.A. 2002. Electrochemical Measurement of Mercury Concentration Profiles in the Pore-waters of Sediments of the Venice Lagoon by Ion-exchange Voltammetry at Polymer Modified Electrodes. *Annali di chimica* **92**, 301-311.

Vanysek, P. 1996. Modern Techniques in Electroanalysis. ISBN 0-471-55514-2. John Wiley & Sons, Inc. *Chemical Analysis Series* **139**, 151-180.

Van Loon, J.C., and Barefoot, R.R. 1992. Overview of Analytical Methods for Elemental Speciation. *The Analyst* 117, 563-570.

Wang, J., Lu, J., Hocevar, S.B., and Farias, P.A.M. 2000. Bismuth-coated Carbon Electrodes for Anodic Stripping Voltammetry. *Analytical Chemistry* **72**, 3218-3222.

Wang, J., Lu, J., Kiegoz, U.A., Hocevar, S.B., and Ogorevc, B. 2001. Insights into the Anodic Stripping Voltammetric Behavior of Bismuth Film Electrodes. *Analytica Chimica Acta* **434**, 29-34.

Wangwongwatana, S. 2003. Cleaning the Air. *ADB Review* **35**, 26-27.

Wantz, F., Banks, C.E., and Compton, R.G. 2005. Edge Plane Pyrolytic Graphite Electrodes for Stripping Voltammetry: a Comparison with other Carbon Based Electrodes. *Electroanalysis* **17**, 655-661.

WHO, 2006. World Health Organization. : ISBN 92 4 154696 4. *Guidelines for drinking-water quality* **1**, 491-493.

Zeng, A., Liu, E., Tan, S.N., Zhang, S., and Gao, J. 2002. Stripping Voltammetric Analysis of Lead at Nitrogen Doped Diamond-like Carbon Film Electrodes, *Electroanalysis*, **14**, 1294-1298.

http://en.wikipedia.org/wiki/Lead (accessed 3/02/2007).

http://electrochem.usask.ca/chem322/Notes_2/Electrochem2.pdf (accessed 31/05/2008).

http://www.cypresssystems.com/Experiments/pulsetechniques.html (accessed 31/05/2008).

APPENDIX A

EFFECT OF COEXISTING IONS ON DETERMINATION OF LEAD

Appendix A-1 Effect of Aluminum on the stripping voltammograms recorded in 0.05 M KNO_3 (pH 1.26), at constant Pb concentration (20.0 µg L^{-1}). Al^{3+} concentration (µg L^{-1}): (1) 0, (2) 10, (3) 20, (4) 30. Stripping Conditions: Deposition potential, -1.3 V vs Ag/AgCl; Deposition time, 10 min; pulse amplitude, 50 mV

Al^{3+} Concentration (µg L^{-1})	Current (µA)			Average	SD	%RSD	Peak current change (%)
	I	II	III				
0	23.150	21.080	21.270	21.830	1.144	5.241	0.00
10	21.790	21.270	20.930	21.330	0.433	2.031	-2.31
20	21.930	20.190	20.150	20.760	1.016	4.896	-4.93
30	18.650	19.690	19.930	19.420	0.680	3.503	-11.04

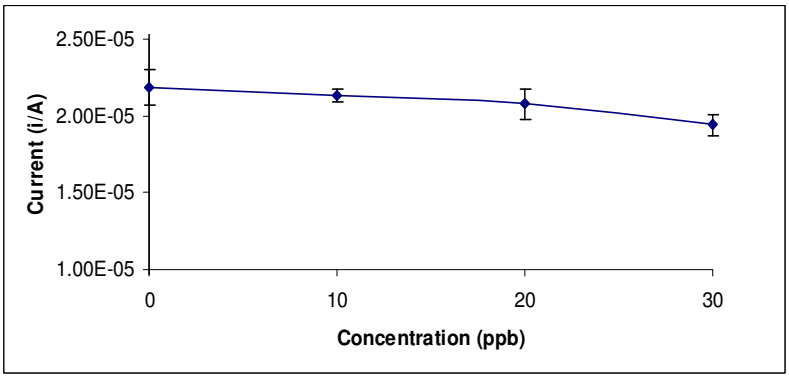

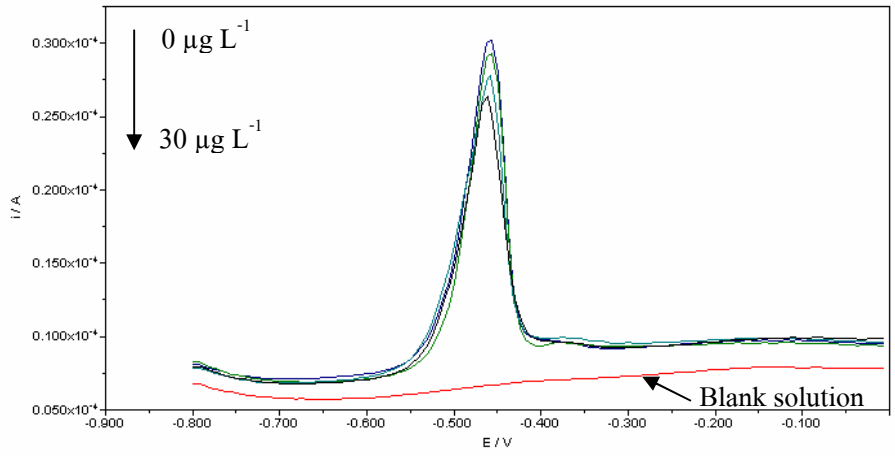

Appendix A-2 Effect of Calcium on the stripping voltammograms recorded in 0.05 M KNO_3 (pH 1.26), at constant Pb concentration (20.0 µg L^{-1}). Ca^{2+} concentration (µg L^{-1}): (1) 0, (2) 1000, (3) 2000, (4) 3000, (5) 4000. Stripping Conditions: Deposition potential, -1.3 V vs Ag/AgCl; Deposition time, 10 min; pulse amplitude, 50 mV

Ca^{2+} Concentration (µg L^{-1})	Current (µA)			Average	SD	%RSD	Peak current change (%)
	I	II	III				
0	22.950	22.660	21.580	22.400	0.722	3.224	0.00
1000	22.940	21.720	21.850	22.170	0.670	3.022	-1.01
2000	21.480	22.160	21.880	21.840	0.342	1.565	-2.49
3000	20.770	22.050	20.950	21.260	0.693	3.260	-5.09
4000	18.770	19.520	20.150	19.480	0.691	3.547	-13.02

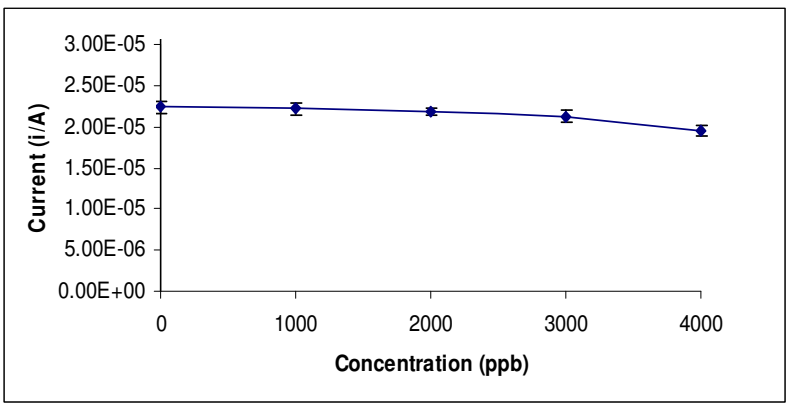

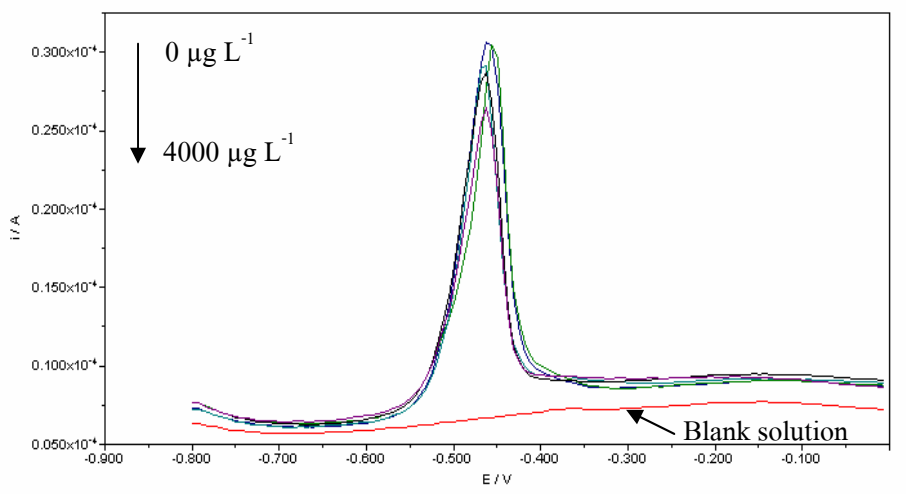

Appendix A-3 Effect of Cadmium on the stripping voltammograms recorded in 0.05 M KNO_3 (pH 1.26), at constant Pb concentration (20.0 µg L^{-1}). Cd^{2+} concentration (µg L^{-1}): (1) 0, (2) 50, (3) 100, (4) 150, (5) 200. Stripping Conditions: Deposition potential, -1.3 V vs Ag/AgCl; Deposition time, 10 min; pulse amplitude, 50 mV

Cd^{2+} Concentration (µg L^{-1})	**Current (µA)**			**Average**	**SD**	**%RSD**	**Peak current change (%)**
	I	**II**	**III**				
0	22.410	23.840	21.800	22.680	1.047	4.616	0.00
50	21.680	20.550	22.080	21.440	0.794	3.702	-5.50
100	19.220	20.430	20.720	20.120	0.796	3.954	-11.29
150	19.740	18.240	19.150	19.040	0.756	3.968	-16.05
200	18.500	17.590	18.510	18.200	0.528	2.903	-19.76

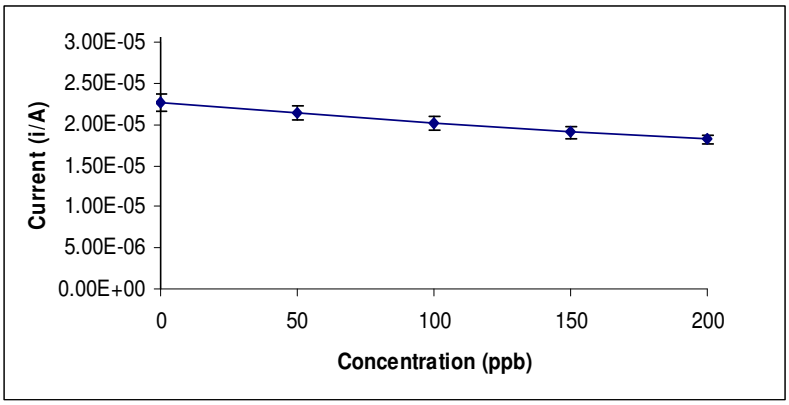

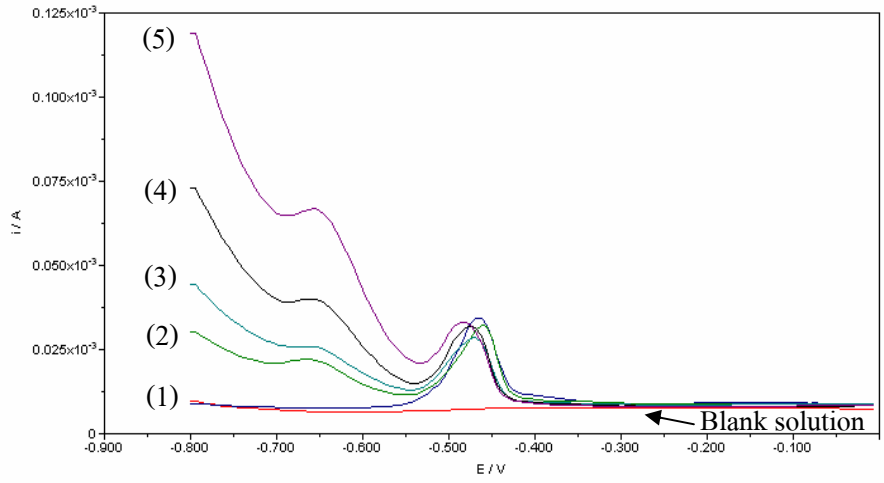

Appendix A-4 Effect of Cobalt on the stripping voltammograms recorded in 0.05 M KNO_3 (pH 1.26), at constant Pb concentration (20.0 µg L^{-1}). Co^{2+} concentration (µg L^{-1}): (1) 0, (2) 5, (3) 10, (4) 15, (5) 20. Stripping Conditions: Deposition potential, -1.3 V vs Ag/AgCl; Deposition time, 10 min; pulse amplitude, 50 mV

Co^{2+} Concentration ($\mu g\ L^{-1}$)	Current (µA)			Average	SD	%RSD	Peak current change (%)
	I	II	III				
0	18.050	19.610	18.430	18.700	0.814	4.351	0.00
5	18.570	19.080	18.060	18.570	0.510	2.746	-0.68
10	19.100	18.970	17.380	18.480	0.958	5.182	-1.14
15	18.730	17.160	18.700	18.200	0.898	4.934	-2.67
20	18.100	17.990	17.050	17.710	0.577	3.258	-5.26

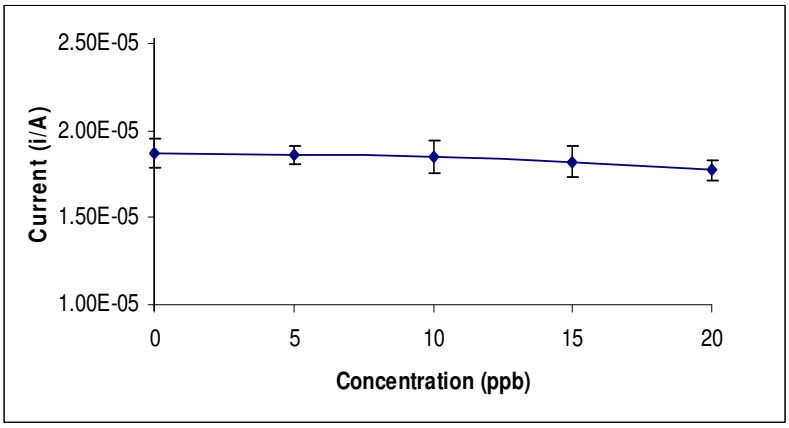

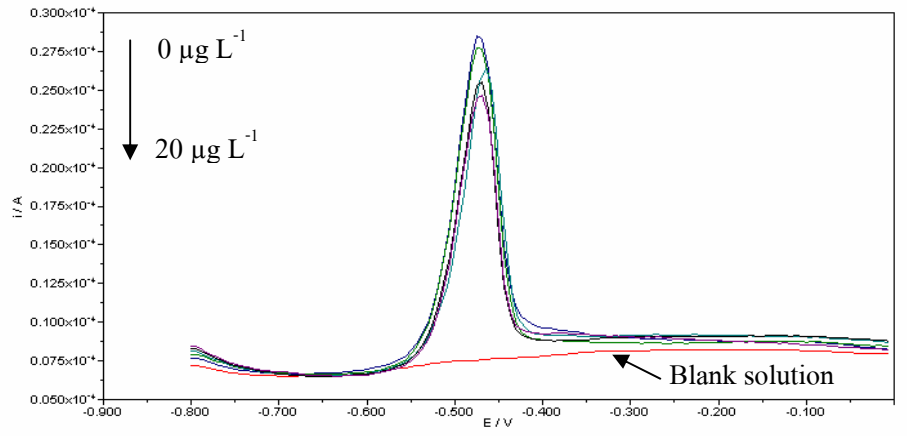

Appendix A-5 Effect of Copper on the stripping voltammograms recorded in 0.05 M KNO_3 (pH 1.26), at constant Pb concentration (20.0 µg L^{-1}). Cu^{2+} concentration (µg L^{-1}): (1) 0, (2) 5, (3) 10, (4) 15, (5) 20. Stripping Conditions: Deposition potential, -1.3 V vs Ag/AgCl; Deposition time, 10 min; pulse amplitude, 50 mV

Cu^{2+} Concentration (µg L^{-1})	**Current (µA)**			**Average**	**SD**	**%RSD**	**Peak current change (%)**
	I	**II**	**III**				
0	38.090	39.510	39.420	39.010	0.795	2.038	0.00
5	37.770	39.500	38.850	38.710	0.874	2.258	-0.77
10	37.070	38.790	39.390	38.420	1.204	3.135	-1.51
15	39.620	36.500	38.240	38.120	1.563	4.100	-2.27
20	35.550	38.000	36.680	36.740	1.226	3.337	-5.80

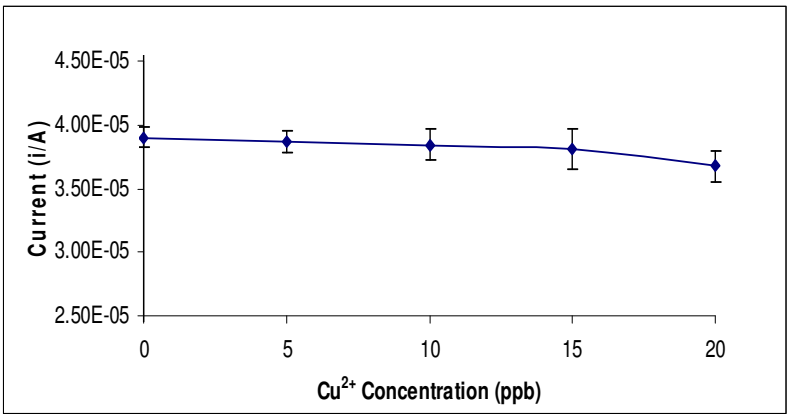

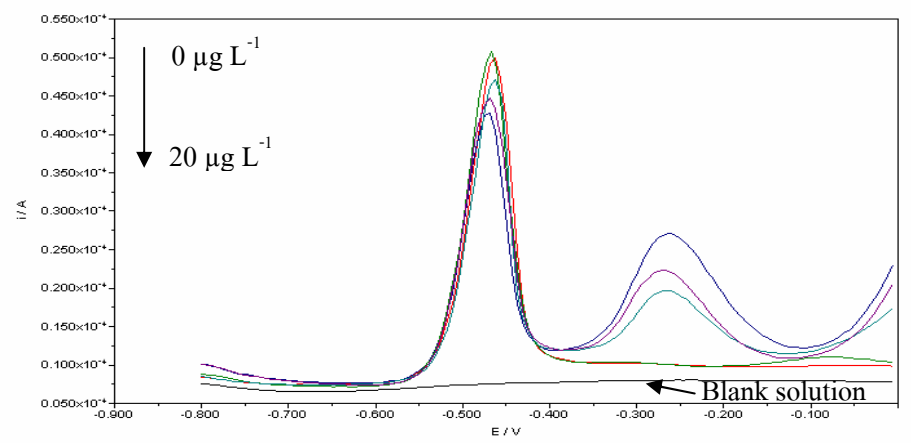

Appendix A-6 Effect of Iron on the stripping voltammograms recorded in 0.05 M KNO_3 (pH 1.26), at constant Pb concentration (20.0 µg L^{-1}). Fe^{2+} concentration (µg L^{-1}): (1) 0, (2) 50, (3) 100, (4) 200, (5) 300. Stripping Conditions: Deposition potential, -1.3 V vs Ag/AgCl; Deposition time, 10 min; pulse amplitude, 50 mV

Fe^{2+} Concentration ($\mu g\ L^{-1}$)	Current (µA)			Average	SD	%RSD	Peak current change (%)
	I	II	III				
0	29.530	27.760	28.950	28.750	0.902	3.139	0.00
50	29.780	30.030	28.690	29.500	0.712	2.415	2.62
100	28.500	29.350	31.210	29.690	1.386	4.669	3.27
200	31.480	28.650	30.550	30.230	1.442	4.772	5.15
300	34.080	31.380	32.990	32.820	1.358	4.139	14.16

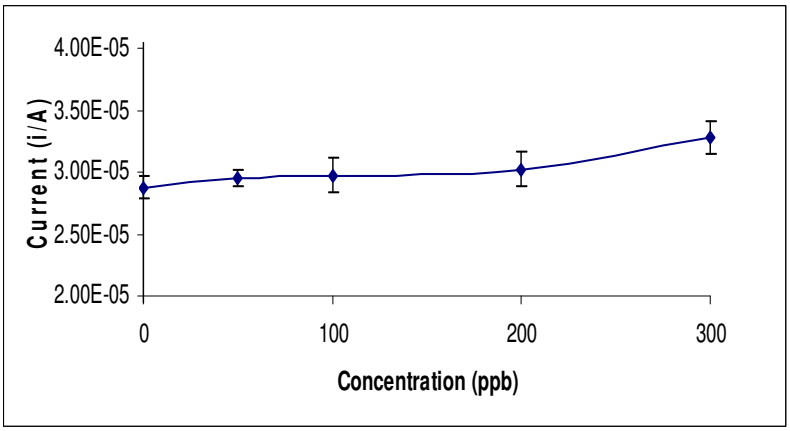

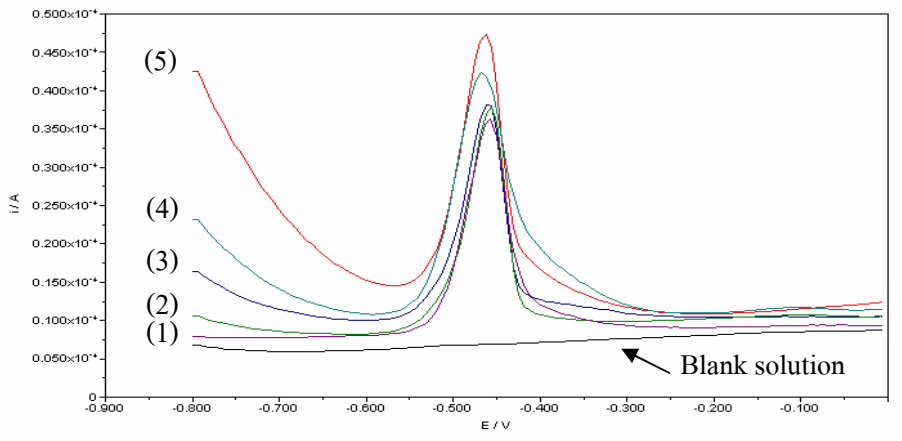

Appendix A-7 Effect of Magnesium on the stripping voltammograms recorded in 0.05 M KNO_3 (pH 1.26), at constant Pb concentration (20.0 µg L^{-1}). Mg^{2+} concentration (µg L^{-1}): (1) 0, (2) 1000, (3) 2000, (4) 3000, (5)

4000. Stripping Conditions: Deposition potential, -1.3 V vs Ag/AgCl; Deposition time, 10 min; pulse amplitude, 50 mV

Mg^{2+} Concentration ($\mu g\ L^{-1}$)	Current (µA)			Average	SD	%RSD	Peak current change (%)
	I	II	III				
0	30.730	29.750	28.580	29.690	1.076	3.626	0.00
1000	28.810	29.250	28.510	28.860	0.372	1.290	-2.80
2000	27.260	28.550	27.680	27.830	0.658	2.364	-6.25
3000	24.260	24.980	24.500	24.580	0.367	1.491	-17.20
4000	17.600	16.760	19.240	17.870	1.261	7.060	-39.82

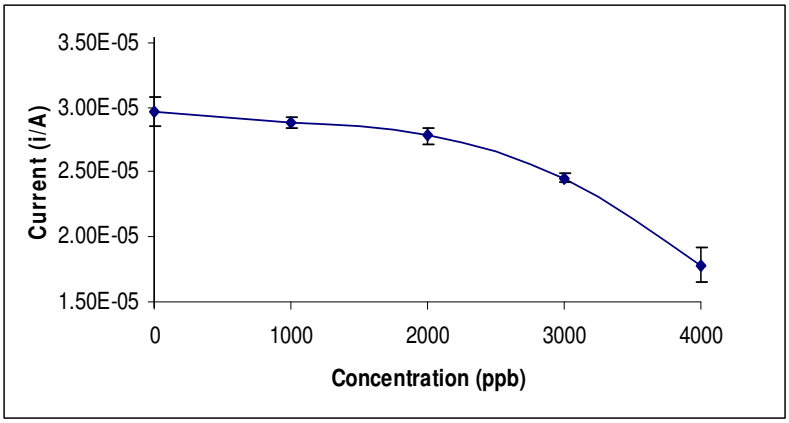

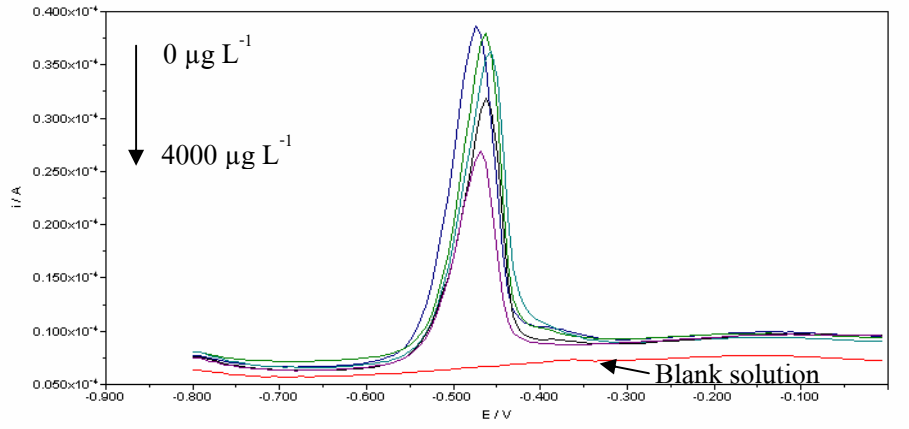

Appendix A-8 Effect of Manganese on the stripping voltammograms recorded in 0.05 M KNO_3 (pH 1.26), at constant Pb concentration (20.0 µg L^{-1}). Mn^{2+}concentration (µg L^{-1}): (1) 0, (2) 500, (3) 1000, (4) 1500, (5) 2000. Stripping Conditions: Deposition potential, -1.3 V vs Ag/AgCl; Deposition time, 10 min; pulse amplitude, 50 mV

Mn^{2+} Concentration (µg L^{-1})	**Current (µA)**			**Average**	**SD**	**%RSD**	**Peak current change (%)**
	I	**II**	**III**				
0	19.860	19.430	19.590	19.630	0.217	1.107	0.00
500	18.050	18.680	18.910	18.550	0.445	2.401	-5.50
1000	17.310	17.250	17.680	17.410	0.233	1.337	-11.28
1500	16.250	15.060	14.540	15.280	0.877	5.736	-22.13
2000	10.930	9.658	9.804	10.130	0.696	6.871	-48.38

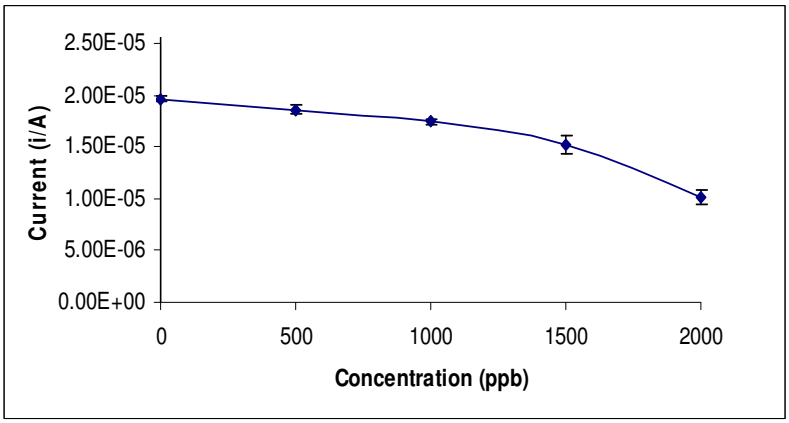

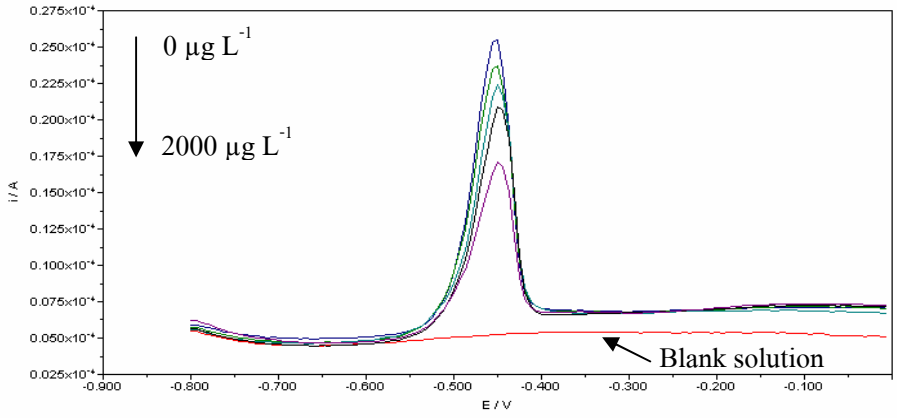

Appendix A-9 Effect of Nickel on the stripping voltammograms recorded in 0.05 M KNO_3 (pH 1.26), at constant Pb concentration (20.0 µg L^{-1}). Ni^{2+} concentration (µg L^{-1}): (1) 0, (2) 50, (3) 100, (4) 200. Stripping Conditions: Deposition potential, -1.3 V vs Ag/AgCl; Deposition time, 10 min; pulse amplitude, 50 mV

Ni^{2+} Concentration ($\mu g\ L^{-1}$)	Current (µA)			Average	SD	%RSD	Peak current change (%)
	I	II	III				
0	27.130	28.760	26.630	27.510	1.114	4.049	0.00
50	25.650	25.530	26.920	26.030	0.770	2.959	-5.36
100	25.500	24.840	24.690	25.010	0.431	1.723	-9.08
200	23.460	21.750	23.580	22.930	1.024	4.464	-16.64

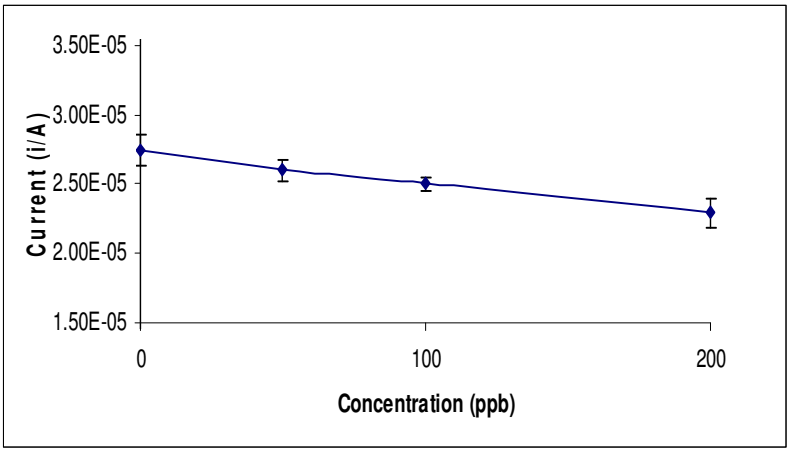

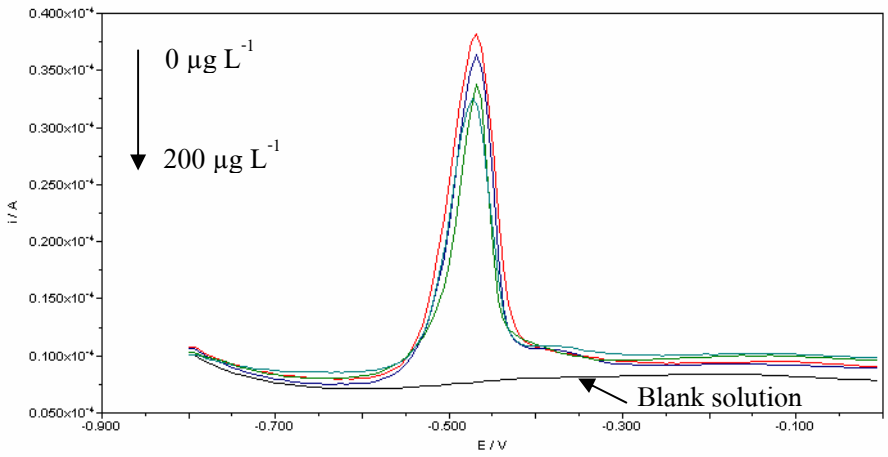

Appendix A-10 Effect of Zinc on the stripping voltammograms recorded in 0.05 M KNO_3 (pH 1.26), at constant Pb concentration (20.0 µg L^{-1}). Zn^{2+} concentration (µg L^{-1}): (1) 0, (2) 50, (3) 100, (4) 200 (5) 300.

Stripping Conditions: Deposition potential, -1.3 V vs Ag/AgCl; Deposition time, 10 min; pulse amplitude, 50 mV

Zn^{2+} Concentration ($\mu g\ L^{-1}$)	Current (µA)			Average	SD	%RSD	Peak current change (%)
	I	II	III				
0	28.410	28.480	31.040	29.310	1.499	5.113	0.00
50	29.66	28.330	27.810	28.600	0.954	3.336	-2.42
100	27.150	27.230	28.480	27.620	0.746	2.700	-5.77
200	26.770	26.610	26.760	26.710	0.090	0.336	-8.86
300	23.500	24.050	23.880	23.810	0.282	1.183	-18.76

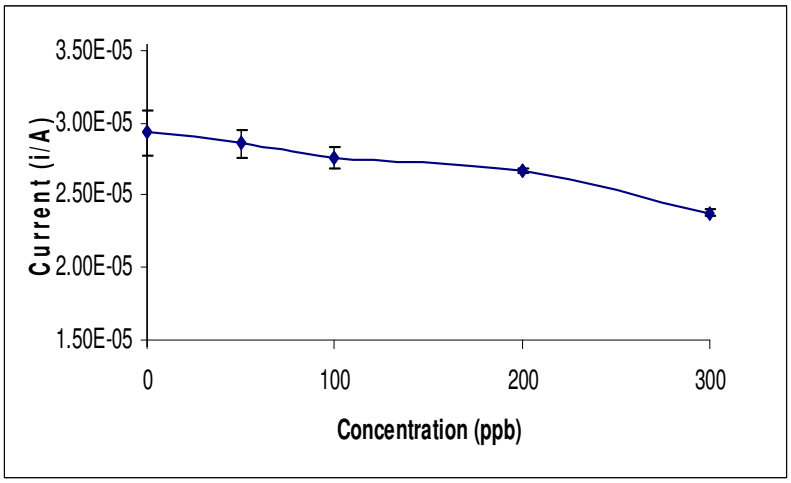

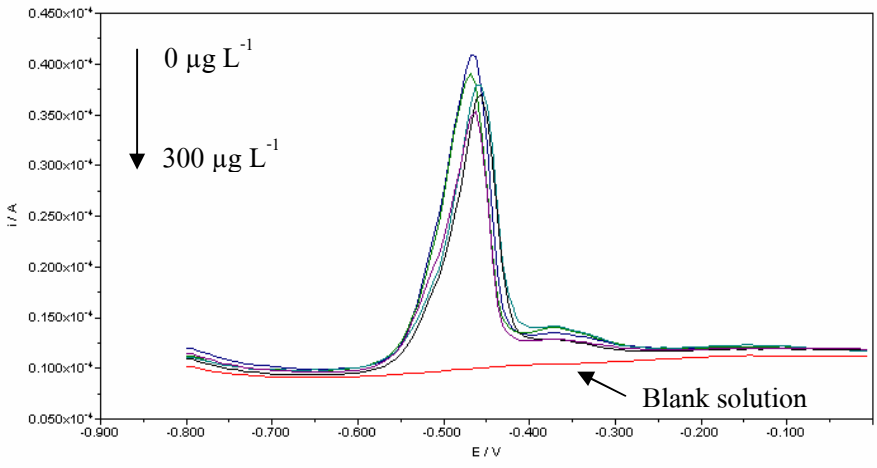

APPENDIX B

ANALYSIS OF A NIST REFERENCE SOLUTION

Appendix B-1 Square wave anodic stripping voltammetry (SWASV) *i-E* curve for a NIST sample (SRM 1640) overlaid with curves for standard solutions of Pb^{2+} ranging in concentration from 2.0 to 10.0 µg l^{-1}: (1) 0.0, (2) 2.0, (3) 4.0, (4) 6.0 (5) 8.0 (6) 10.0. in 0.10 M KNO_3 (pH 1.00). Stripping Conditions: Deposition potential, -1.3 V vs Ag/AgCl; Deposition time, 10 min; pulse amplitude, 50 mV

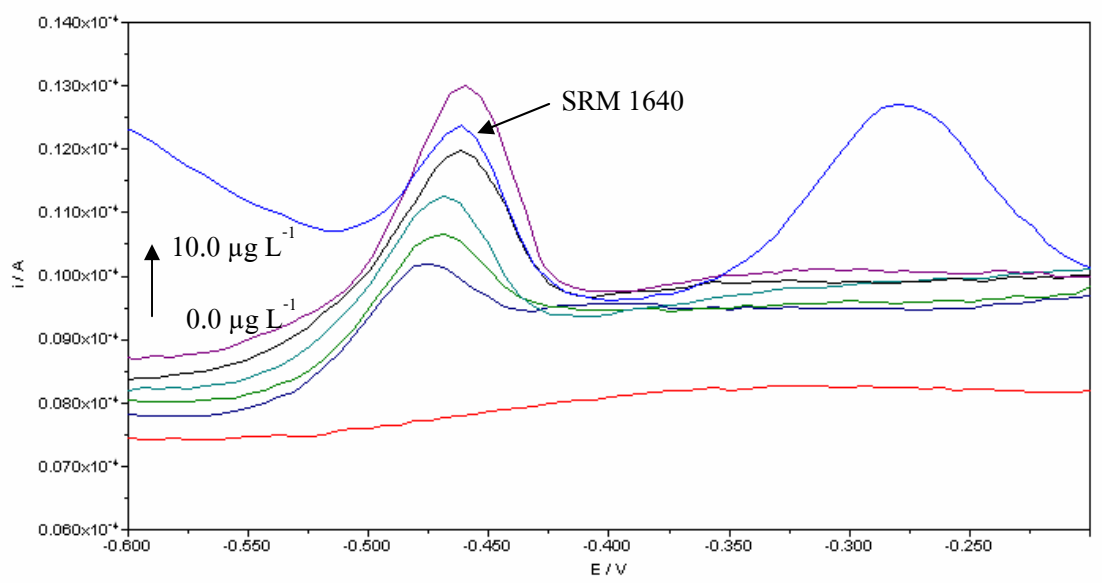

APPENDIX C

STATISTICAL ANALYSIS

Appendix C-1 The compared of slopes of standard addition and calibration curve for Pb^{2+} by using two-way ANOVA (F-test)

Anova: Two-Factor With Replication

SUMMARY	2.0 µg L^{-1}	5.0 µg L^{-1}	10.0 µg L^{-1}	20.0 µg L^{-1}	Total
Calibration Curve					
Count	3	3	3	3	12
Sum	4.418E-06	8.553E-06	1.726E-05	3.647E-05	6.670E-05
Average	1.473E-06	2.851E-06	5.754E-06	1.216E-05	5.559E-06
Variance	1.505E-15	1.660E-14	4.967E-14	1.457E-13	1.847E-11
Standard addition					
Count	3	3	3	3	12
Sum	5.789E-06	1.177E-05	2.114E-05	4.219E-05	8.089E-05
Average	1.930E-06	3.924E-06	7.047E-06	1.406E-05	6.741E-06
Variance	5.572E-15	2.143E-14	4.997E-14	1.704E-13	2.317E-11
Total					
Count	6	6	6	6	
Sum	1.021E-05	2.032E-05	3.840E-05	7.866E-05	
Average	1.701E-06	3.387E-06	6.401E-06	1.311E-05	
Variance	6.549E-14	3.604E-13	5.409E-13	1.217E-12	

ANOVA

Source of Variation	*SS*	*df*	*MS*	*F*	*P-value*	*F crit*

Sample	8.385E-12	1	8.385E-12	145.542	1.905E-09	4.494
Columns	4.556E-10	3	1.519E-10	2635.825	9.221E-22	3.239
Interaction	1.612E-12	3	5.374E-13	9.329	8.415E-04	3.239
Within	9.218E-13	16	5.761E-14			
Total	4.665E-10	23				

APPENDIX D

MAP OF SAMPLE COLLECTED

Appendix D-1 Map of tap water samples collected at Hatyai city, in the South of Thailand, approximately 30 km. from Songkhla; in February 2008 (Zoom 1st step)

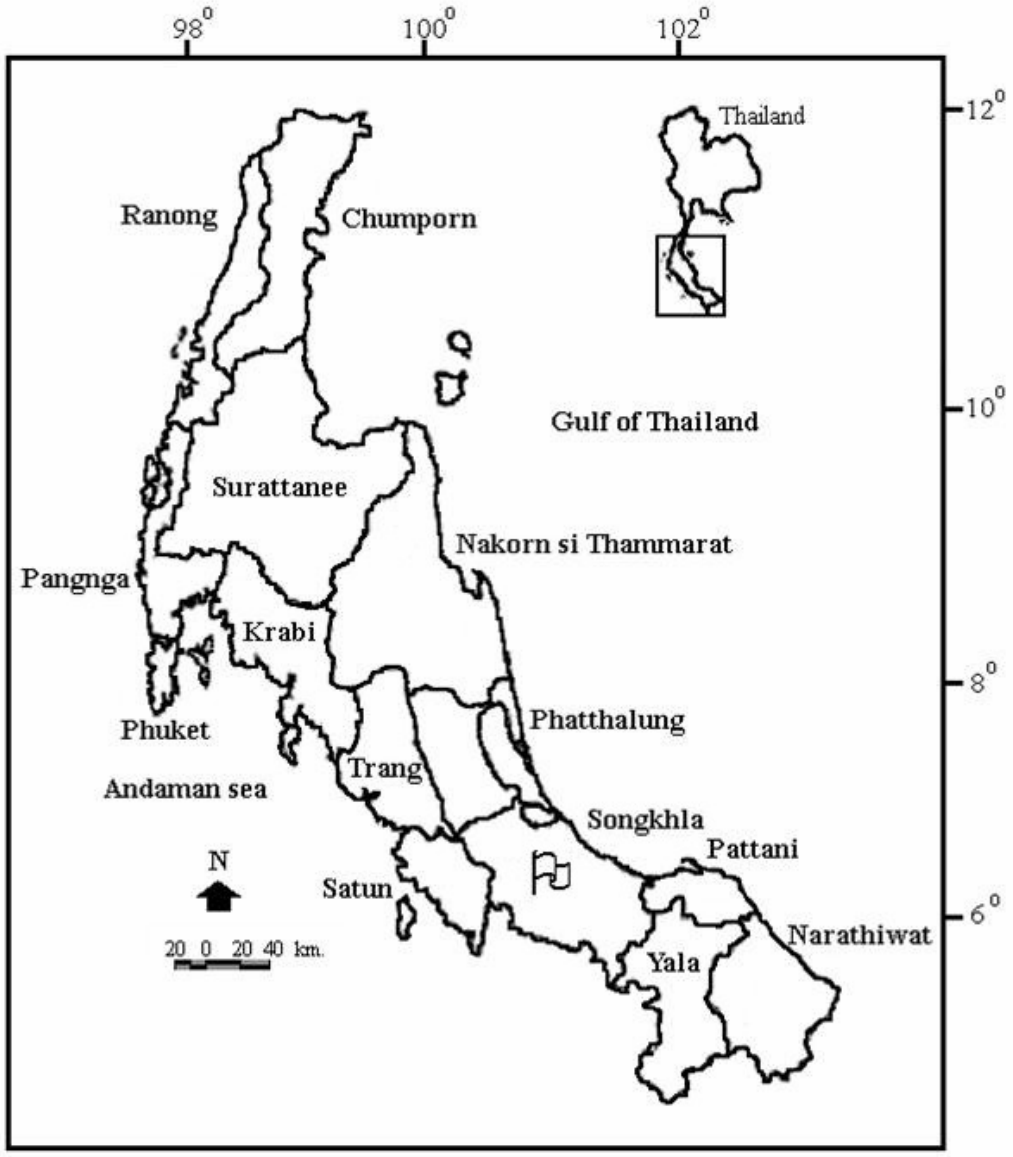

Source; http://www.nbids.org/nbidsdata/images/S map.jpg

Appendix D-2 Map of tap water samples collected at Hatyai city, in the South of Thailand, approximately 30 km. from Songkhla; in February 2008 (Zoom 2nd step)

Source; Provincial Waterworks Authority (http://www.pwa.co.th)

Appendix D-3 Map show the location to collect tap water samples around Hatyai city, in the South of Thailand, approximately 30 km. from Songkhla; in February 2008 (Zoom 3rd step)

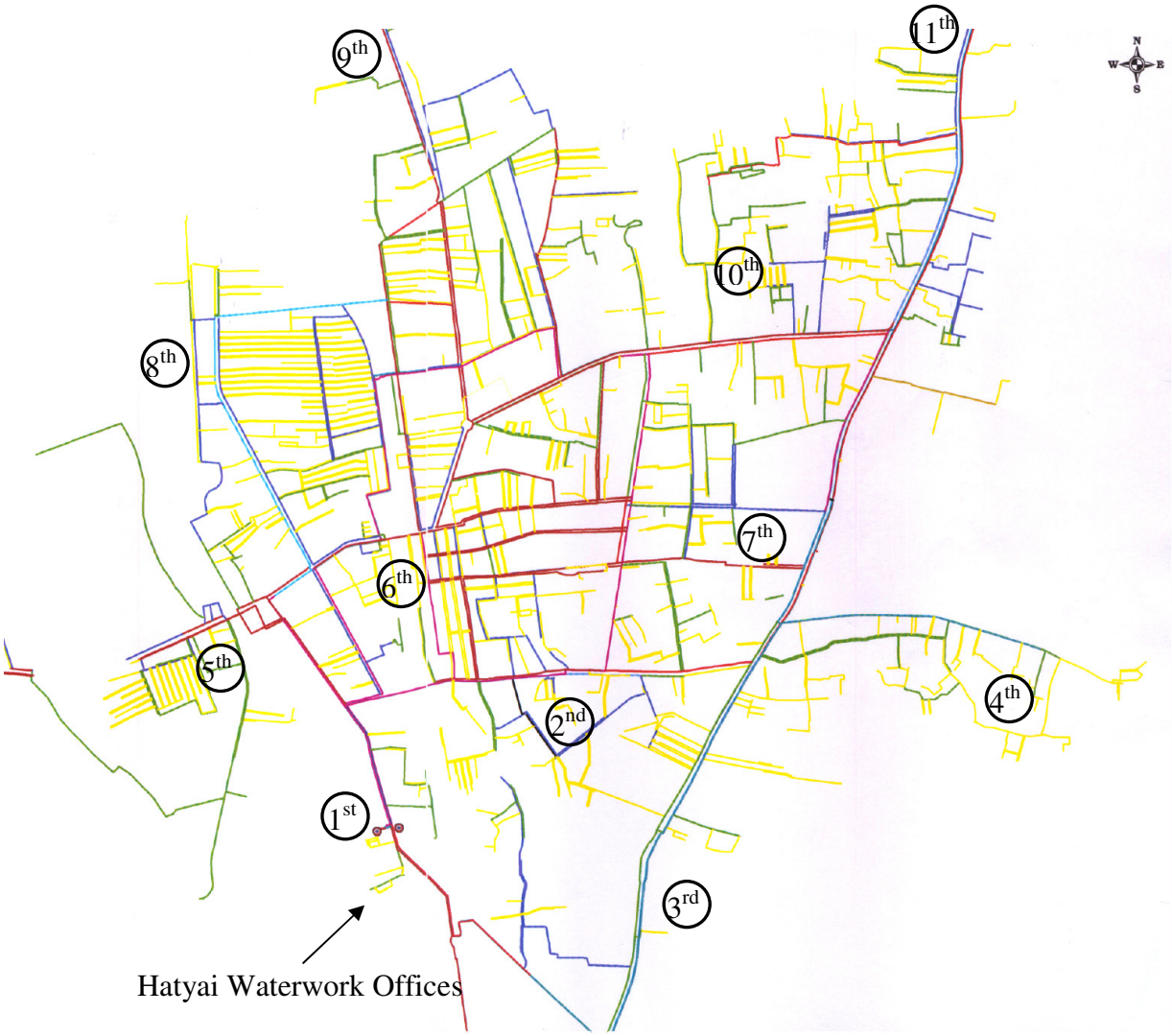

Source; Hatyai Waterwork Offices, 2007

VITAE

Name Mr. Chalermpol Innuphat

Student ID 4722012

Education Attainment

Degree	Name of Institution	Year of Graduation
B.Sc. (General Science)	Prince of Songkla University	2001

List of Publication and Proceeding

Chalermpol Innuphat, Pipat Chooto and Puchong Wararatananurak. Detection of trace levels of Pb^{2+} in tap water by stripping voltammetry with boron-doped diamond (BDD) electrode. The 33rd Congress on Science and Technology of Thailand, October 18-20, 2007, Nakorn Si Thammarat, Thailand.